Paster

ASR72-294

NASA CR-
141673

SPACE SHUTTLE ORBIT MANEUVERING ENGINE DEMONSTRATION THRUST CHAMBER DESIGN REPORT

TASK III

(NASA-CR-141673) SPACE SHUTTLE ORBIT MANEUVERING ENGINE DEMONSTRATION THRUST CHAMBER DESIGN REPORT (Rocketdyne) 97 p

N75-73334

Unclas
00/98 13656

Prepared by

R. P. Pauckert
Member-Technical-Staff
Advanced Programs

NAS 9-12802

Approved by

R. D. Paster
Project Engineer
SS/OME Program

ROCKETDYNE A DIVISION OF NORTH AMERICAN ROCKWELL CORPORATION
6633 Canoga Avenue, Canoga Park, Cal

13656 JSC

INTRODUCTION

A regeneratively cooled thrust chamber using NTO/MMH propellants is a primary candidate for the Orbital Maneuvering Engine of the Space Shuttle. The design requirements for the OME are listed in Table 1 and a typical OME engine assembly is shown in Fig. 1. Engine characteristics are described in Fig. 2 and a weight breakdown is given in Table 2. As part of Contract NAS9-12802, a regeneratively cooled thrust chamber is being designed, fabricated, and tested to evaluate the critical design factors of this configuration. Particular factors which will be evaluated during this program are:

1. The fuel injection temperature and inlet temperature requirements resulting from the regenerative cooling mode
2. Performance
3. Sensitivity to inlet pressure variations
4. Start and transient soakback characteristics
5. Chamber durability
6. Combustion stability

The thrust chamber will be tested with an injector having performance, heat flux, and stability characteristics similar to that of the flight OME injector. A short radiation cooled nozzle will be used to simulate the nozzle attached geometry and thermal soakback characteristics. In this report are discussed the similarities between the demonstrator and flight OME thrust chambers, the logic and analyses used to select the design details for the thrust chamber assembly, the operating characteristics of the thrust chamber, and the fabrication methods and schedule.

Table 1. OME DESIGN REQUIREMENTS

• PROPELLANTS	NTO/MMH
• THRUST	6000 POUNDS
• CHAMBER PRESSURE	125 PSIA
• MIXTURE RATIO	1.65 O/F
• SERVICE LIFE	10 YEARS 100 MISSIONS 1000 STARTS 4×10^8 LB-SEC TOTAL IMPULSE
• DUTY CYCLE	10 STARTS 6×10^6 LB SEC MAXIMUM BURN TOTAL IMPULSE 1 SECOND MINIMUM BURN MINIMUM RESTART CONSTRAINTS
• PROPELLANT TEMPERATURE	30 - 120°F AT START 40 - 90°F STEADY-STATE
• ENGINE TEMPERATURE	600°F MAXIMUM EXTERNAL TEMPERATURE UPSTREAM OF NOZZLE EXTENSION

4

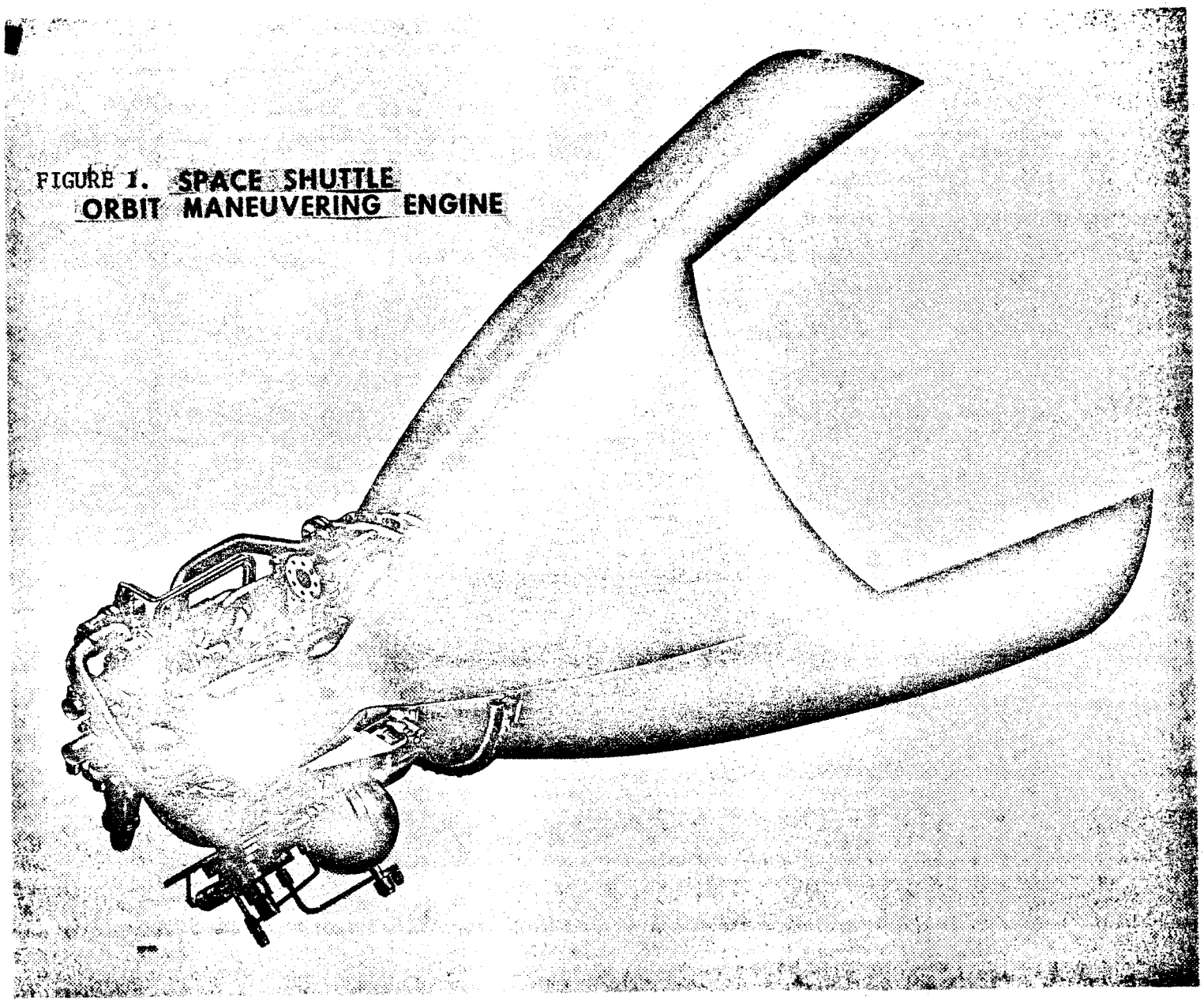

FIGURE 1. SPACE SHUTTLE ORBIT MANEUVERING ENGINE

FIGURE 2. **STORABLE OME ASSEMBLY**

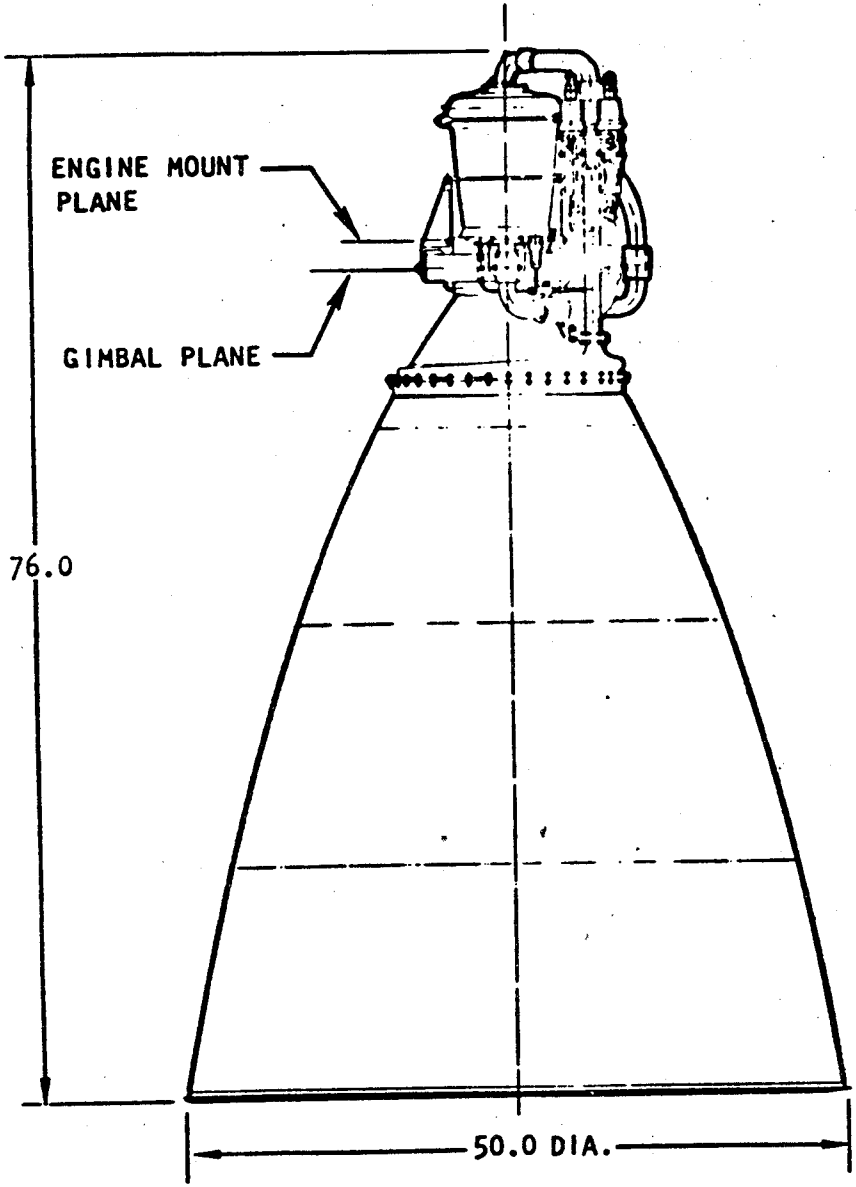

ENGINE CHARACTERISTICS

THRUST POUNDS	6000
PROPELLANTS	N_2O_4/MMH
MIXTURE RATIO, O/F	1.65
CHAMBER PRESSURE, PSIA	125
NOZZLE AREA RATIO,	72
I_S, SECONDS	313
COOLING	
REGENERATIVE	$\epsilon = 7$
FILM, % W	2.4
RADIATION	Cb/Ti SKIRT
VALVE TYPE	QUAD-REDUNDANT BALL VALVE
TVC	GIMBAL ($\pm$7 DEG)
COMBUSTION STABILITY	AC. CAV.
WEIGHT, LBS	180

Table 2

ORBIT MANEUVERING ENGINE WEIGHT BREAKDOWN

	WEIGHT, POUNDS
REGENERATIVE CHAMBER	37.4
RADIATION NOZZLE	41.2
INJECTOR	23.6
PROPELLANT VALVE	38.0
GIMBAL, RING, BEARING, ATTACHMENTS	26.0
DUCTING	10.7
ELECTRIC	2.7
TOTAL	179.6

DISCUSSION

The flight configuration of the OME thrust chamber assembly shown in Fig. 3 includes the injector, the regeneratively cooled chamber and the radiation cooled nozzle. The radiation cooled nozzle attaches at an area ratio of 7 and extends to an area ratio of 72 which corresponds to an external exit diameter of 50 inches at the 6000 pound thrust level for a chamber pressure of 125 psia. Characteristics of this thrust chamber assembly are described in Table 3. Safety, reliability, and maintainability features are shown in Fig. 4. A Failure Mode and Effects Analysis of the injector and chamber are presented in Appendix A. The regeneratively cooled thrust chamber uses channel wall construction with an uppass coolant circuit from an area ratio of 7 to the injector and has a contraction area ratio of 2. The tapered contour from the injector to the throat favors boundary layer buildup and enhances coolant characteristics at the throat. The chamber has an integral auxiliary fuel cooling ring which contains 180 orifices using 6.4 percent of the fuel (2.4 percent of the propellants). This auxiliary film coolant lowers the regenerative coolant jacket Δp to 15 psi and the fuel temperature rise to 175 F. The regenerative coolant channels are machined into a CRES liner and closed out with electroformed nickel.

DEMONSTRATOR CONFIGURATION

The demonstrator thrust chamber assembly is shown in Fig. 5. The injector, film coolant ring, and thrust chamber are bolted together to allow greater flexibility during the test program. The injector and the film coolant ring can be readily changed and the fuel flow can be controlled separately to the injector, coolant ring, and regenerative coolant jacket. The radiation cooled nozzle extension has soakback characteristics similar to that of the flight nozzle and is similarly attached.

Figure 3. OME THRUST CHAMBER ASSEMBLY FLIGHT CONFIGURATION

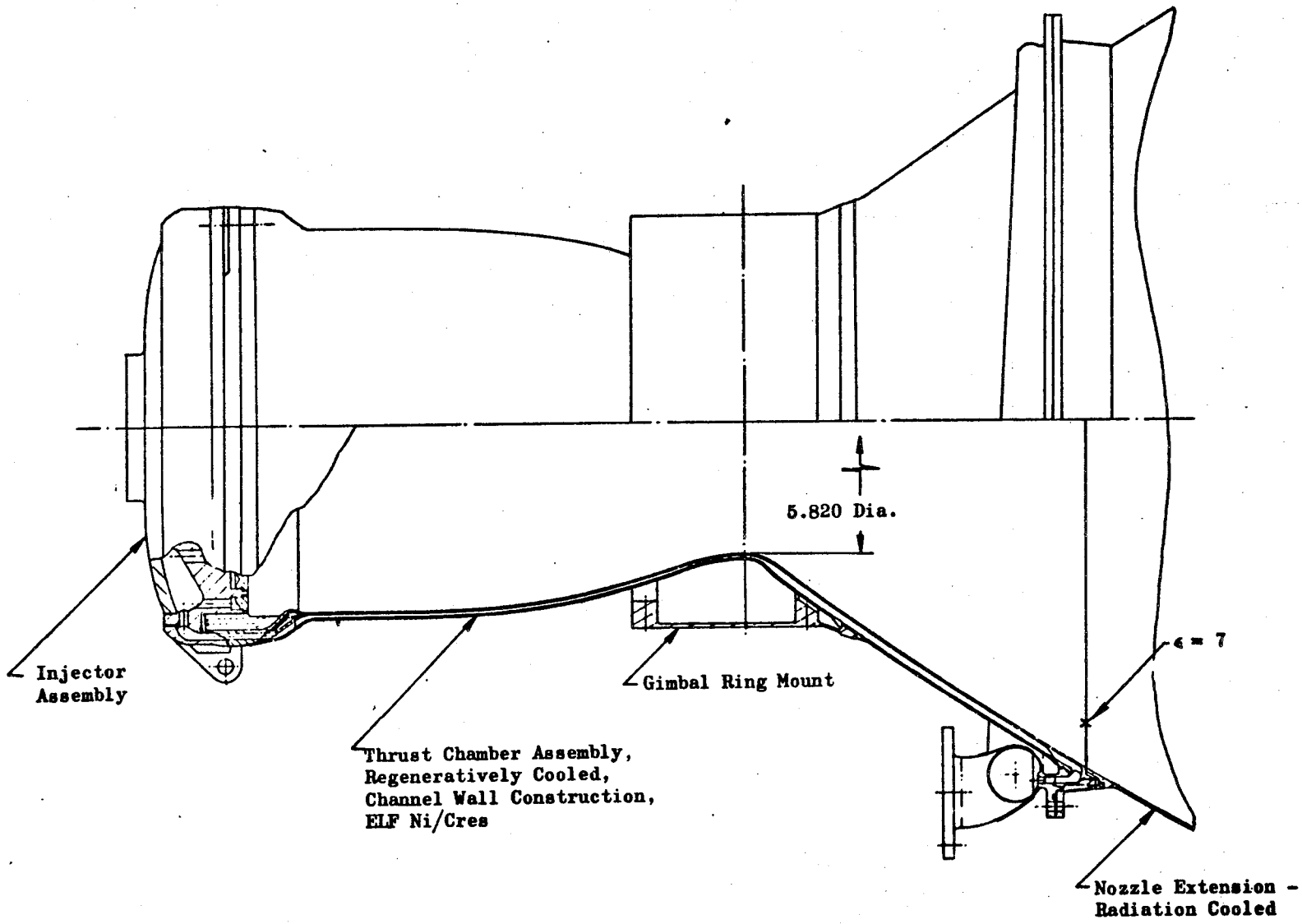

Table 3. THRUST CHAMBER CHARACTERISTICS

● COMBUSTOR	
CONTRACTION RATIO	2:1
LENGTH	14.7 IN
CONTOUR	TAPERED FROM 7 IN. UPSTREAM OF THROAT
● NOZZLE	
REGEN SECTION EXPANSION RATIO	TO 7:1
CONTOUR	FLIGHT PARABOLIC
NOZZLE EXTENSION EXPANSION RATIO	7:1 TO 9:1
CONTOUR	30° CONICAL
● COOLANT	
CIRCUIT	UPPASS
NUMBER OF REGEN COOLANT CHANNELS	180
COOLANT PRESSURE DROP	15 PSID
COOLANT BULK TEMPERATURE RISE	175F
AUXILIARY FILM COOLANT	2.4% TOTAL PROPELLANT

Figure 4. **OME DESIGN FEATURES**

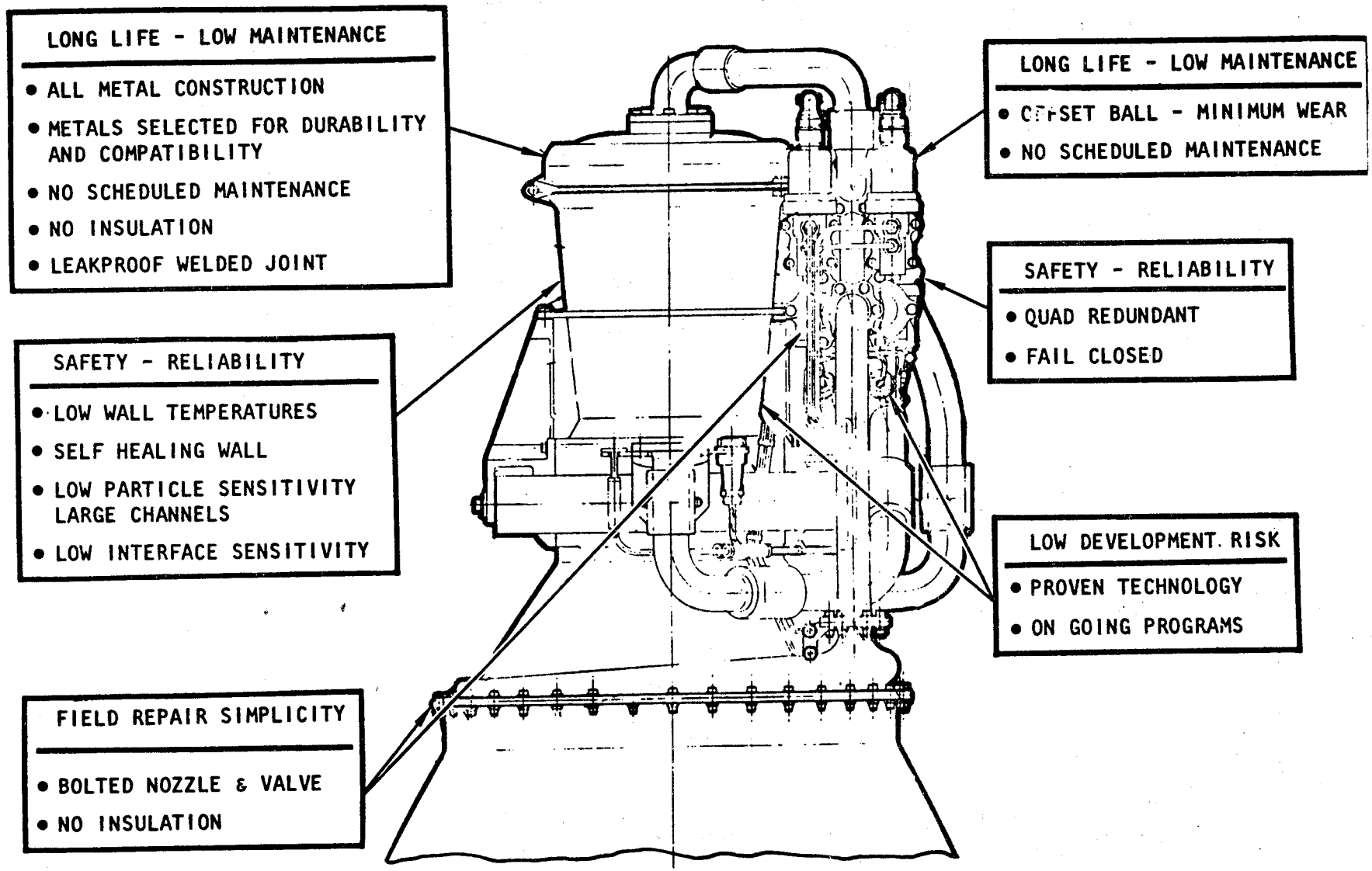

Rocketdyne
North American Rockwell

Figure 5. OME THRUST CHAMBER ASSEMBLY DEMONSTRATOR CONFIGURATION

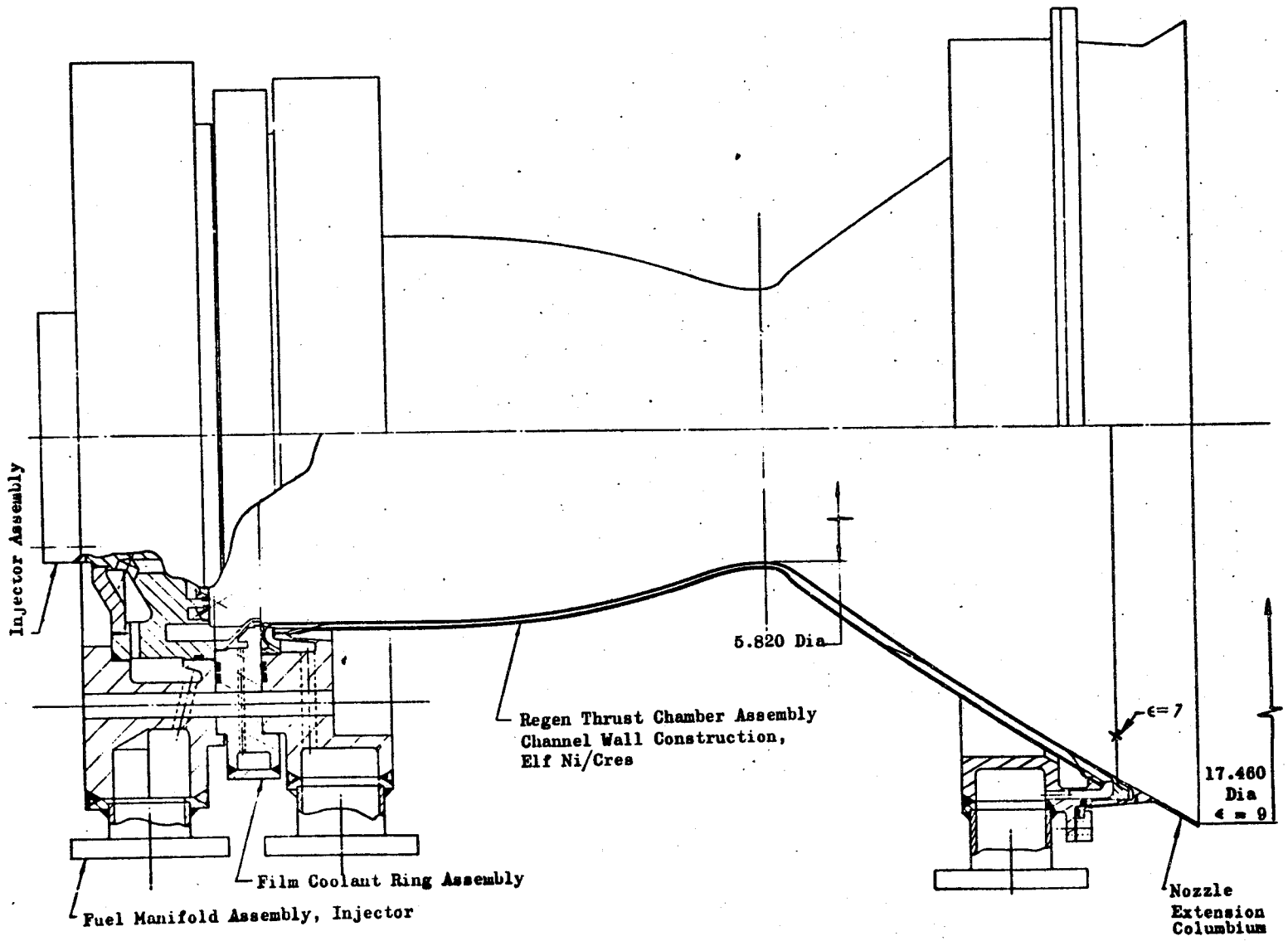

Predicted performance of both the flight and demonstrator thrust chamber assemblies are shown in Table 4 and the pressure budgets in Table 5. The coolant jacket pressure drop of the demonstrator chamber is identical to that of the flight configuration. The demonstrator fuel volumes are greater than that of the flight configuration because of the greater flexibility designed into the demonstrator to provide for injector and film coolant ring changes and to permit testing with separate flows to the coolant jacket and injector. The volume difference primarily effects the start transient and will be compensated for during the demonstrator test program by sequencing of the propellant valves.

Materials for the flight and demonstrator thrust chamber assemblies are shown in Table 6. Thus, the propellant compatibility, thermal expansion effects, and operating stress levels experienced by the demonstrator chamber will be identical to that of the flight configuration.

The head end configuration of the flight chamber is shown in Fig. 6. The CRES film coolant ring forms a part of the acoustic cavity and also directs film coolant from the regenerative coolant jacket to the injector. The ring is EB welded to the CRES liner and nickel is electroformed over the liner/ring assembly. The injector and manifold are then EB welded in place. All welds are inspectable and no weld is required to seal hot gases from the chamber directly. The head end configuration of the demonstrator chamber is shown in Fig. 7. Fuel flows from the regenerative coolant jacket collector manifold to the transfer manifold into the injector and film coolant manifolds by transfer tubes. The injector fuel transfer tube is shown in the figure. Fuel from the regenerative coolant jacket is dumped during the bypass mode of operation. Double seals are used to prevent hot gas leakage during operation of the bolted assembly. As in the flight configuration, the nickel is bonded to the CRES at all points during the electroforming operation. No weld or braze joint of the two dissimilar metals is required.

The flight and demonstrator nozzle joint configurations are shown in Fig. 8 and 9 respectively. The bolted assembly facilitates shipping of the engine and allows simple replacement of the nozzle if damaged during ground operations. Columbium

Table 4. OME SPECIFIC IMPULSE

	FLIGHT	DEMONSTRATOR
NOZZLE AREA RATIO	72	9
TDK SPECIFIC IMPULSE (ADJUSTED FOR δ *), SEC	326.7	274.8
TDK FLOWRATE (ADJUSTED FOR δ *), LB/SEC	19.19	19.19
VAPORIZED MASS FLOWRATE, LB/SEC	18.84	18.84
INVISCID FLOW THRUST, LB	6128.3	5154.1
BOUNDARY LAYER THRUST DECREMENT, LB	-128.5	-58.5
THRUST CHAMBER THRUST, LB	6000	5097
THRUST CHAMBER SPECIFIC IMPULSE, SEC	312.7	265.7

17

Table 5. OME PRESSURE BUDGET

FLIGHT CONFIGURATION				DEMONSTRATOR	
OXIDIZER	FUEL	OXIDIZER	FUEL	OXIDIZER	FUEL
211*	211*	$P_{Engine\ Inlet}$			
15	16	$\Delta P_{Feed\ \&\ Valve}$			
196	195	$P_{T/C\ Inlet}$		196	198
	17	ΔP_{Jacket}			17
3	2	$\Delta P_{Inj.\ Man.}$		3	5
62	45	$\Delta P_{Inj.\ Orifice}$		62	45
131		$P_{Chamber(Inj.\ End)}$		131	
6		$\Delta P_{Chamber}$		6	
125		$P_{Chamber\ (Nozzle\ Stag.)}$		125	

* SPACE DIVISION

18

Table 6. THRUST CHAMBER ASSEMBLY MATERIAL SELECTION

COMPONENT	FLIGHT CONFIGURATION	DEMONSTRATOR CONFIGURATION
INJECTOR	321 CRES	304L CRES
THRUST CHAMBER LINER	321 CRES	321 CRES
THRUST CHAMBER SHELL	ELECTROFORMED NICKEL	ELECTROFORMED NICKEL
NOZZLE EXTENSION	DISILICIDE COATED COLUMBIUM/ TITANIUM (ϵ = 38)	DISILICIDE COATED COLUMBIUM

Figure 6. FLIGHT HEAD-END CONFIGURATION

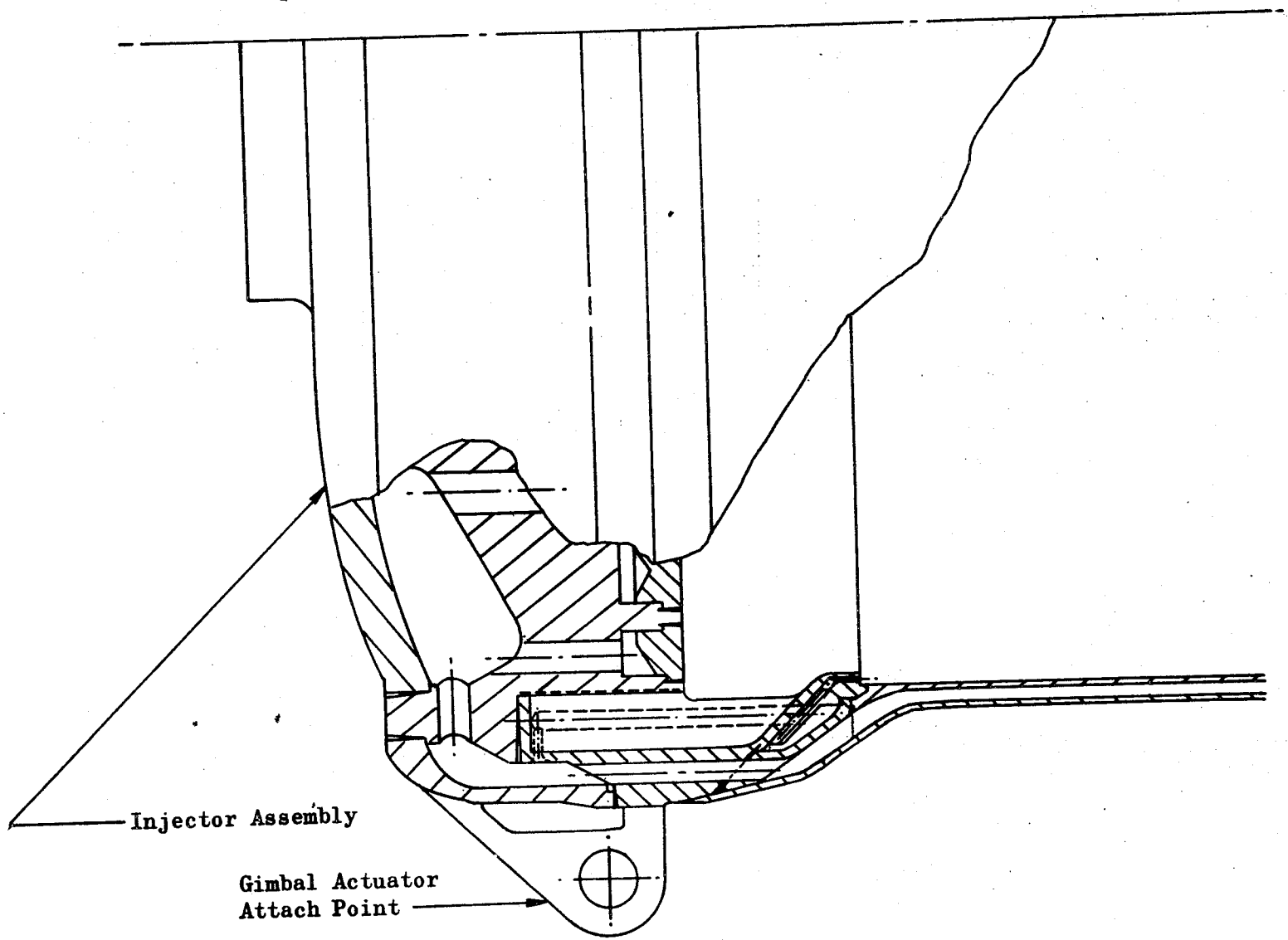

Figure 7. DEMONSTRATOR ENGINE HEAD, END CONFIGURATION

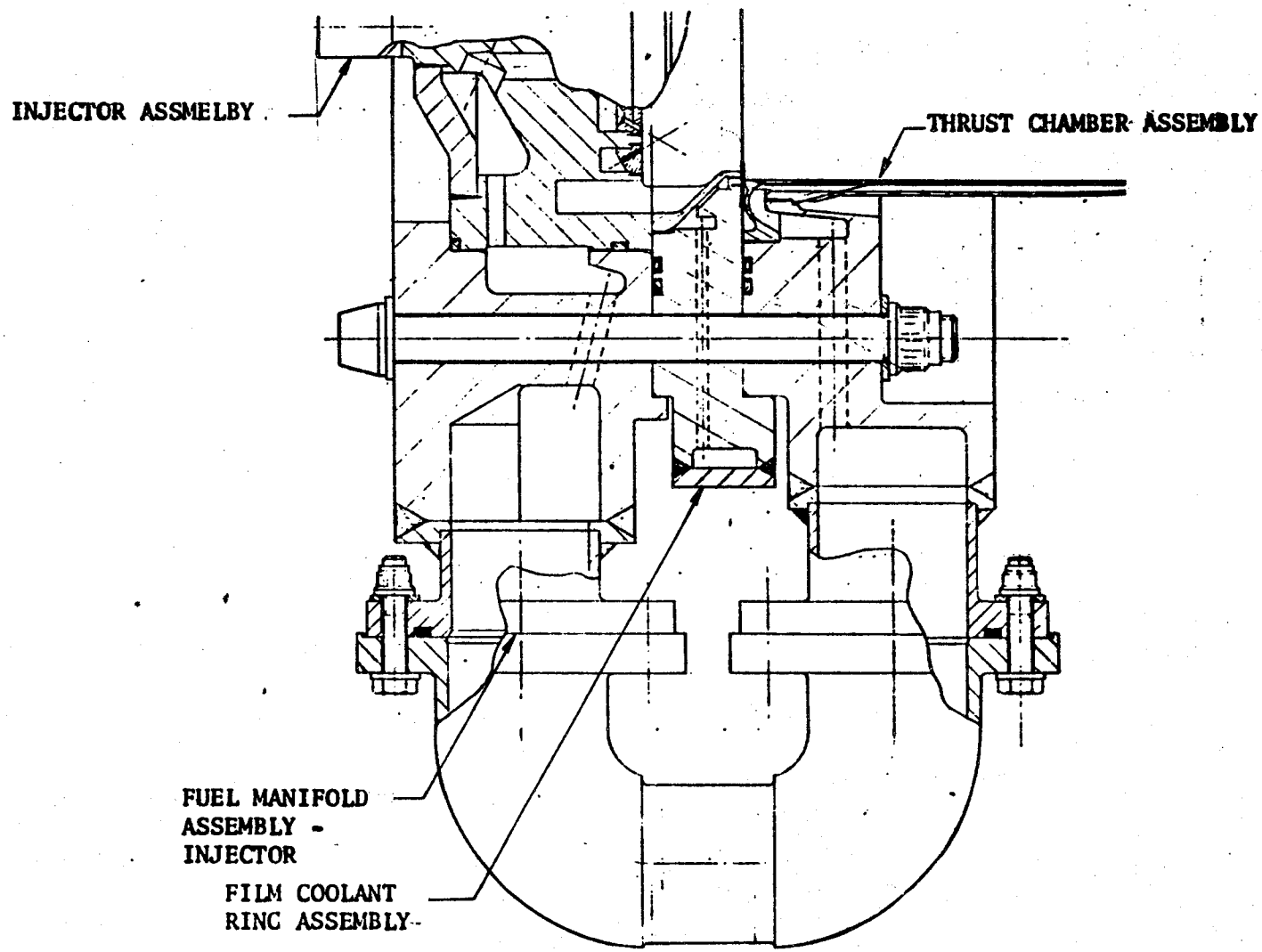

14

Figure 8. **FLIGHT ENGINE NOZZLE JOINT CONFIGURATION**

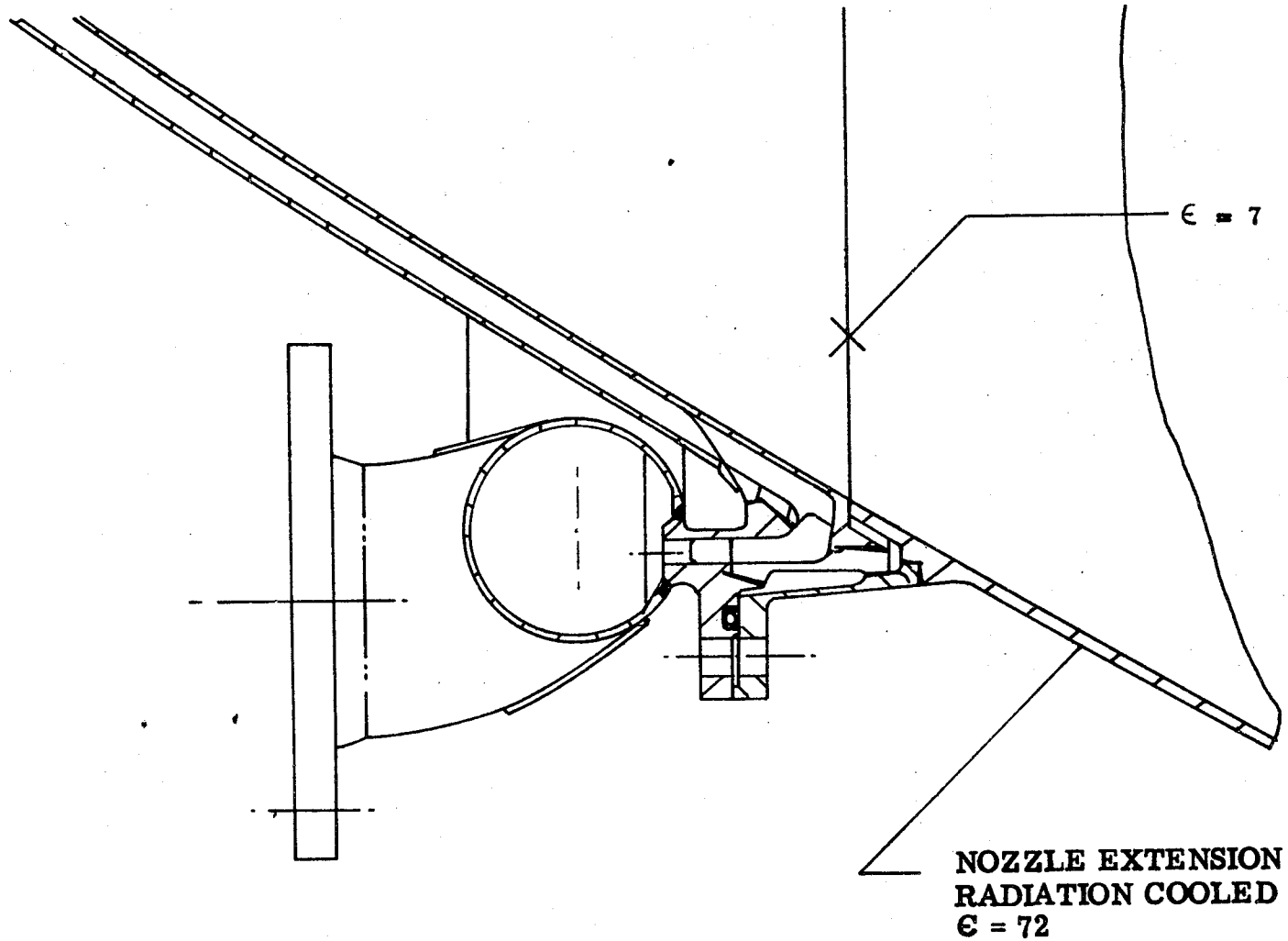

FIGURE 9. DEMONSTRATOR ENGINE NOZZLE JOINT CONFIGURATION

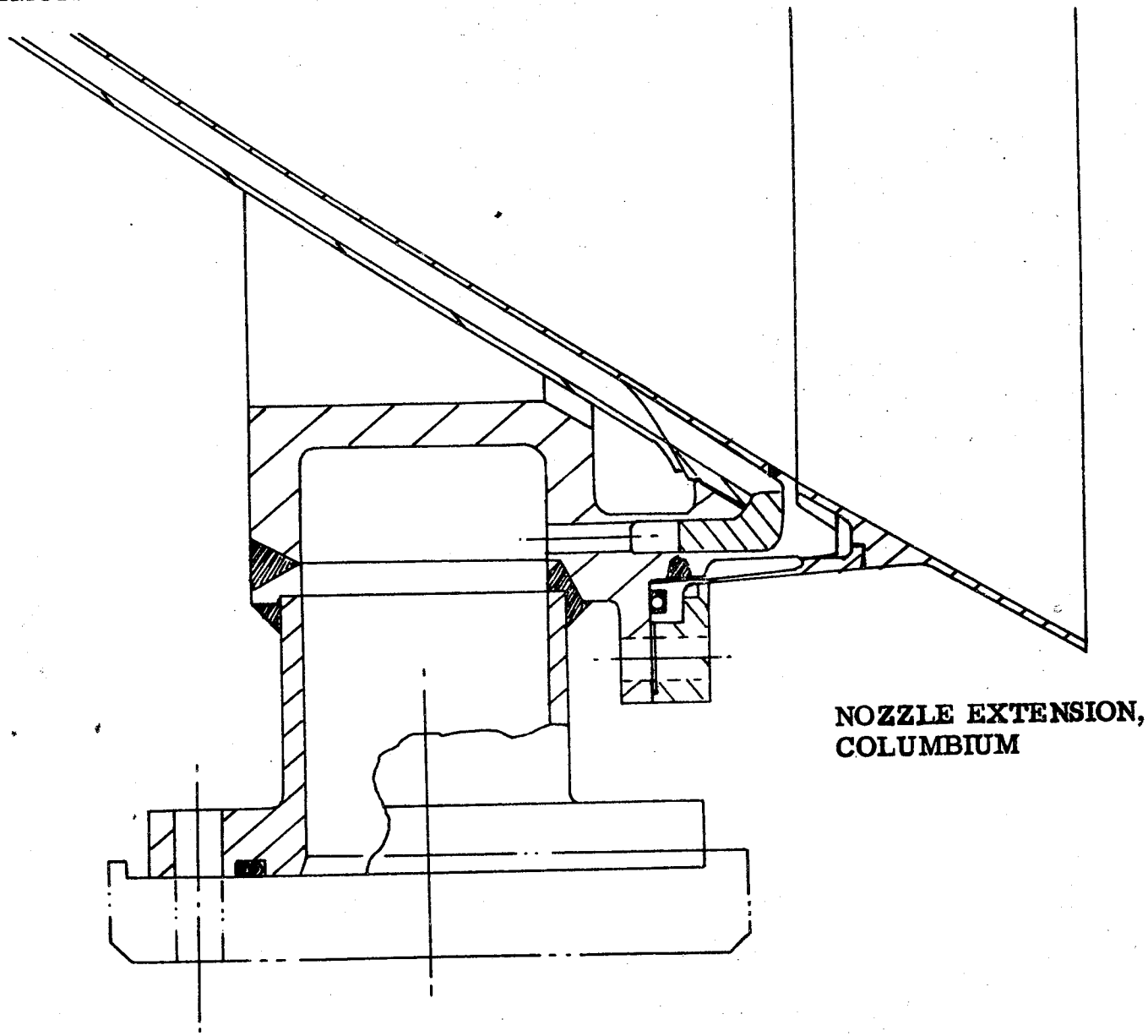

16

(WC-103) is used for the nozzle at the joint to permit high temperature operation and minimize the area ratio at which the attachment takes place. The nozzle is coated inside and outside with a 0.003 inch thickness of silicide to increase durability and enhance radiation emissivity. A metal O-ring seal is used between the regenerative and radiation nozzle sections. A tolerance allowance is made for the thermal growth of the radiation nozzle during operation. The flight nozzle is 0.030 inches thick at the attached point compared to 0.050 inches for the demonstrator nozzle. The mass and thickness distribution of the demonstrator nozzle downstream of the joint results in a soakback transient which is similar to that of the flight nozzle. The regenerative coolant inlet manifold on the demonstrator chamber is simpler than that of the flight version although heavier.

THRUST CHAMBER DESIGN DETAIL SELECTION

The area ratio at which the transition from regenerative to radiation cooling is made is determined by the radiation cooling capability of the nozzle as shown in Fig. 10. An operating temperature of 2400 F is assigned to the Columbium nozzle and results in an attached area ratio of 7 at a chamber pressure of 125 psia. The transition from Columbium to titanium takes place at 1600 F at an area ratio of 38.

The chamber contraction ratio selection is based on consideration of vaporization efficiency, auxiliary film coolant flow requirements, and the attendant performance losses, pressure budget factors, engine weight effects, and stability characteristics as expressed in Table 7. and Fig. 11. The vaporization efficiency increase as the contraction ratio is increased is based on company-sponsored injector test results. Film coolant flow requirements decrease with increasing contraction ratio because of the reduced heat flux in the combustor. This effect also reduces the regenerative coolant jacket pressure drop requirements and the pressure drop of the combustion gases in the chamber decreases. Increasing the contraction ratio increases the weights

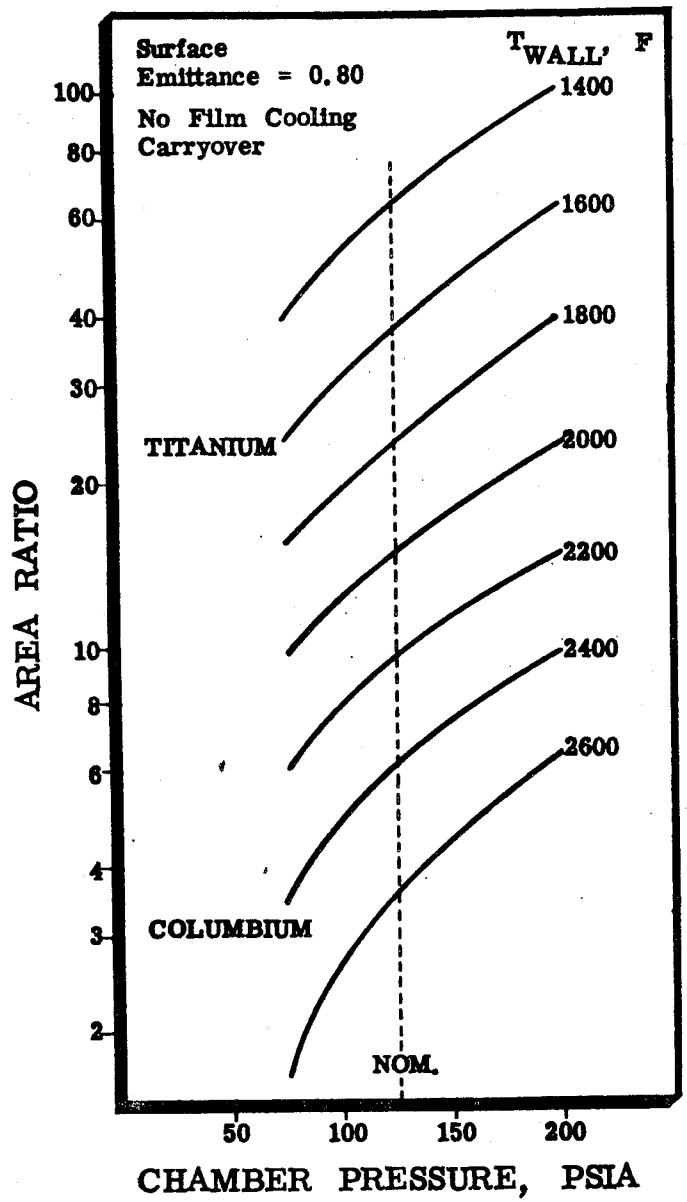

Figure 10

EFFECT OF CHAMBER PRESSURE AND WALL TEMPERATURE ON RADIATION NOZZLE ATTACH POINT

22

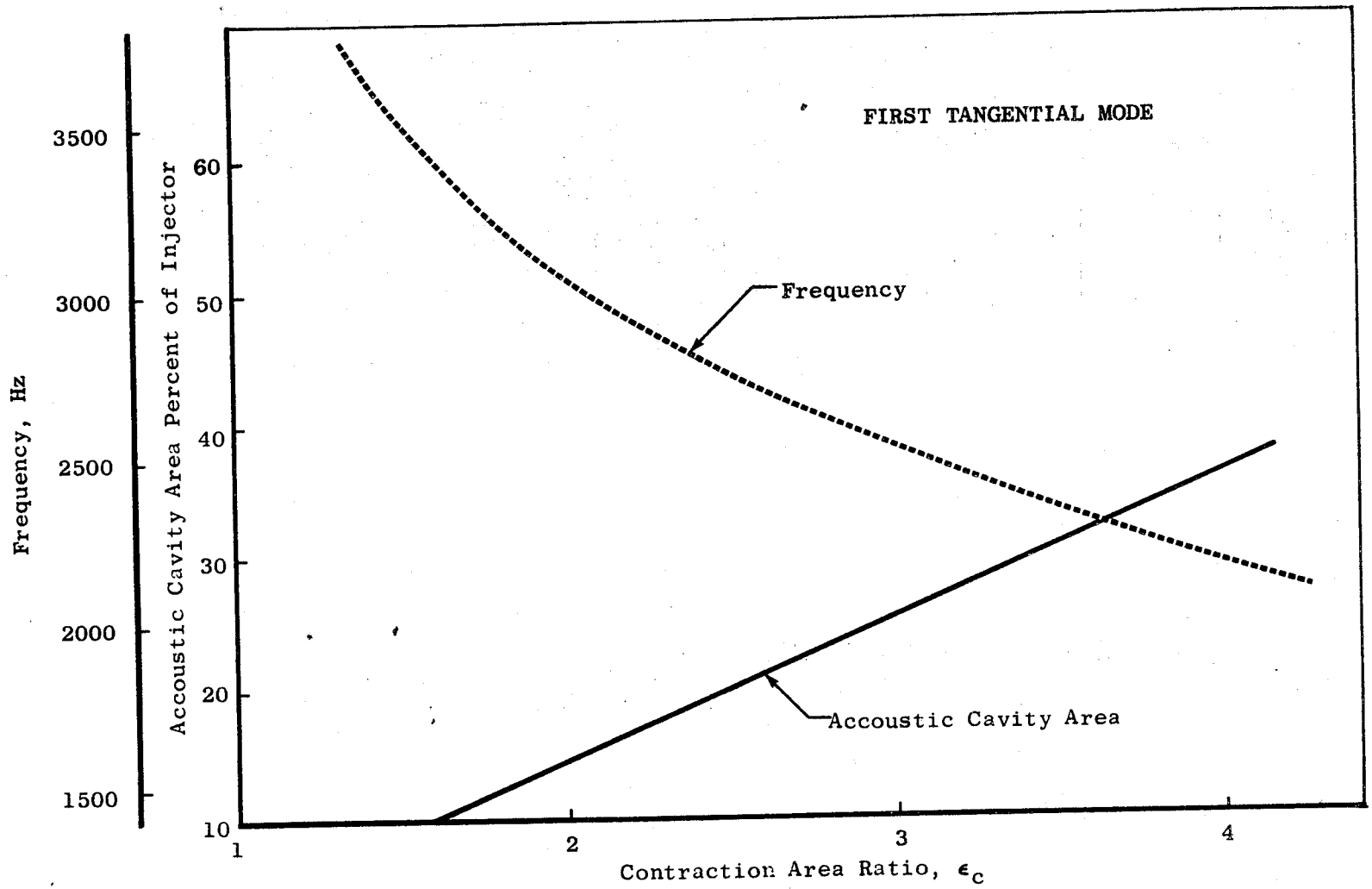

Figure 11 . Variation of Chamber Natural Frequency with Contraction Area Ratio

Table 7. **CONTRACTION RATIO SELECTION**

ϵ_C	D_{INJ}, IN.	η_{C^*VAP}	$\Delta I_{S_{vap}}$, SEC	$\%\dot{W}_C$	ΔI_{S_C}, SEC	ΔP COMB. PSI	ΔP RGEN. PSI	$\Delta I_{S_{\Delta P}}$, SEC	ΔW_{ENG}, LB	ΔI_{S_W}, SEC	$\Sigma \Delta I_S$, SEC
1.5	7.1	0.986	-0.3	2.9	-0.3	12.0	21	-1.3	-15.1	+0.7	-1.2
2	8.2	0.987	Ref	2.4	Ref	6.3	17	Ref	Ref	Ref	Ref
3	10.0	0.989	+0.6	1.6	+0.3	2.8	16	+0.6	+37.2*	-1.6	-0.1

* INCLUDES BAFFLES

CONCLUSION: $\epsilon_{OPT} \approx 2.3$, $\Sigma \Delta I_s = 0.2$ SEC ABOVE REFERENCE

RECOMMENDATION: USE $\epsilon_C = 2$ TO AVOID BAFFLES

of the combustor, injector, gimbal ring, and ducting. Combination of all of these effects indicates that the contraction ratio of 2 provides higher equivalent performance than either the contraction ratios of 1.5 or 3.

The natural frequency in the first tangential mode of a thrust chamber is shown as a function of the contraction ratio in Fig. 11. The lower the natural frequency, the more susceptible the chamber is to acoustic instabilities and the larger the acoustic cavity must be to effectively suppress them. Thus, stability considerations tend to drive the contraction ratio to lower values. Baffles can be installed at the expense of complexity and weight.

[illegible] bulk [illegible]

The regenerative coolant bulk temperature safety factor is described in Table 8. The factor is applied to the most severe conditions that the coolant will experience. This occurs at off-design conditions where the propellant temperature is the highest, chamber pressure is the lowest, and mixture ratio is the highest. The minimum subcooling occurs at the injector discharge location where the temperature is the highest and the pressure is the lowest. Long combustor lengths and low film coolant flow-rates tend to decrease the subcooling as shown in Fig. 12. Thus these two parameters may be traded off against each other at a constant value of subcooling as in Fig. 13. Variations in the injector-to-throat length effect the vaporization efficiency of the engine and changes in the film cooling flowrate effect the stratification losses. The combined effects of both parameters on the delivered specific impulse are shown in Fig. 14. Optimization of combustor length based on delivered specific impulse in a fixed length engine is shown in Fig. 15. Inclusion of engine weight and inlet pressure has a small effect on the optimization as indicated in Fig. 16. Performance variations are quite small for lengths ranging from 14 to 17 inches.

The final dimensions and contour for the regeneratively cooled demonstrator thrust chamber are shown in Fig. 17. The large contour convergent radius, R_2, was a compromise between preventing excessive reductions in the local

Table 8. REGENERATIVE COOLANT SAFETY FACTORS

- MAXIMUM COOLANT TEMPERATURE MAINTAINED BELOW BULK BOILING POINT (I. E., MINIMUM SUBCOOLING)
  - MINIMUM ΔT_{SUB} = 50F BASED ON EXISTING DATA
  - MINIMUM ΔT_{SUB} OCCURS IN INJECTOR AT OFF-DESIGN CONDITIONS*
  - USED IN DETERMINING COMBUSTOR LENGTH AND SUPPLEMENTAL FILM COOLANT FLOWRATE

* OFF-DESIGN CONDITIONS: T_{in} = 90F, P_c = 112 psia, MR = 1.85

Figure 12. INFLUENCE OF COMBUSTOR LENGTH AND FILM COOLANT ON BULK TEMPERATURE RISE

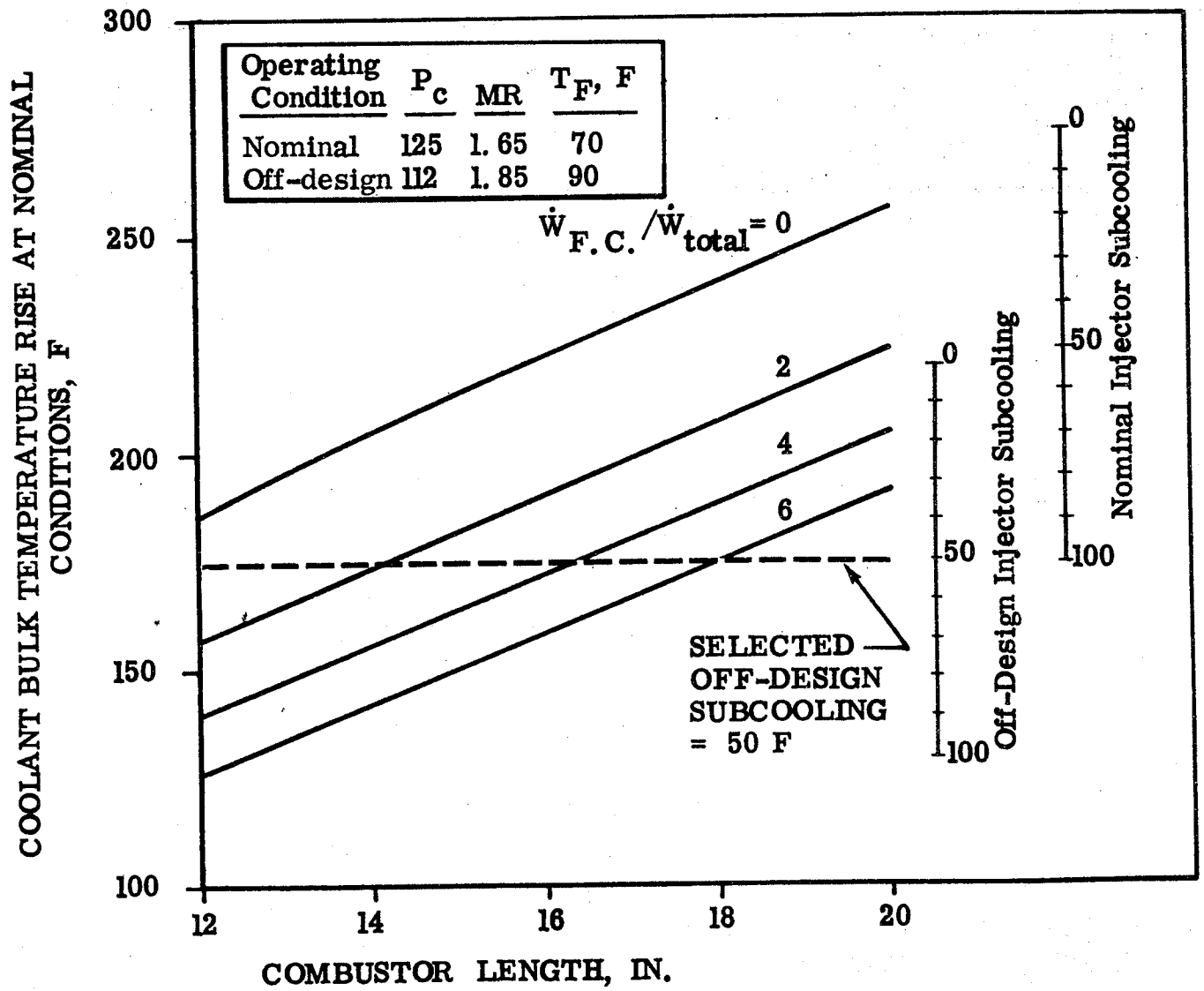

27

Figure 13. SUPPLEMENTAL FILM COOLANT REQUIREMENTS AS A FUNCTION OF TOTAL COMBUSTOR LENGTH

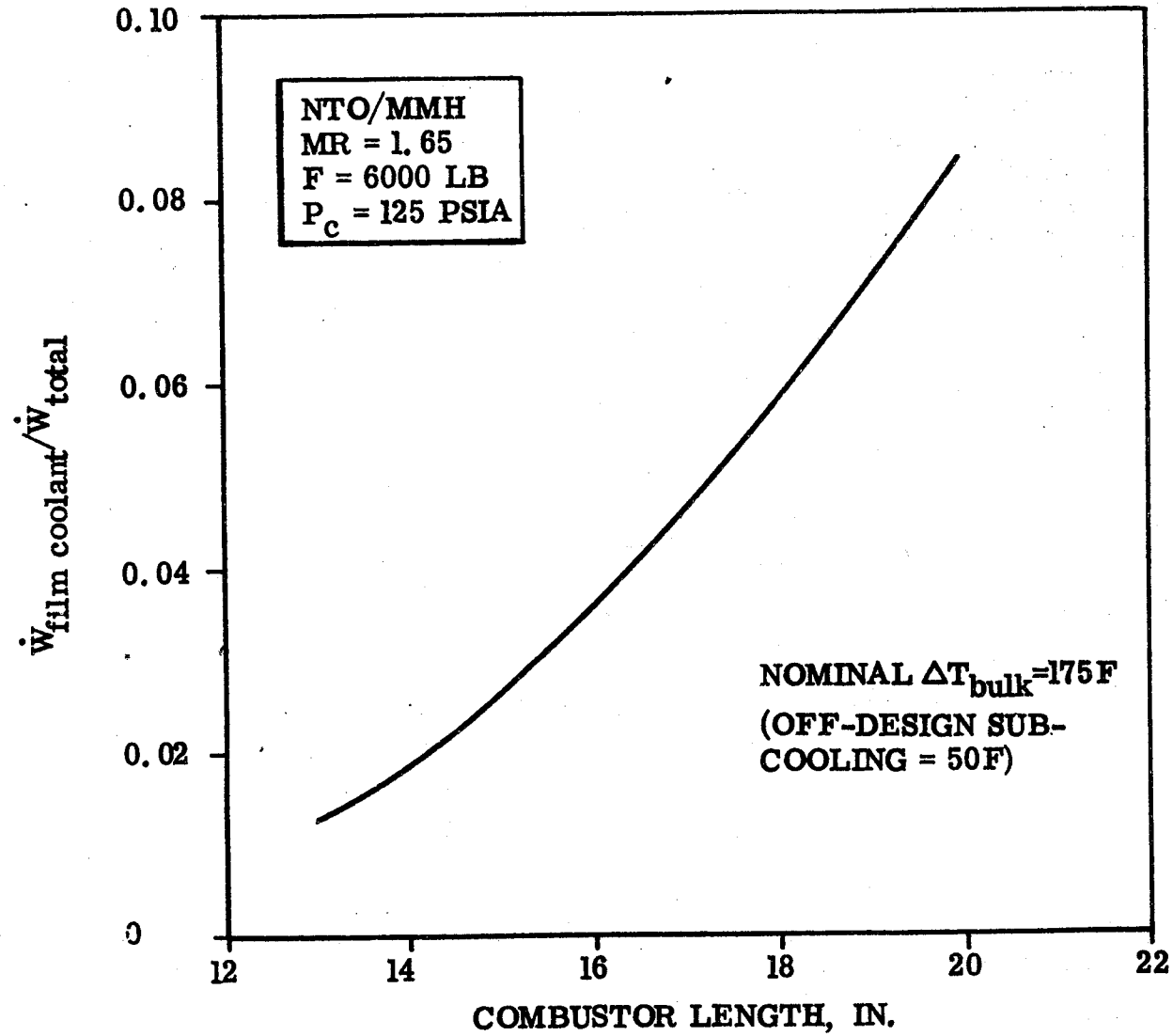

28

Figure 14. EFFECT OF COMBUSTOR LENGTH AND FILM COOLANT FLOW ON OME PERFORMANCE

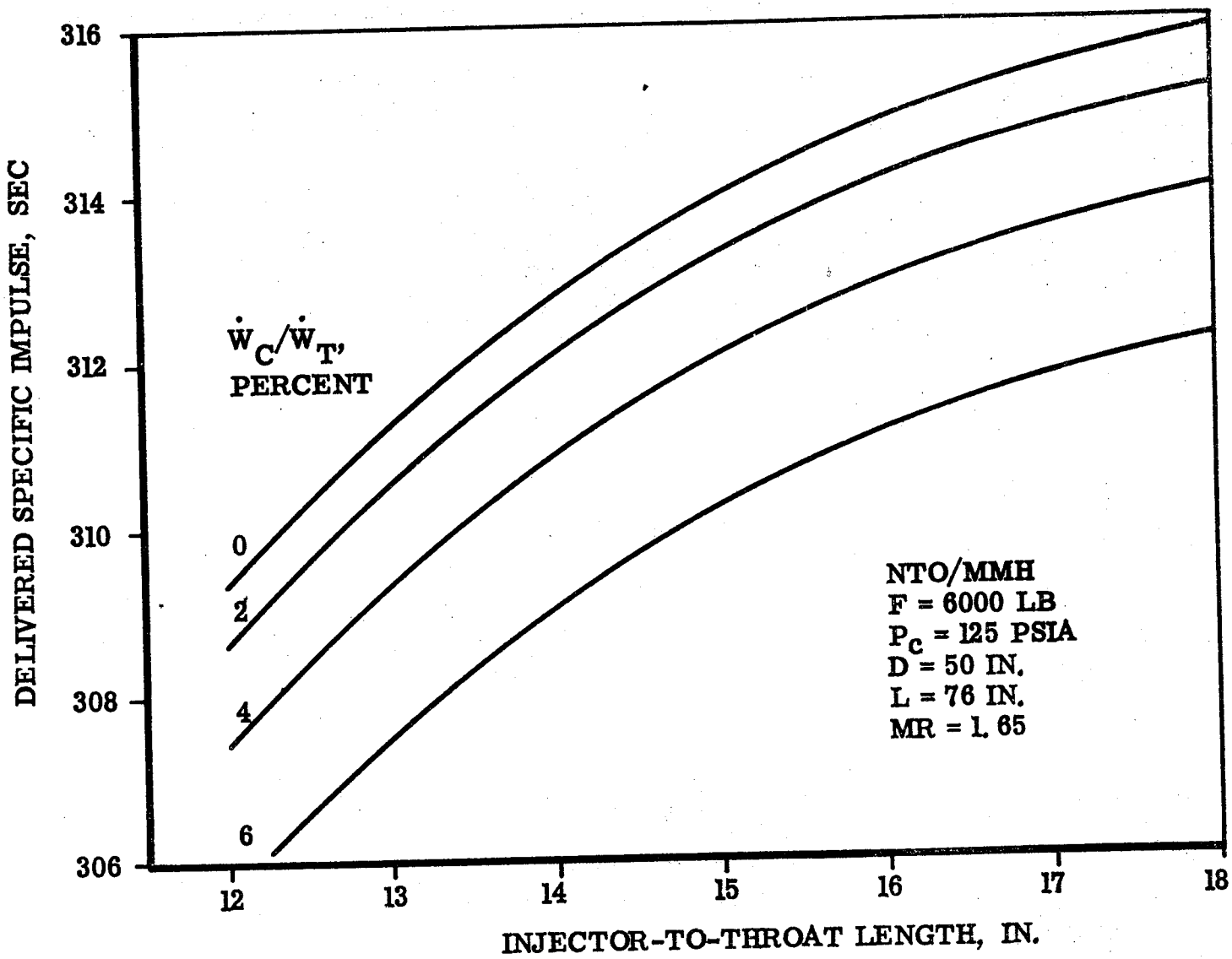

30

Figure 15. PERFORMANCE OF FIXED ENVELOPE SYSTEM

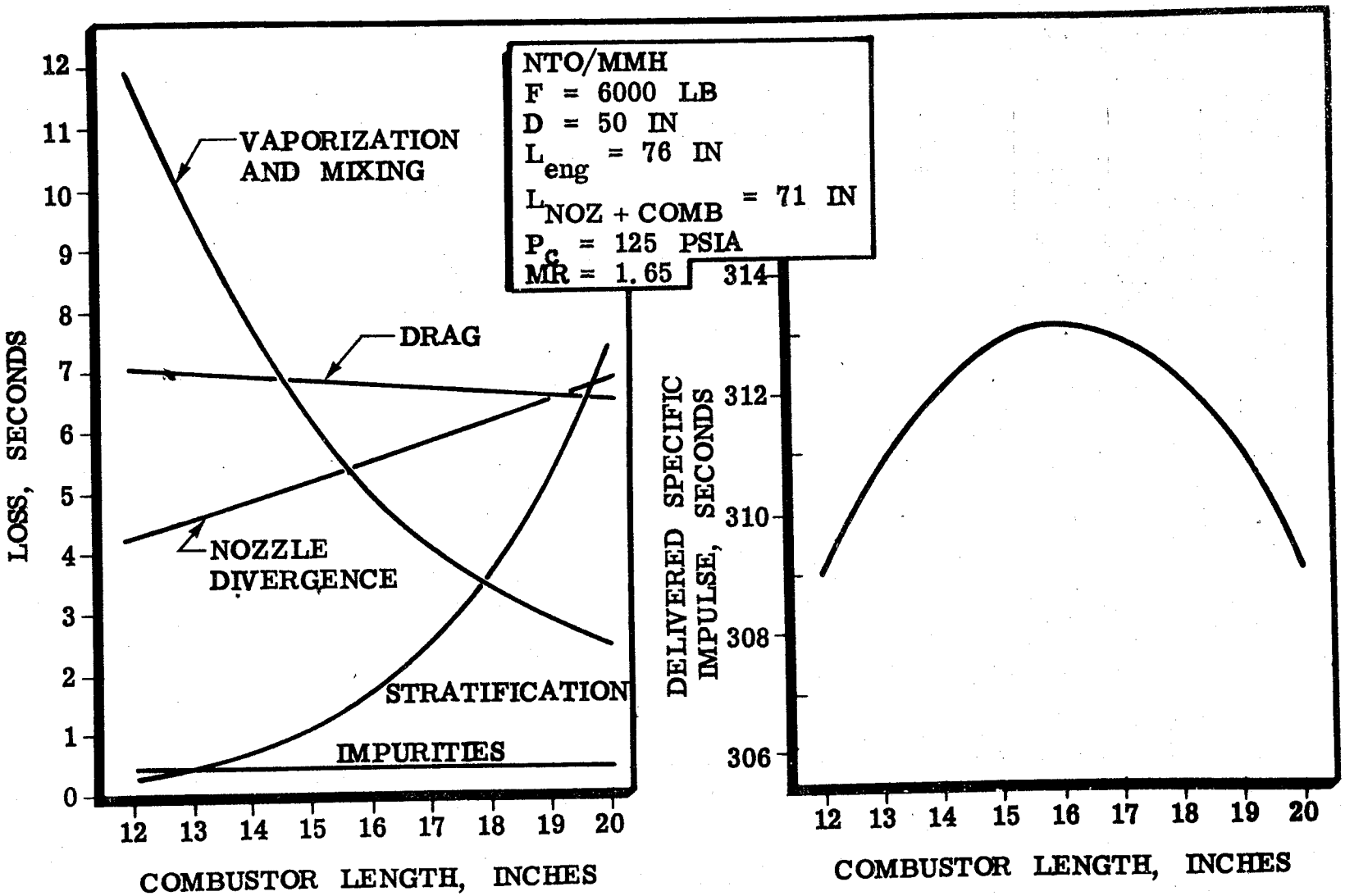

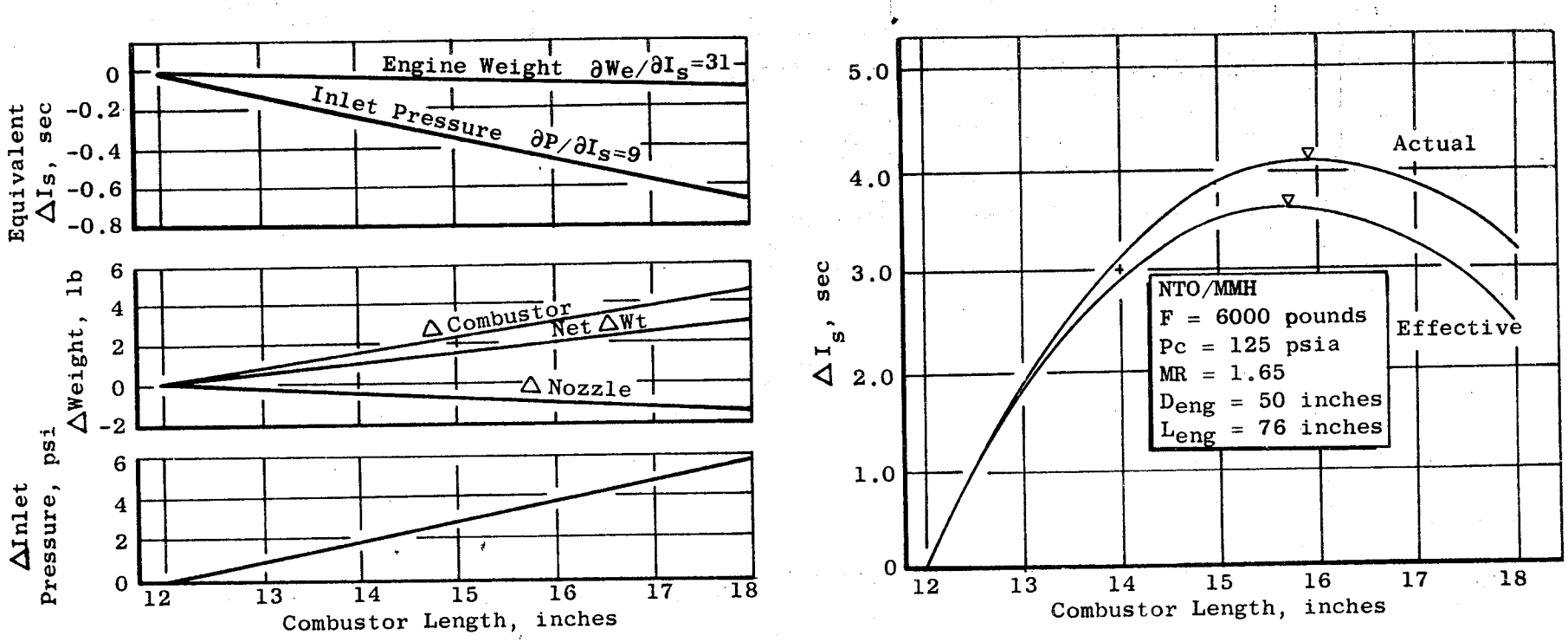

Figure 16 . Combustor Length Optimization including Engine Weight and Inlet Pressure Effects

Figure 17. SS/OME DEMONSTRATOR CHAMBER CONTOUR

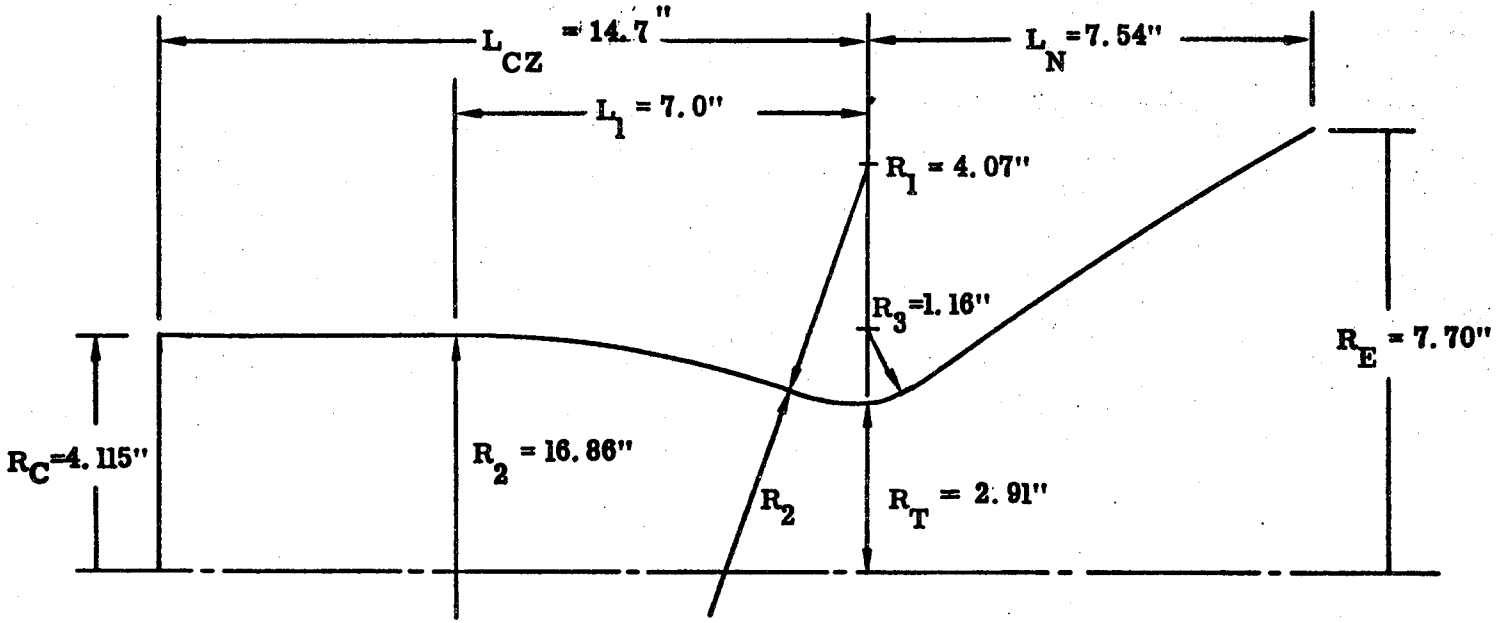

COMBUSTOR GEOMETRY

L_1 BASED ON MINIMUM LIKELY TEST LENGTH

R_T BASED ON F=6K, P_c=125 PSIA

R_C BASED ON CONTRACTION RATIO = 2:1

R_1/R_T (= 1.4) COMPROMISE OF HEAT TRANSFER (LOW ΣQ) AND AERODYNAMICS (HIGH DISCHARGE COEFFICIENT)

R_2/R_T SELECTED TO MINIMIZE TURNING OF COMBUSTION GASES

NOZZLE GEOMETRY

R_3/R_T (= 0.4) SELECTED TO PROVIDE FOR POSSIBLE COOLANT CURVATURE ENHANCEMENT

L_N, R_E BASED ON RADIATION ATTACH POINT AT AREA RATIO = 7:1

NOZZLE CONTOUR: TRUNCATED 70% LENGTH PARABOLIC OPTIMUM BELL CONTOUR TO AREA RATIO = 72 BASED ON EXIT DIAMETER = 50 INCHES

contraction area ratio and providing a gradual turn to enhance boundary layer buildup. The throat approach radius, R_1, was selected by again avoiding large regions of low contraction area ratio while at the same time avoiding too rapid a turn at the throat which would decrease the aerodynamic discharge coefficient. The value of the downstream throat contour radius, R_3, was based on considerations of fabrication, coolant enhancement due to high curvature, and maintaining a low area in the high heat flux region.

Having selected the contour, the alternatives of the flow configuration and the wall construction were evaluated. Tube wall, channel wall, and double wall construction were considered. Channel wall was selected in preference to tube wall construction. Heat load is an important consideration in this design and the tube wall has a greater surface area because of the curvature of the tubes. The tube wall chamber also presents potential hot gas leak paths where the tubes are brazed together. The time and cost of fabricating dies for the tube wall chamber would favor the channel wall from the standpoints of development flexibility and development economy. Double wall construction is similar to the channel wall construction except that the inner and outer walls are joined only at the injector and exit ends. Analysis has indicated that the channel wall construction would have a greater life expectancy than the double wall construction.

The selected flow path was an uppass configuration with the coolant entering at an area ratio of 7, flowing through the throat and combustor regions, and exiting directly into the integral manifold of the injector. The downpass configuration has the additional complexity of a return tube to conduct the coolant from the nozzle to the injector at one or more points and the added complexity and weight of the separate injector fuel manifold. A one and one-half pass configuration with the coolant entering the nozzle near the throat region, flowing to the nozzle exit, and then returning through the nozzle, throat region, and combustor region, and discharging into the injector was also considered. This configuration would be more expensive to fabricate and would have a slightly higher pressure drop than the uppass configuration.

The channel geometry and wall thicknesses were next determined. The hot wall thickness is determined primarily from thermal fatigue considerations. The hot wall gas side surface temperature increases as the wall thickness is increased while the outer surface of the closeout is not affected as shown in Fig. 18. The difference between these two temperatures influences the life of a chamber. As the hot wall thickness is reduced, the closeout thickness is also reduced in order that the strains may be balanced between the hot inner wall and the cold outer wall. Reducing the thicknesses in this manner results in increasing life as shown in Fig. 18. However, the closeout thickness cannot be reduced much below 0.030 inches because of pressure considerations and the life decreases for hot wall thicknesses below 0.030 inches. The value of 0.030 was therefore selected as the thickness for both the hot wall and the cold wall.

The selection of the actual number of channels and the channel geometry are based on two-dimensional conduction considerations as shown in Fig. 19. This geometry is most critical in the injector region where the heat fluxes are reasonably high and the land width is considerably greater than at the throat position. Specifying the minimum land width and the number of channels essentially specifies the channel width. The ordinate in Fig. 19 is the maximum heat flux to a channel calculated by two dimensional analysis compared to that calculated by one dimensional analysis. Since a two dimensional analysis is more realistic, it is desirable to have as low a value of this parameter as possible. It can be seen from the figure that reducing the land width reduces the value of the parameter. Hence a land width of 0.040 inches was selected based on fabrication ease and convenience.

Having selected the land width, it is seen that increasing the number of channels reduces the heat flux. However, the number of channels must be increased from the selected value of 180 to approximately 250 in order to effect a 5 percent decrease in the heat flux. Reducing the number of channels would simplify fabrication but would induce additional pressure stresses into the hot and cold walls. Furthermore, a square channel provides the greatest hydraulic radius for a given cross sectional area and the selected number of channels result in a nearly square geometry in the throat region where the pressure drop is concentrated.

Figure 18. EFFECT OF WALL THICKNESS ON WALL TEMPERATURE AND FATIGUE LIFE

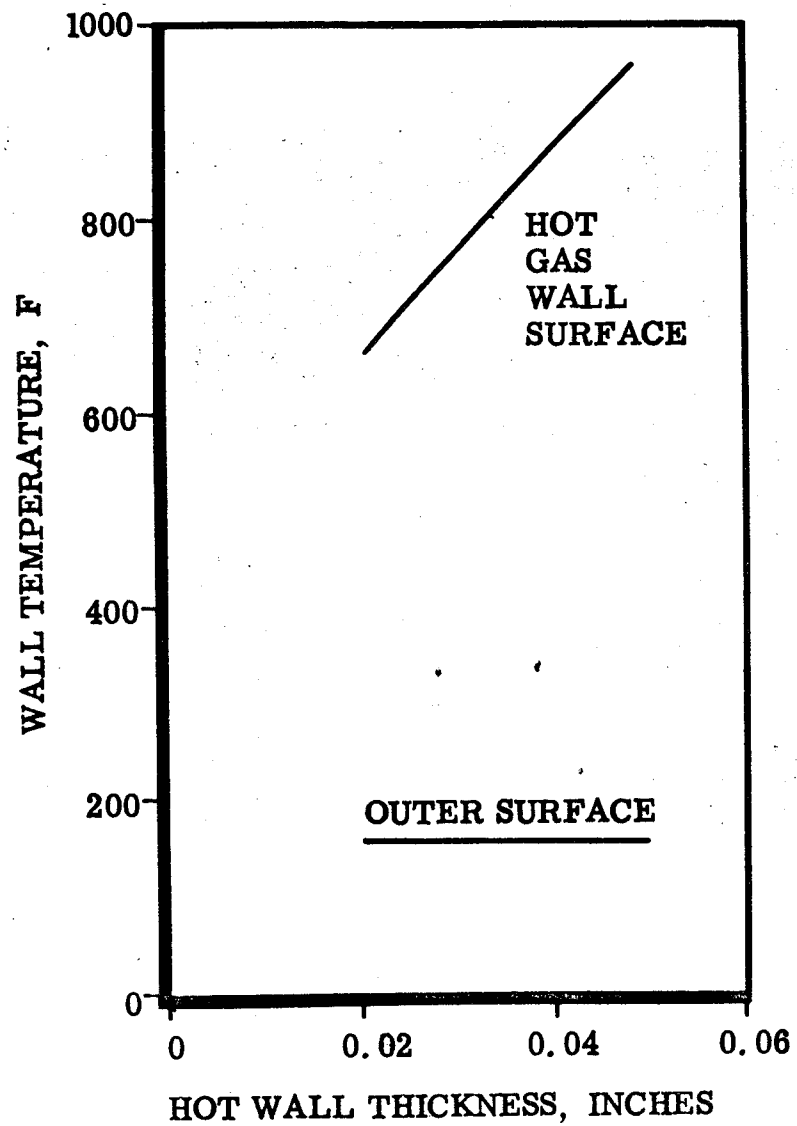

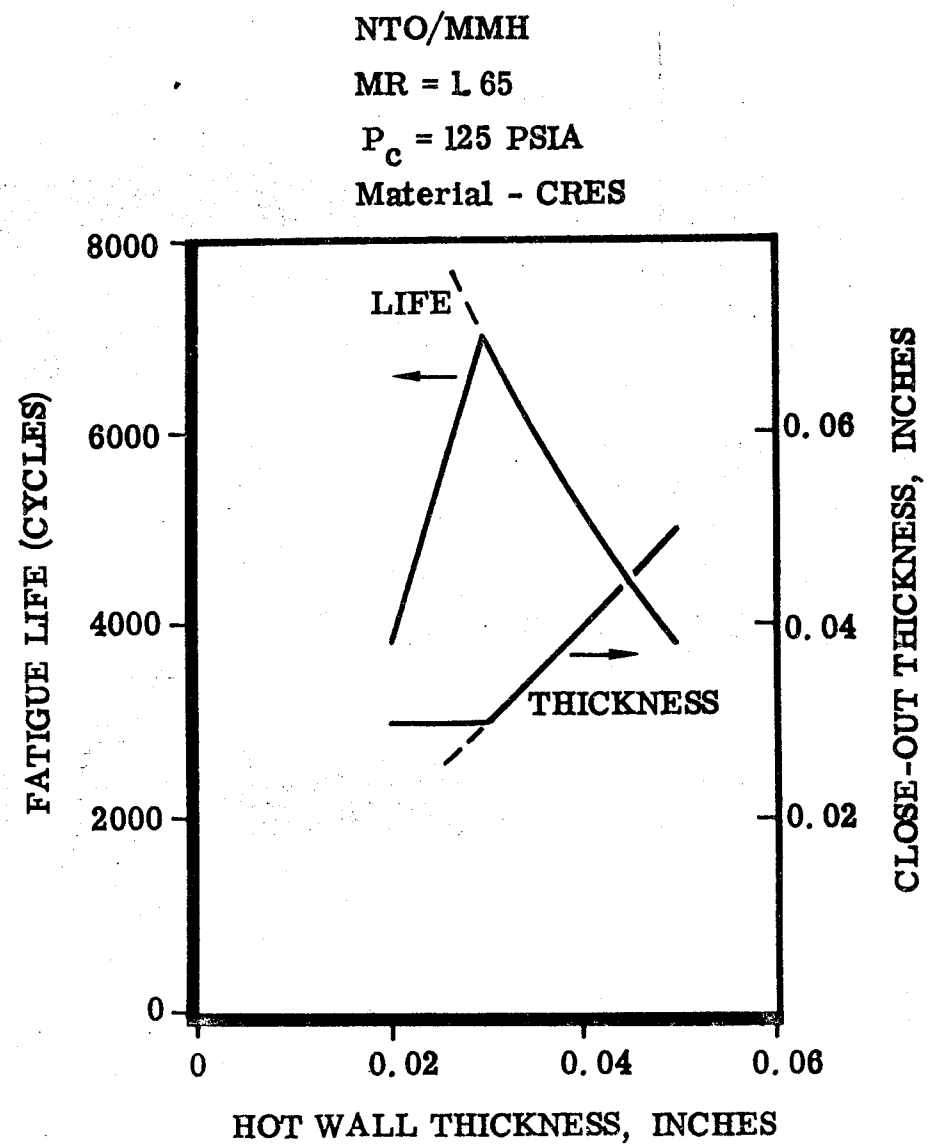

34

Figure 19. EFFECT OF CHANNEL GEOMETRY ON THE RELATIVE INJECTOR END COOLANT SIDE HEAT FLUX

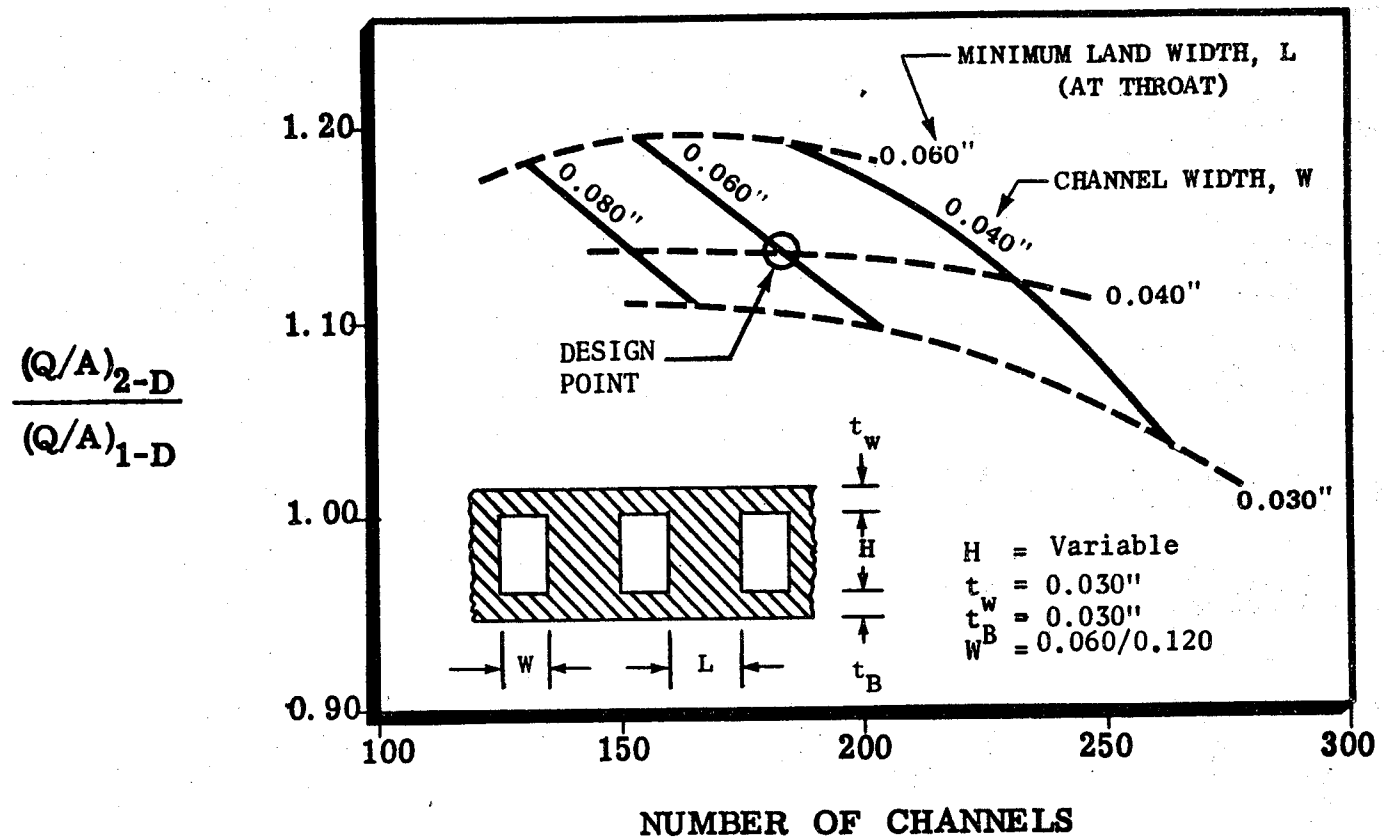

THERMAL CHARACTERISTICS

The safety factors applied to the channel geometry design are shown in Table 9. The required coolant velocity at each point is such that the burnout heat flux capability will always be at least twice the expected value at nominal design conditions and will be at least 1.5 times the expected value at all points in the chamber for the extreme off-design conditions. The predicted burnout heat flux is shown as a function of the local coolant velocity and subcooling in Fig. 20. These curves were based on experimental data from contract and IR&D heated tube test programs. The predicted heat flux profile (Fig. 21) was derived from tests with a solid-wall chamber and results in the coolant bulk ture profile shown in Fig. 22 which, together with the local pressures, determines the coolant subcooling profile through the chamber. The predicted heat flux profile, the subcooling profile, and the cooling correlations result in specification of the coolant velocity profile.

The channel height profile shown in Fig. 23 is that which results after such other restrictions as minimum coolant velocity and maximum channel height have been imposed. A minimum coolant velocity of 5 feet per second and a step change in the channel width from 0.06 to 0.12 inches in the nozzle to reduce channel height and nozzle weight were specified for final design. The channel height was limited to 0.175 inches. The resulting coolant velocity and wall temperature profiles are shown in Fig. 24 and 25, respectively. At no point does the wall temperature exceed 800 F. The wall temperature in the combustor region is generally less than 650 F.

Total and static pressure profiles resulting from the selected geometry are shown in Fig. 26. In addition to these pressure losses a loss of 1 psi is assigned to the inlet manifold and 1 psi to the turning of the flow from the coolant jacket into the injector. The resulting safety factor profiles at nominal conditions and at the most severe off design conditions are shown in Fig. 27. These safety factor profiles include the two dimensional effects which are most prominent in the injector region.

Table 9. REGENERATIVE COOLING DESIGN SAFETY FACTORS

- LOCAL COOLANT HEAT FLUX CAPABILITY MAINTAINED GREATER THAN LOCAL IMPOSED HEAT FLUX LEVEL - PREVENT TRANSITION TO FILM BOILING (I. E., BURN-OUT)
  - MINIMUM SAFETY FACTOR: $\frac{(Q/A)_{burn\text{-}out}}{(Q/A)_{local}} = 2.0$ AT NOMINAL DESIGN**
  - MINIMUM SAFETY FACTOR ≈ 1.5 AT EXTREME OFF-DESIGN CONDITIONS*
  - LOCAL SAFETY FACTOR USED TO DETERMINE REQUIRED VELOCITY AND CHANNEL HEIGHT PROFILE

* OFF-DESIGN CONDITIONS: $T_{in} = 90F$, $P_c = 112$ psia, MR = 1.85

** NOMINAL DESIGN CONDITIONS: $T_{in} = 70F$, $P_c = 125$ psia, MR = 1.65

Figure 20. EXPERIMENTAL BURNOUT HEAT FLUX CORRELATION FOR MMH

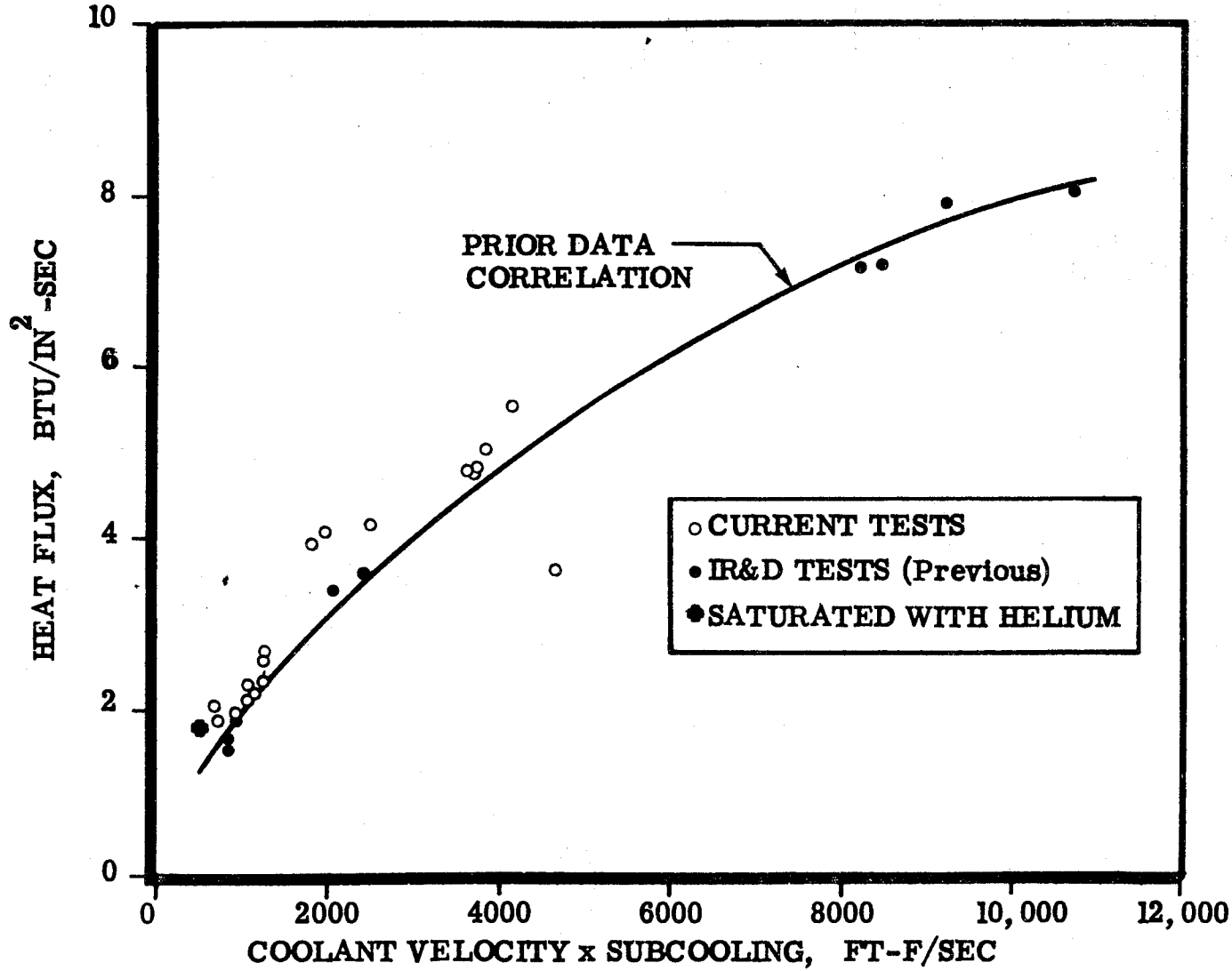

81

Figure 21. DEMONSTRATOR CHAMBER HEAT FLUX PROFILE

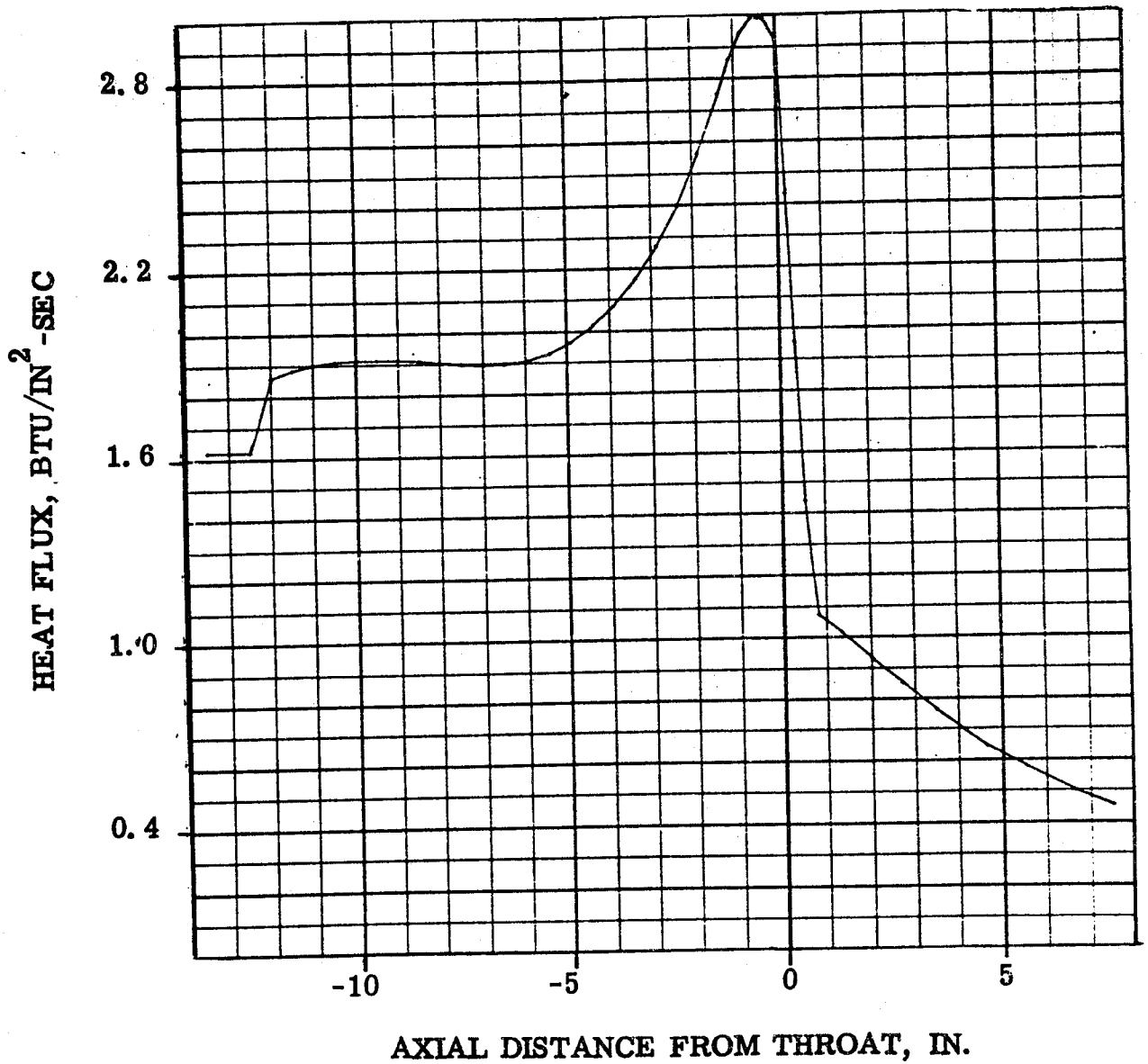

36

Figure 22. DEMONSTRATOR REGENERATIVE COOLANT BULK TEMPERATURE PROFILE

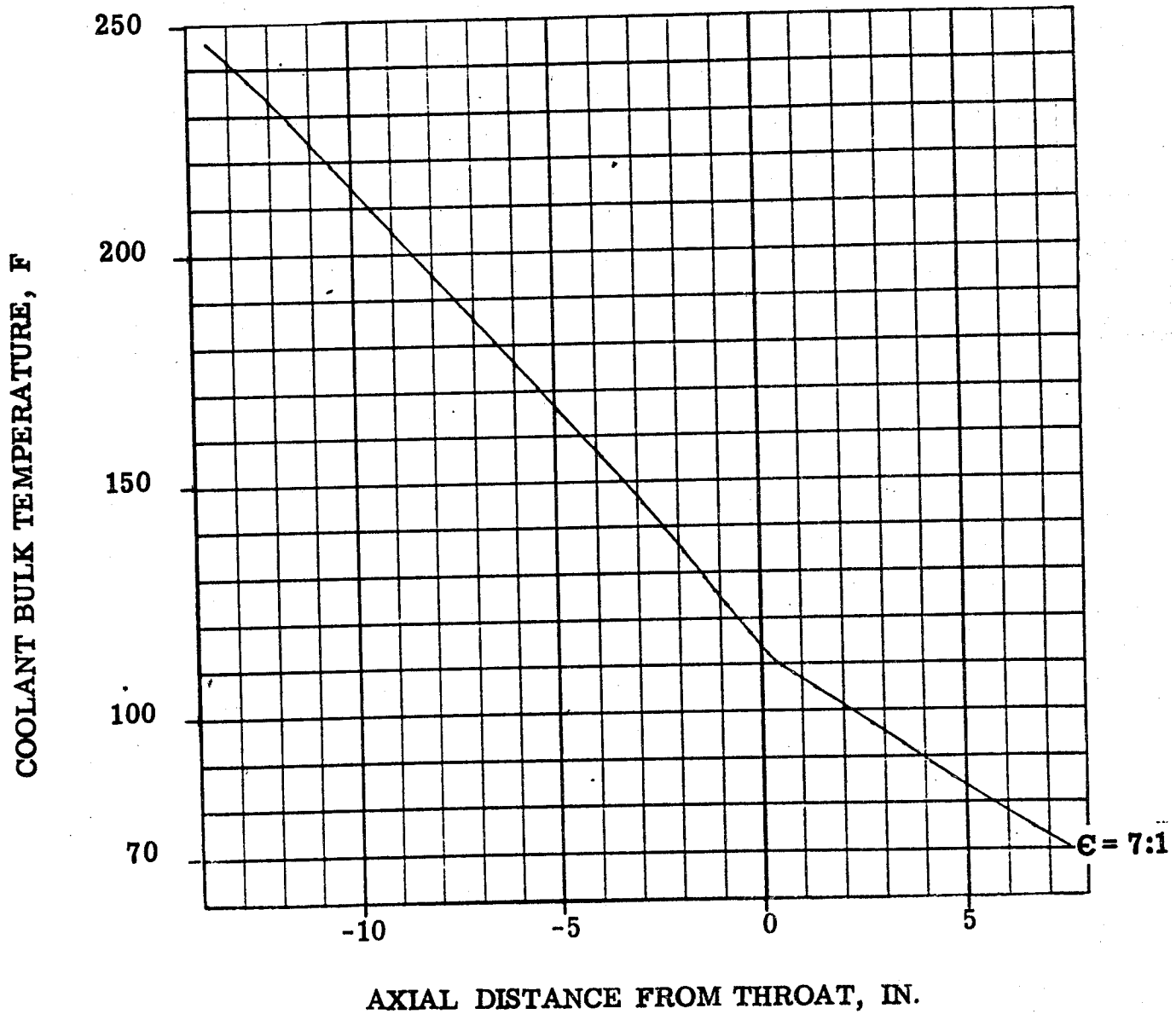

40

Figure 23. DEMONSTRATOR CHANNEL HEIGHT PROFILE

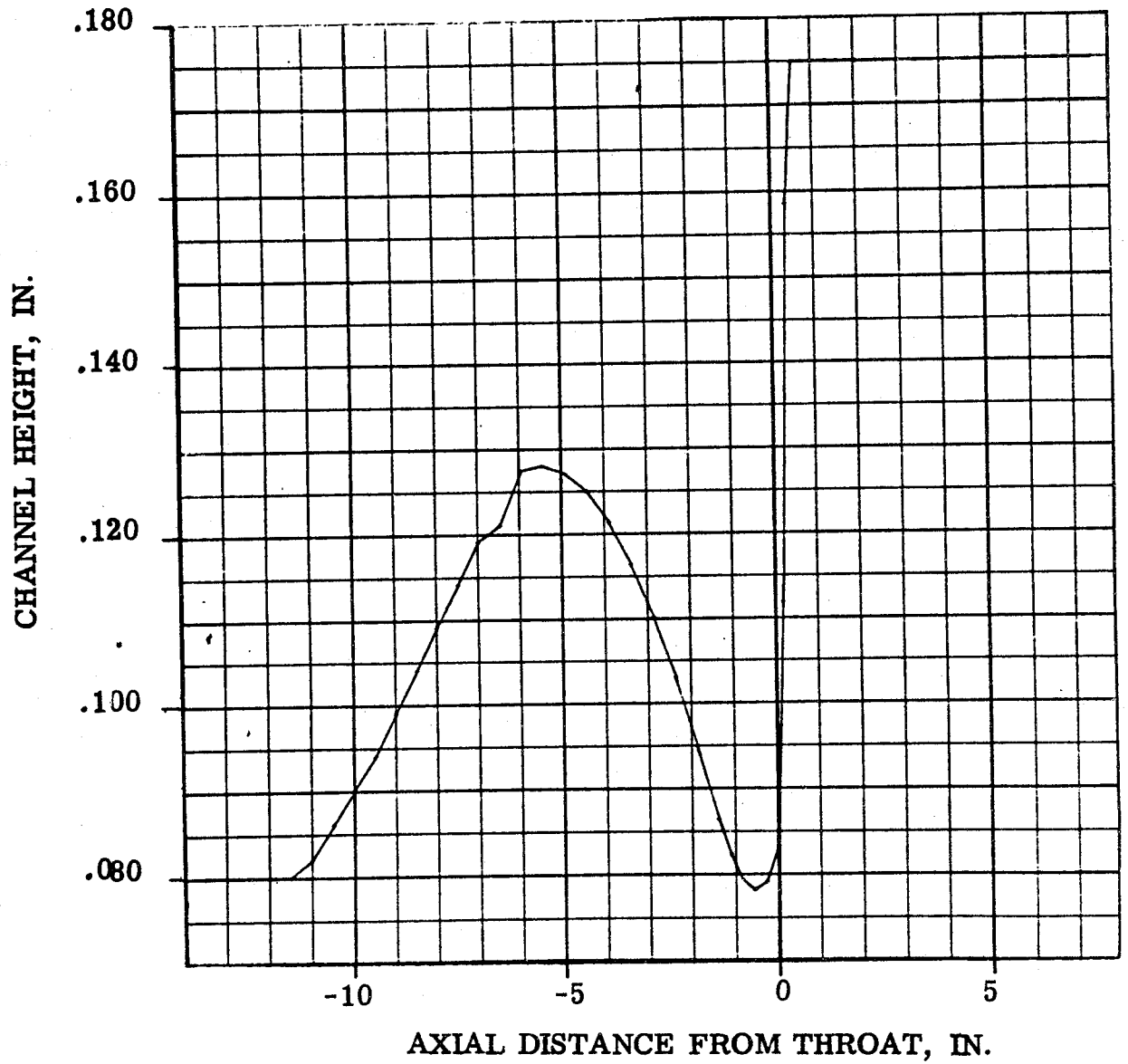

37

Figure 24. DEMONSTRATOR REGENERATIVE COOLANT VELOCITY PROFILE

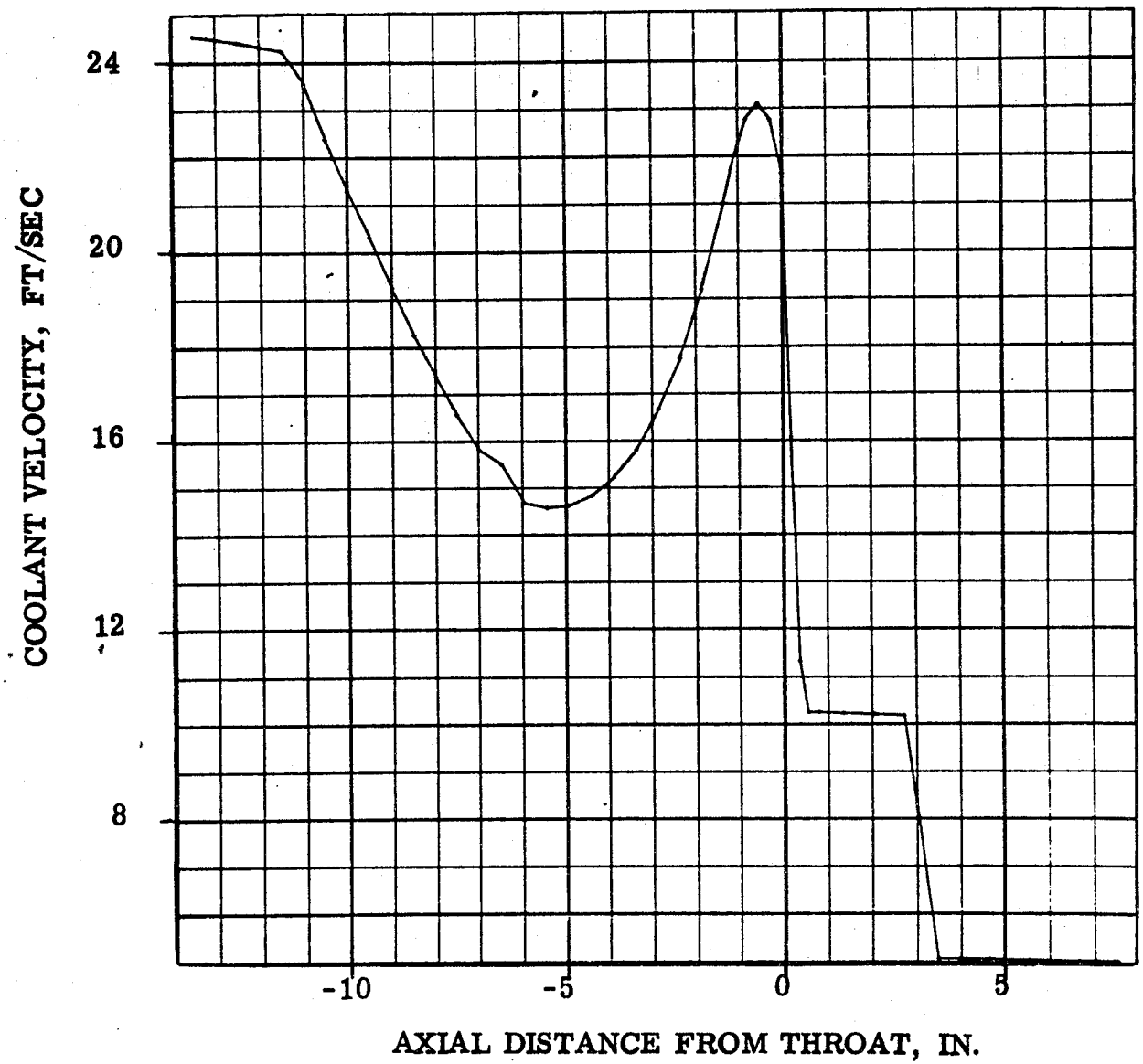

38

Figure 25. DEMONSTRATOR WALL TEMPERATURE PROFILES

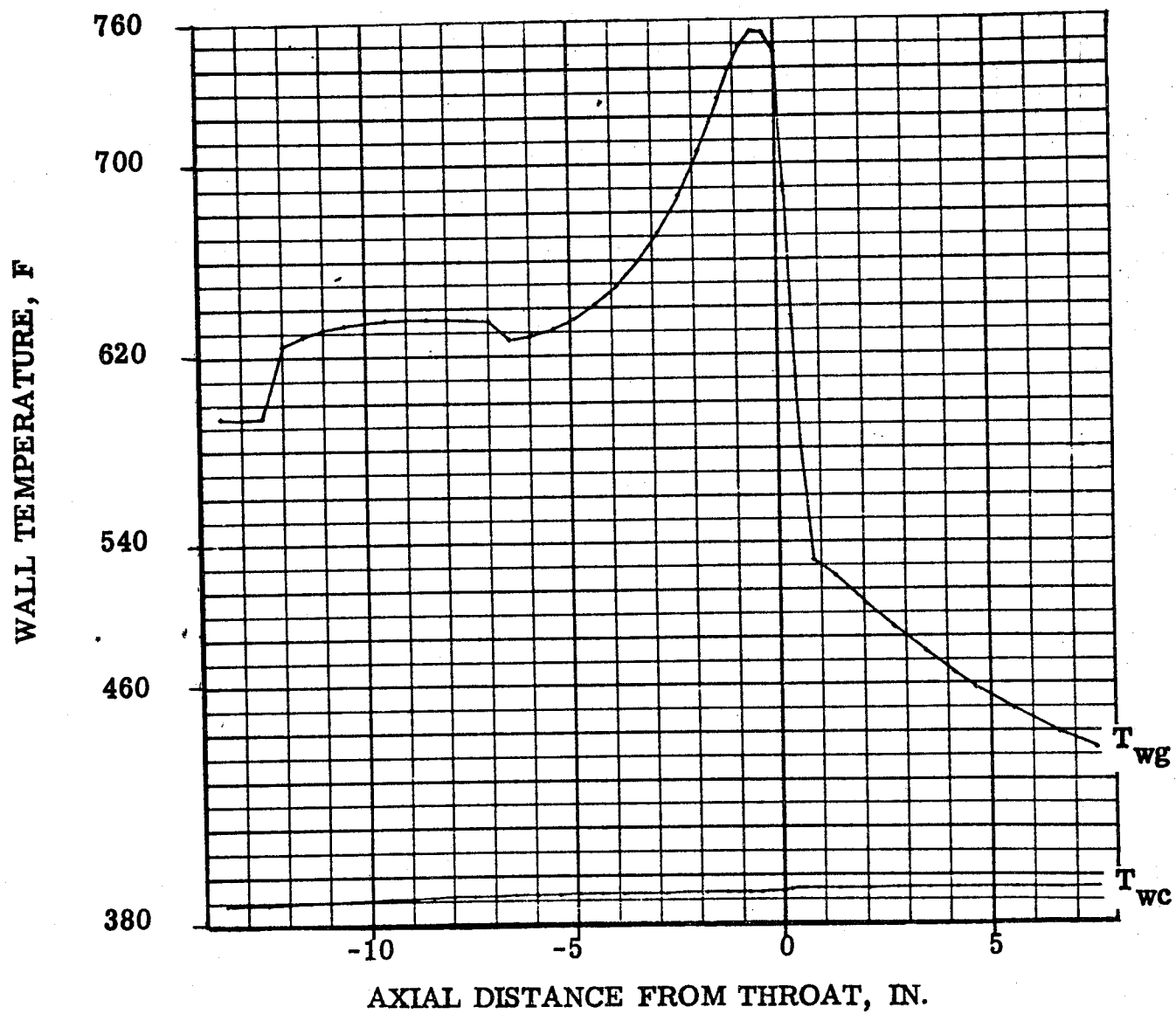

39

Figure 26. DEMONSTRATOR REGENERATIVE COOLANT PRESSURE PROFILES

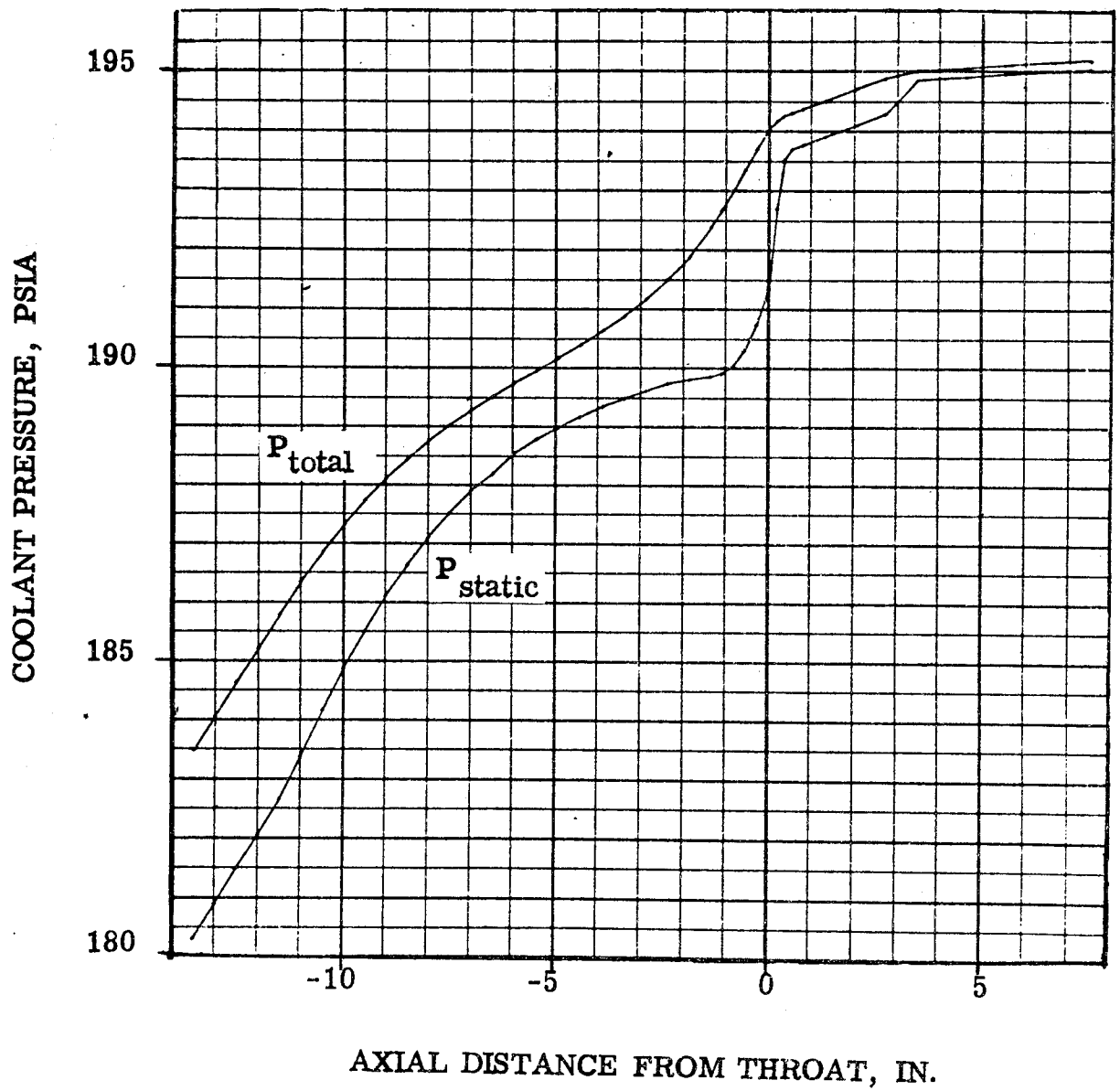

Figure 27. COOLANT SAFETY FACTOR PROFILE

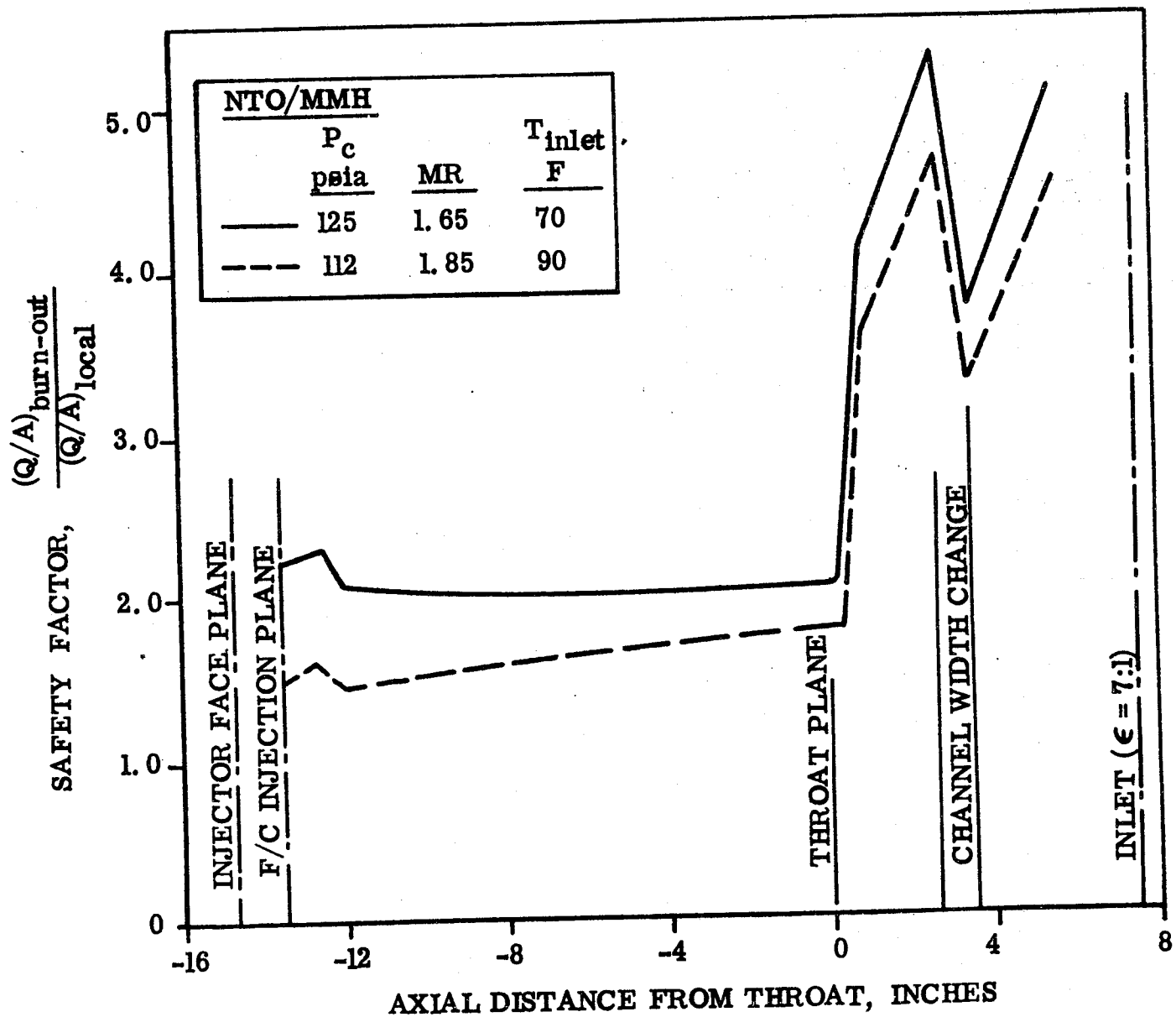

42

THRUST CHAMBER LIFE

The factors which enter into the thrust chamber life analysis are shown in Fig. 28. The life analysis includes the effect of both creep and fatigue damage. However, the creep damage for the regeneratively cooled engine is extremely small as shown in Fig. 9 . For CRES at 1000 F which is considerably in excess of the wall temperature even at off-design conditions, the damage fraction is only 0.2 percent.

The Universal Slopes prediction for the cyclic life of stainless steel under various strain ranges is shown in Fig. 30 for conditions of ambient temperature and 1000 F. The strain induced into the stainless steel liner of the chamber result primarily from thermal gradients between the hot inner wall and the cold outer wall. Strains due to pressures and thrust are negligible. The strain distribution is shown in Fig. 31 and reaches a maximum of approximately 7.5×10^{-3} inches per inch slightly upstream of the throat. This results in the fatigue life profile shown in Fig. 32. The minimum life region is again immediately upstream of the throat where the predicted life is approximately 7000 cycles. Since the required life is 1000 starts this provides a safety factor of approximately 7 on fatigue life.

A two dimensional analysis of the nozzle and attached flange was performed in order to indicate the maximum temperatures, the O-ring seal, and the regenerative inlet manifold will experience during operation. The results are shown in Fig. 33. These analyses indicated a maximum temperature of 2300 F, slightly below the 1 dimensional prediction. Temperatures at the inlet manifold somewhat in excess of 100 F were predicted. The minimum fatigue life of the nozzle joint was calculated to be approximately 5000 cycles.

Life analyses were conducted for all critical portions and failure modes of the radiation cooled nozzle. The most critical location for creep on the Columbian nozzle is at low area ratios where the temperature and the pressure and thrust stresses are most severe. Even under these conditions the stress rupture time as determined from the data of Fig. 34 is in excess of 10^4 hours.

Figure 28. ENGINE LIFE ANALYSIS

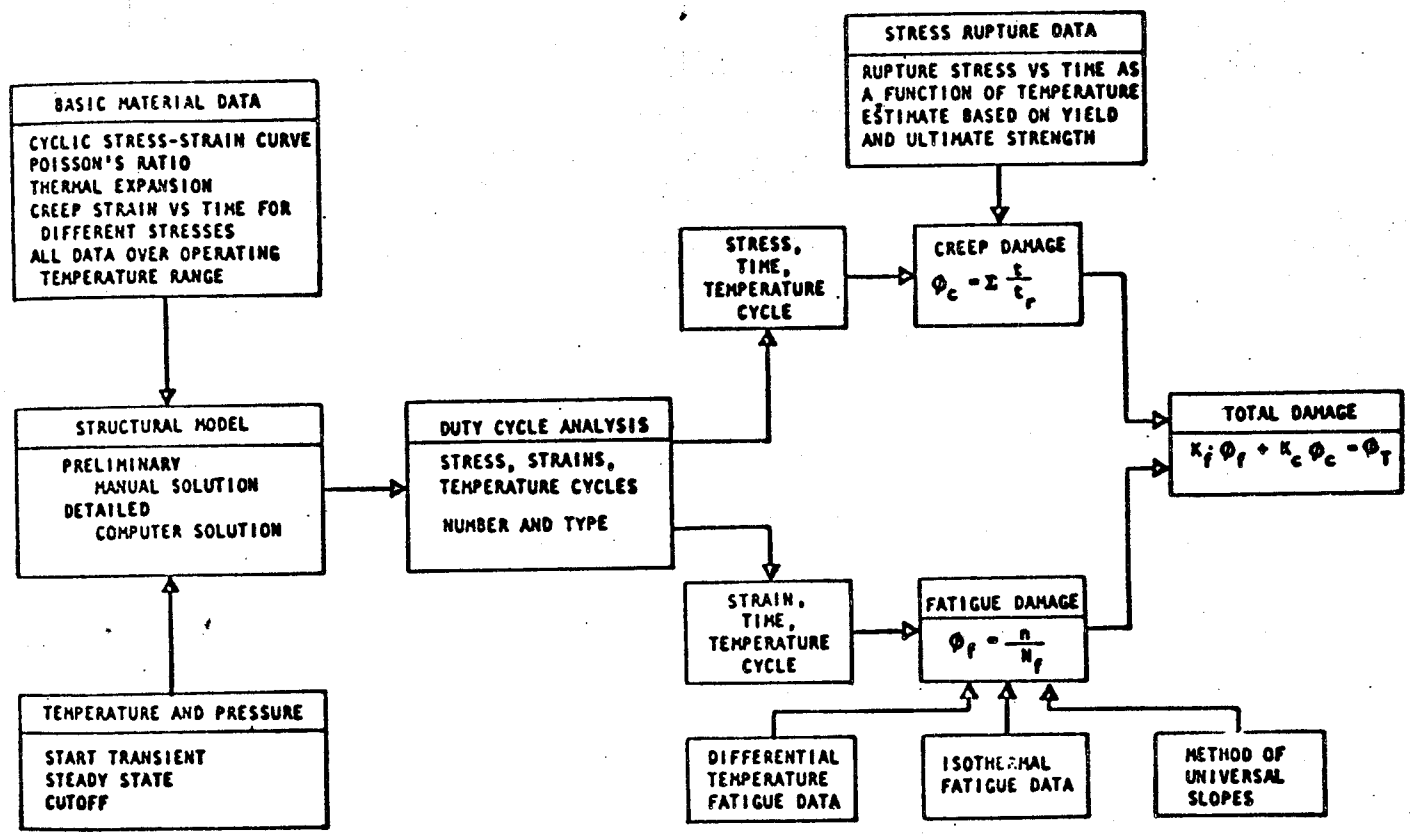

Figure 29. REGENERATIVE COOLED CHAMBER CREEP DAMAGE

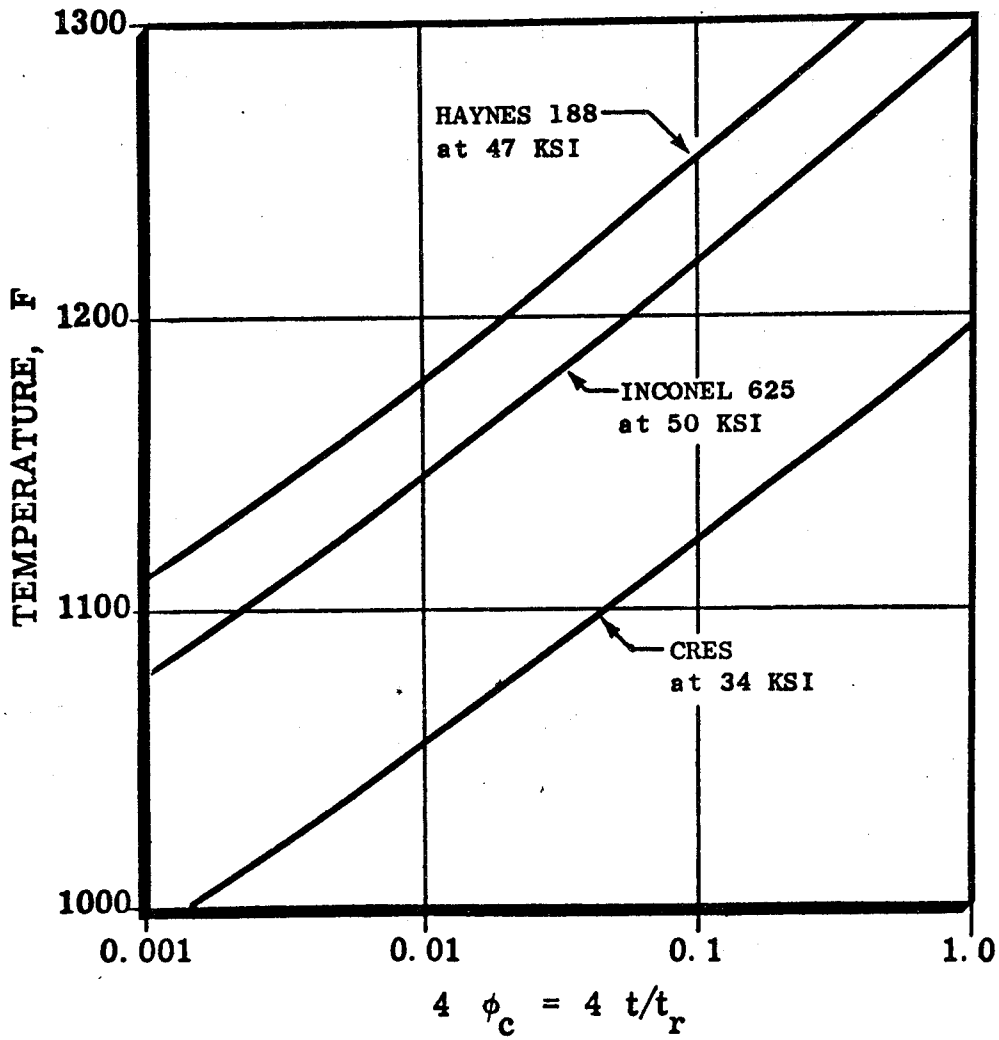

t = 15 HOURS

t_r = TIME TO RUPTURE

NOTE:

THE STRESS LEVELS INDICATED FOR EACH PLOT TYPIFY THE MAXIMUM HOT GAS WALL STRESS. STRESS RELAXATION HAS NOT BEEN INCLUDED

CONCLUSION:

NO SIGNIFICANT CREEP DAMAGE ON REGEN CHAMBER

Figure 30. UNIVERSAL SLOPES EQUATION FATIGUE DATA
STAINLESS STEEL TYPE 321

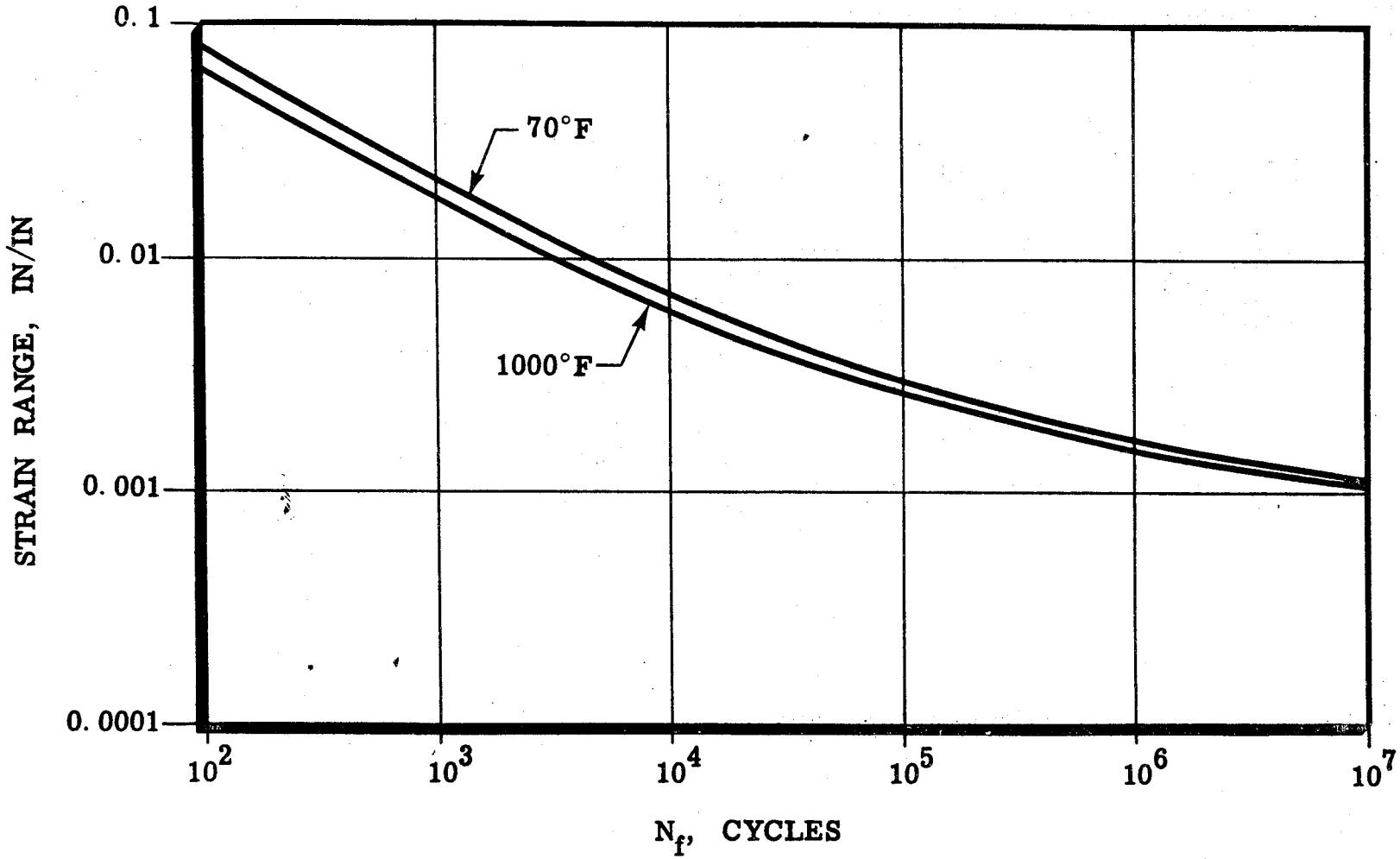

Figure 31. THRUST CHAMBER HOT WALL STRAIN DISTRIBUTION

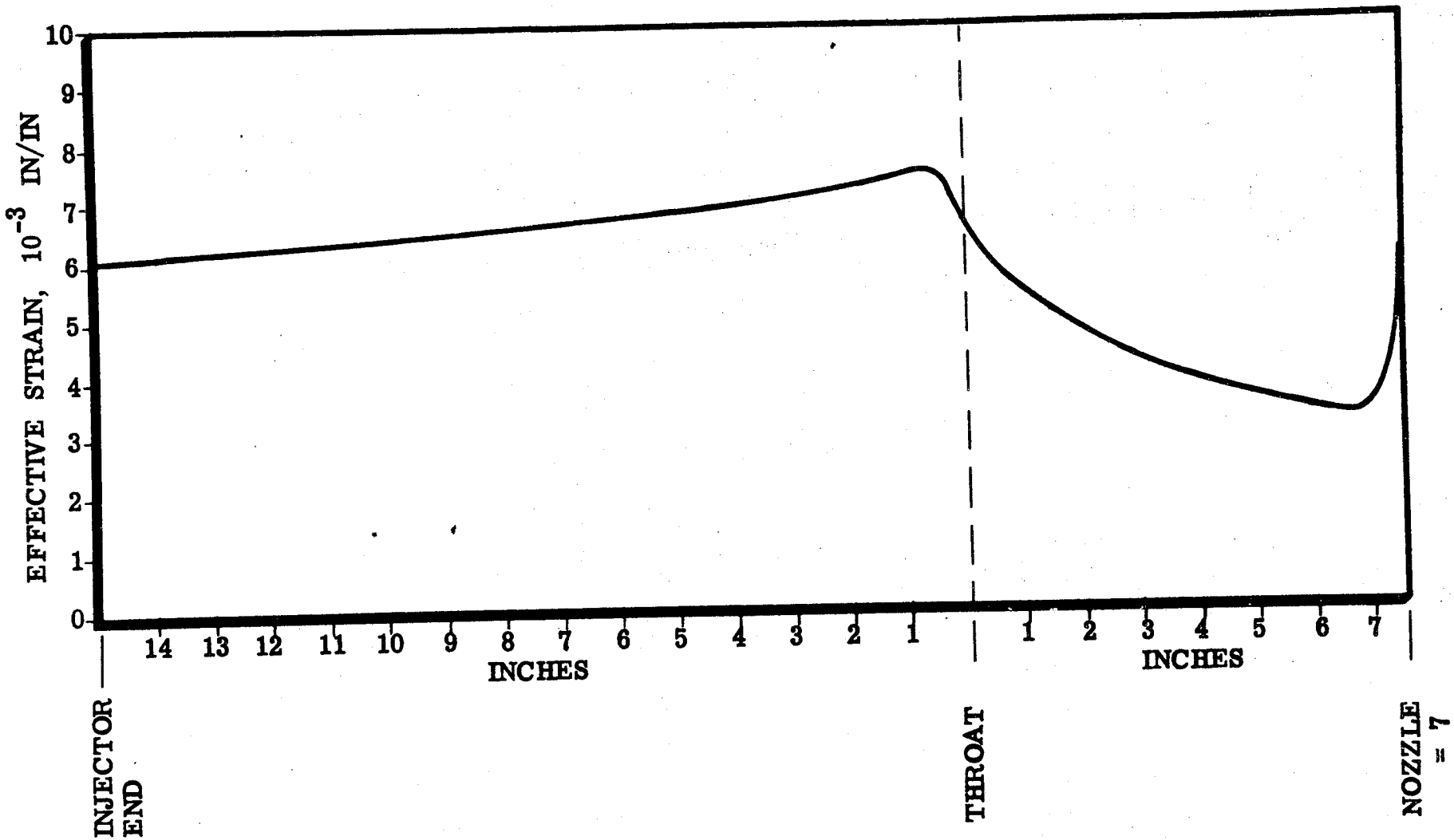

Figure 32. THRUST CHAMBER CYCLE LIFE CAPABILITY

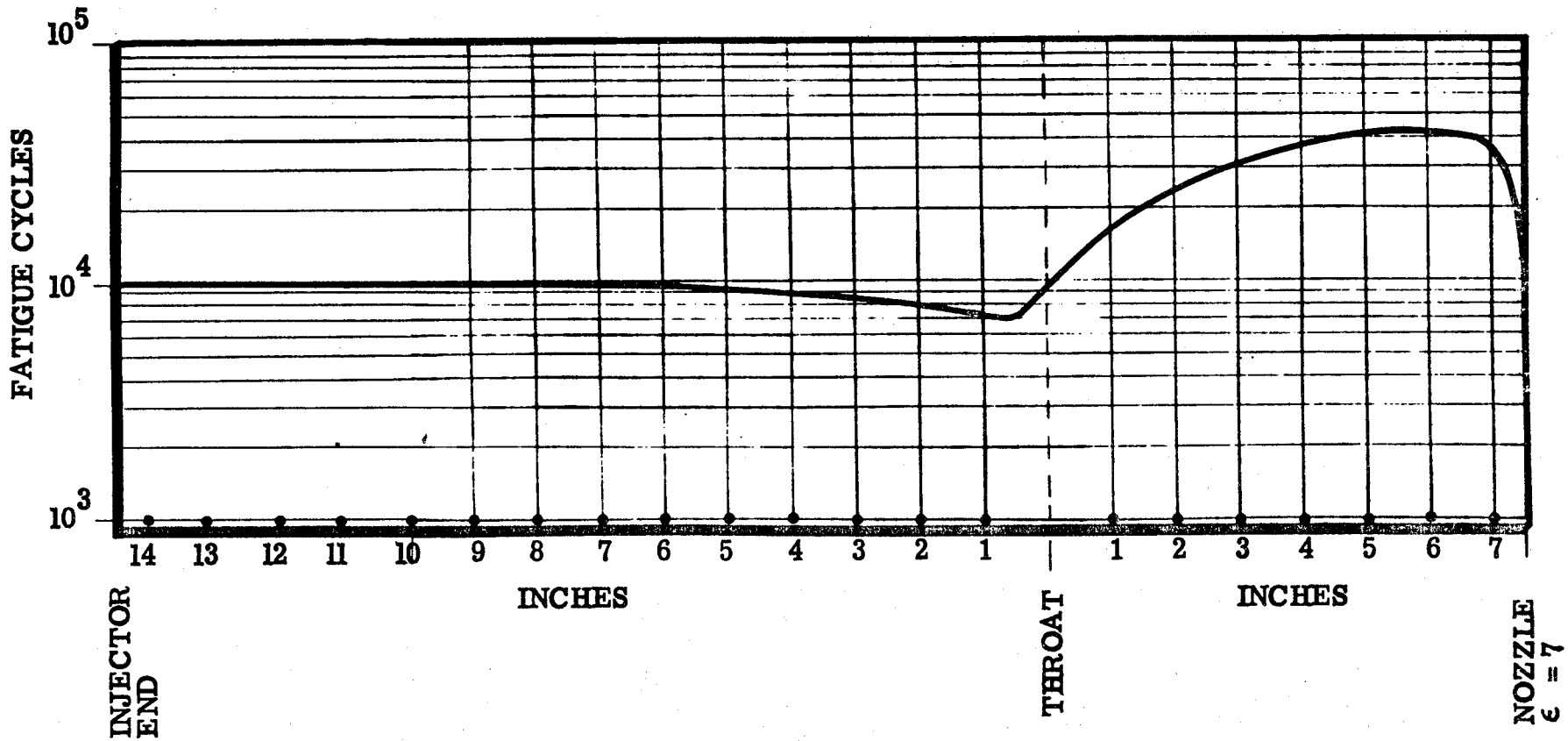

61

Figure 33. NOZZLE JOINT TEMPERATURE PROFILE

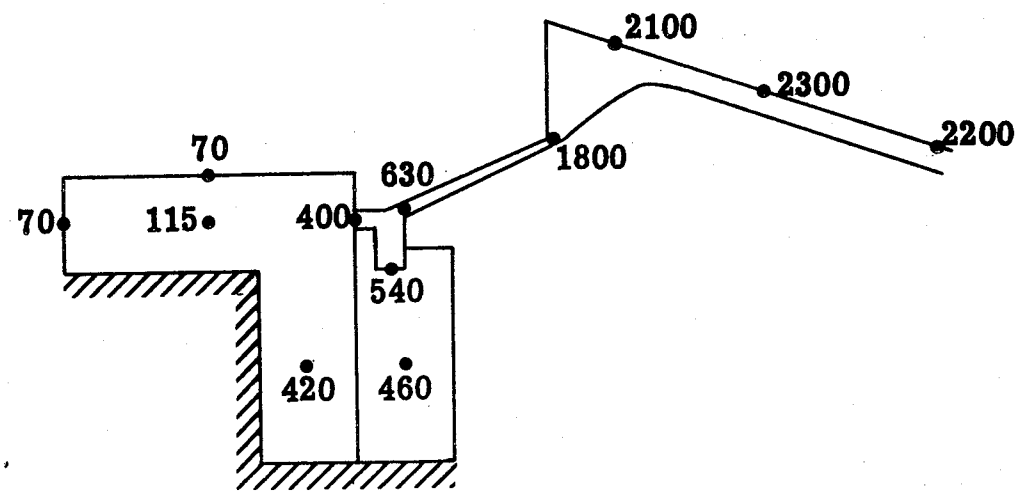

Figure 34. STRESS RUPTURE DATA
COLUMBIUM ALLOY WC-103

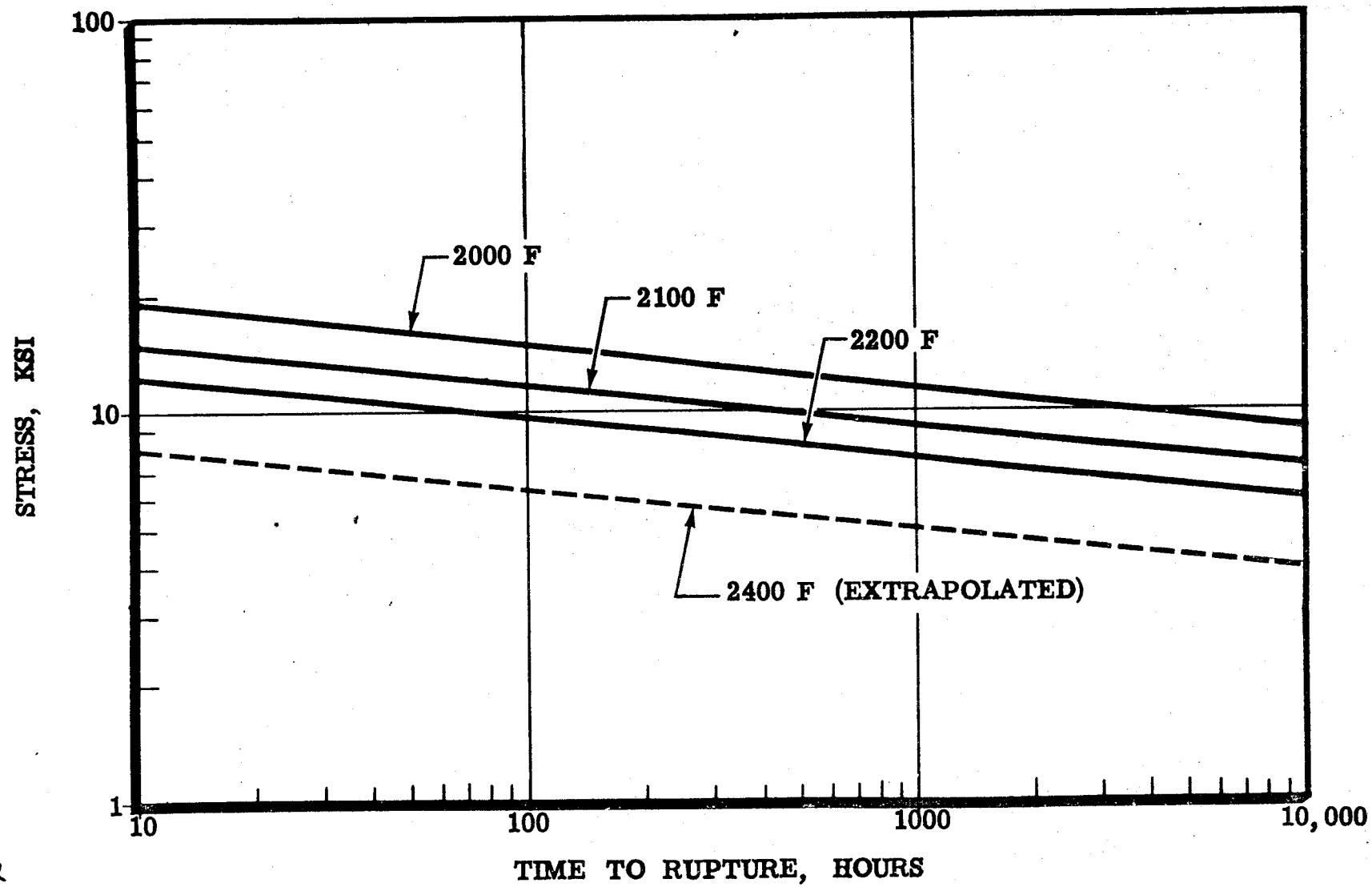

62

The weight advantages of using titanium for part of the radiation cooled nozzle are shown in Fig. 35. The transition from Columbium to titanium is nominally at an area ratio of 38 which corresponds to a wall temperature of 1600 F. Designing to 1800 F could save another 10 pounds per engine. However, structural reinforcing of the nozzle would probably be required which would negate most or all of the gain. Designing for 1400 F would put the transition point so close to the nozzle exit that the bimetalic construction would not be practical. The Columbium/titanium interface is prone to fatigue damage because of the differential thermal expansion between the two materials. However, the fatigue life of this joint was calculated to be in excess of 10^4 cycles. Stress on the titanium due to pressure and thrust loads was calculated to be 375 psi which appears to be well below the creep curve for titanium (5 Al - 2.5 Sn alloy) shown in Fig. 35.

TRANSIENT THERMAL ANALYSIS

Start and shutdown analyses were conducted to uncover potential problem areas in the flight OME, to verify similarity between the thermal transient characteristics of the flight and demonstrator thrust chambers, and to determine the test durations required to obtain steady-state thermal conditions.

Hot wall temperature transients are shown for the regeneratively cooled thrust chamber in Fig. 36. The transients are the same for the flight and for the demonstrator chambers. Time is measured from the beginning of P_c rise. Throat temperatures stabilize within approximately 1 second while the slowest responding temperatures at the coolant inlet location are nearly stabilized in 5 seconds. Temperature transients for the demonstrator nozzle extension are shown in Fig. 37. In 20 seconds the maximum temperatures are nearly reached. Even at 10 seconds of operation almost 90 percent of the equilibrium temperature rise has taken place. Complete equilibrium requires approximately 30 seconds. Temperature transients for the flight nozzle are somewhat more rapid as shown in Fig. 38. In the attached region thermal equilibrium occurs within 20 seconnds. At the exit of the nozzle (ϵ = 72) more than 60 seconds are required to reach complete thermal equilibrium.

Figure 35. TITANIUM RADIATION-COOLED NOZZLE EXTENSION

- 30 LB WEIGHT SAVING OVERALL - COLUMBIUM NOZZLE
- 1600F MAXIMUM OPERATING TEMPERATURE
- 375 PSI MAXIMUM STRESS DUE TO THRUST AND PRESSURE
- FABRICATION SEQUENCE: FABRICATE Cb AND Ti SECTIONS
  - SILICIDE COAT Cb SECTION
  - WELD Cb AND Ti SECTIONS
  - ALUMINIDE COAT Ti/Cb JOINT AND Ti SECTION
- ALUMINIDE LIFE EXPERIENCE: 3 SPS CHAMBERS
  - ALUMINIDE ON COLUMBIUM
  - 150 THERMAL CYCLES EACH
  - 2000 SEC CUMULATIVE - NO DAMAGE

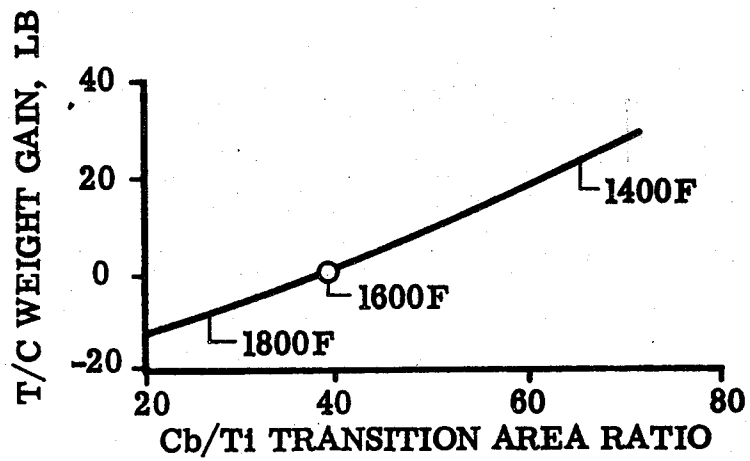

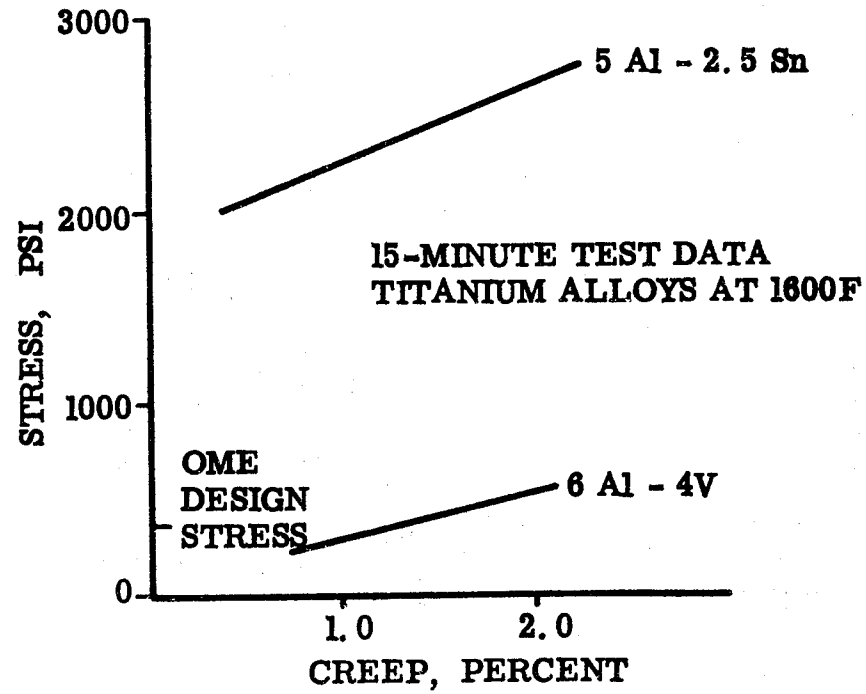

63

Figure 36. FLIGHT AND DEMONSTRATOR CHAMBER WALL TEMPERATURE RESPONSE

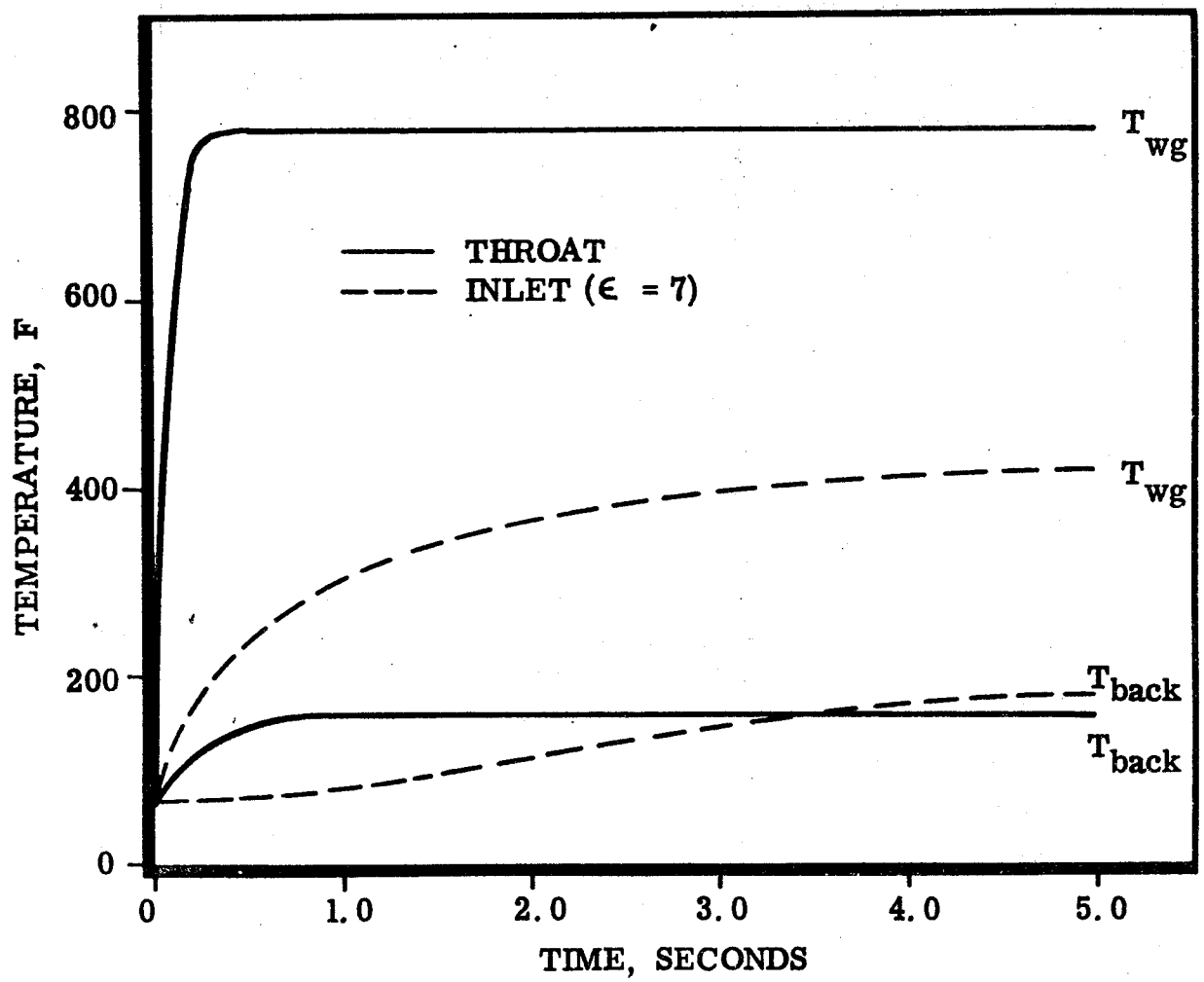

43

Figure 37. DEMONSTRATOR NOZZLE EXTENSION START TRANSIENT

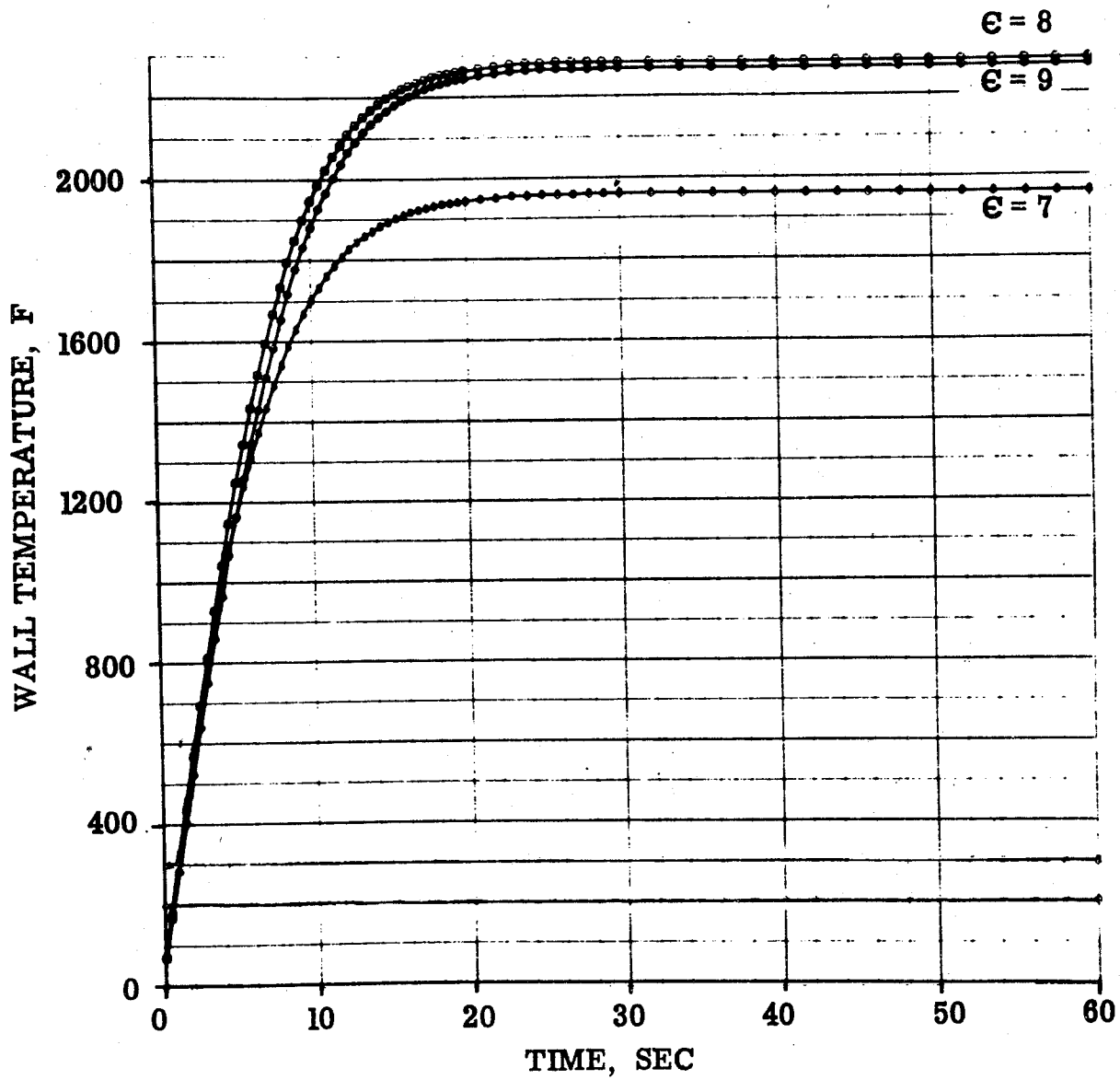

45

Figure 38. FLIGHT NOZZLE EXTENSION START TRANSIENT

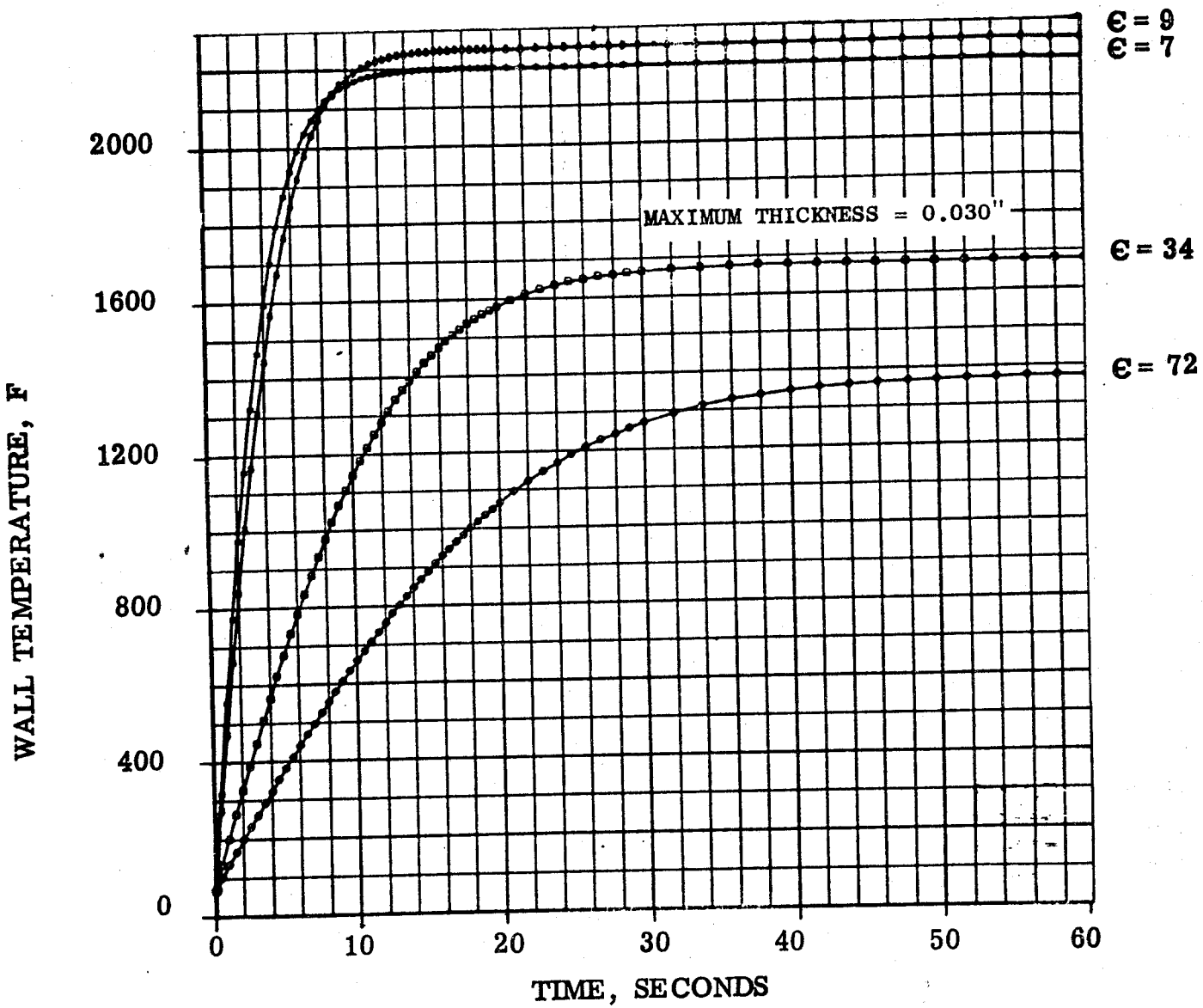

44

To analyze orbital start and soakback conditions a thermal model was made which is described in Fig. 39 and Table 10. Major components of the engine were modeled and the vehicle view factors estimated from vehicle contractor drawings. Engine soakback transients immediately following shutdown are shown in Fig. 40. The residual fuel in the jacket is sufficient to prevent any temperature spikes at cutoff and the temperatures of all components decrease monotonically. The temperature transient for a 7 day soakout in space is shown in Fig. 41. Heat loss to space is balanced after approximately one day by heat gain from the surrounding vehicle. After one day no further change in temperature takes place. All temperatures in the regeneratively cooled portion of the engine are well above the freezing point of the fuel and the injector and valve temperatures are above the freezing point of the oxidizer. Thus, no freezing problem is seen to exist during a long soak in space.

The primary concern during a start in space is that propellant will freeze through vaporization and plug injector or coolant jacket passages. To evaluate this, the start model was used to simulate a start after a long chill in a space environment. The results are shown in Fig. 42. In the analysis, the fuel temperature is calculated at various locations through the system as the fuel loses heat through vaporization and transfers heat with the surrounding materials. Initial material temperatures are based on the results of the soakout analysis. The fuel temperature decreases at first, then very rapidly begins to increase in temperature and through heat transfer to the surrounding materials so that even at an inlet temperature of 40 F the fuel does not freeze.

The most severe freezing condition would be encountered if, after a space chill of longer than one day, the OME were fired for a short duration so that propellants primed the engine but only a small amount of heat was generated by the firing. The results of such a condition with a one second firing of the OME are described in Fig. 43. Components in contact with the MMH remain above the freezing point (-62F) of the fuel. Components in contact with the oxidizer reach the NTO freezing point (12 F) indicating some degree of freezing of residual NTO and potential restart problems. None of the current mission

Figure 39. THERMAL ANALYTICAL MODEL
NODAL SCHEMATIC
ORBITAL CHILL AND START - OFF TIME HOT SOAK BACK

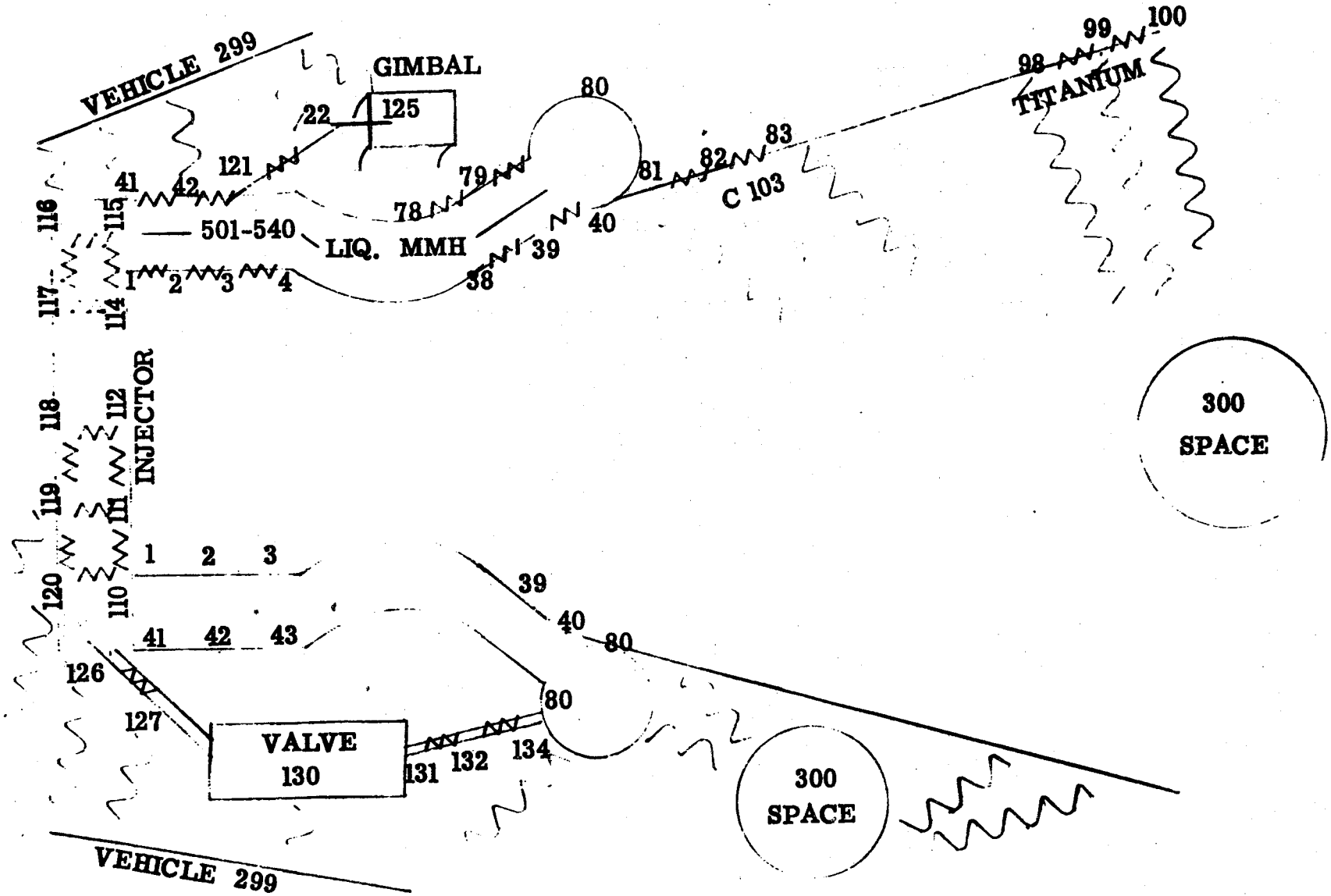

46

Table 10. **ASSUMPTIONS FOR THERMAL TRANSIENT ANALYSES**

- 40F VEHICLE - SYSTEM PRE ORBIT INITIAL TEMPERATURE
  - MODEL 049 VEHICLE - ENGINE SYSTEM CONFIGURATION
- 7 DAY RADIATION TO SPACE
  - NO SUN HEATING
  - NO EARTH ALBEDO VIEW
  - INJECTOR END ENGINE SYSTEM PARTIAL SPACE VIEW (NO RADIATION SHIELD)
  - ENGINE SYSTEM EMISSIVITY > .6
- ONE SECOND COLD START
- EVAPORATIVE CHILL OF BOTH RESIDUAL PROPELLANTS
  - 137 CU. INCHES MMH
    - FREEZES AT -62.5F
  - 22 CU. INCHES NTO
    - FREEZES AT 11.8F
  - 5 PERCENT OF RESIDUAL LIQUID EXPELLED AS LIQUID THROUGH INJECTOR ORIFICES DUE TO TURBULENCE OF EVAPORATION

46A

Figure 40. SS/OME HOT SOAK FOLLOWING STEADY STATE OPERATION

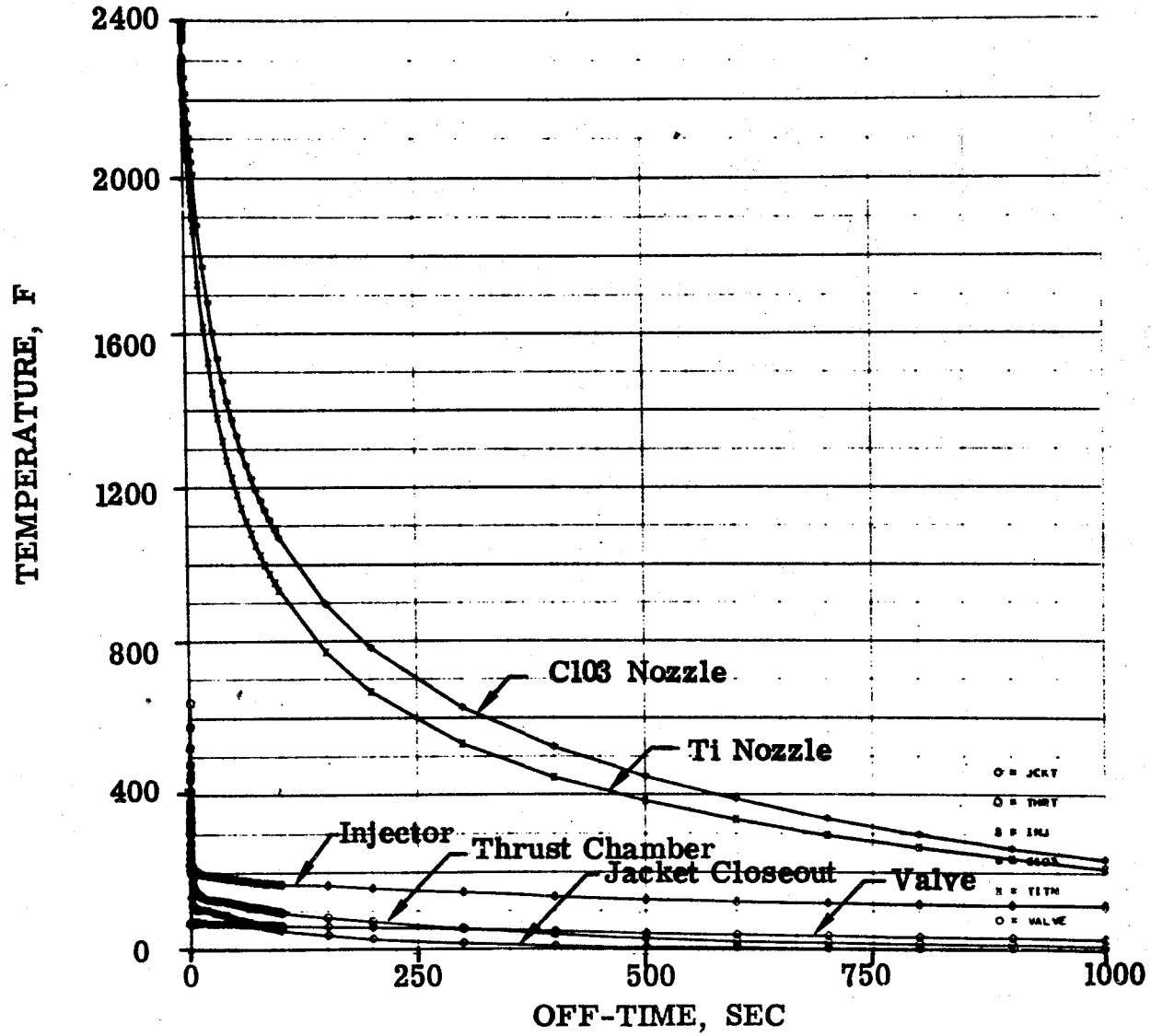

Figure 41. OME COMPONENT TEMPERATURES DURING SPACE SOAK

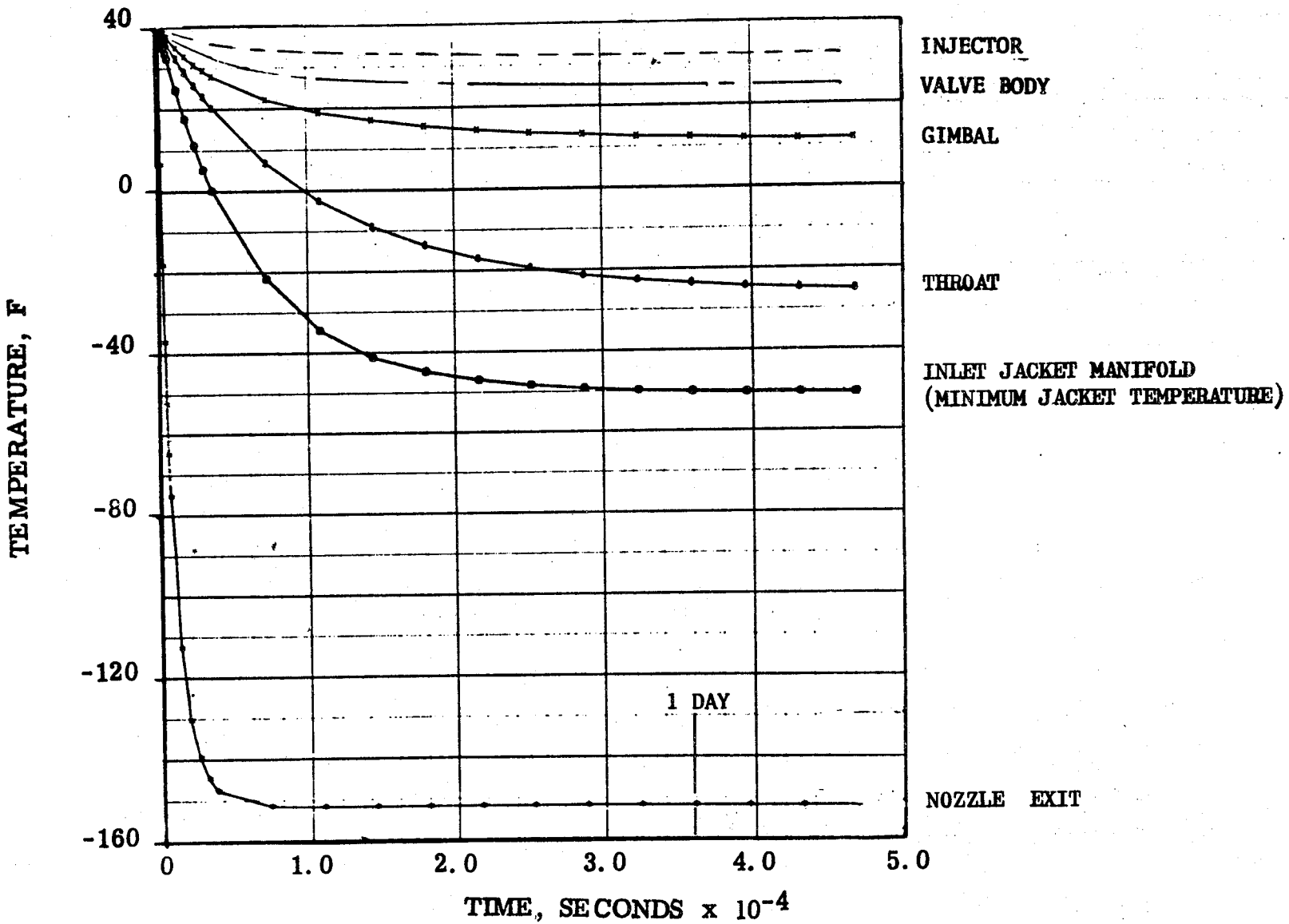

15

Figure 42. OME START FOLLOWING SPACE CHILL

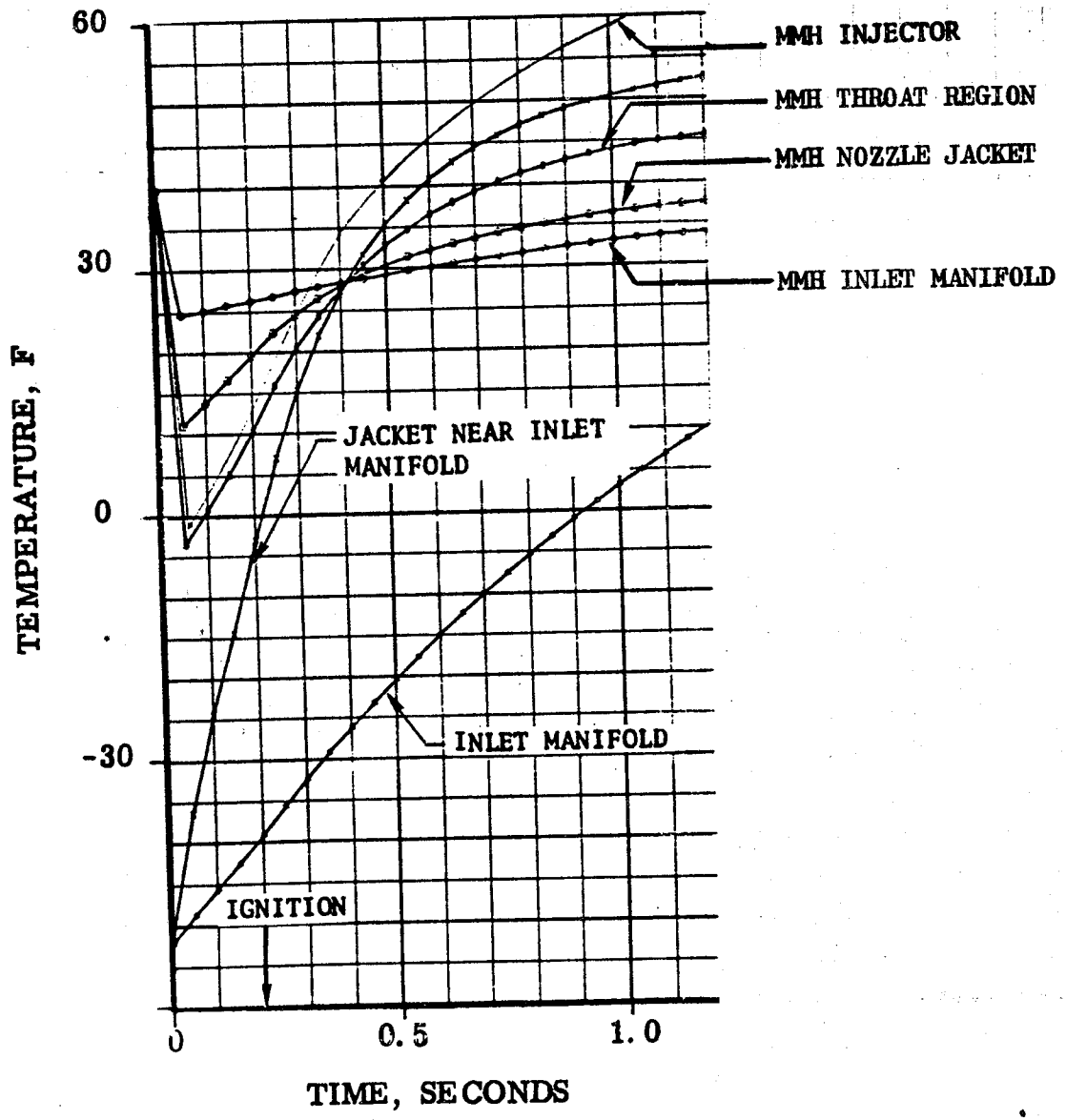

16

Figure 43. EVAPORATIVE CHILL OF OME PROPELLANTS

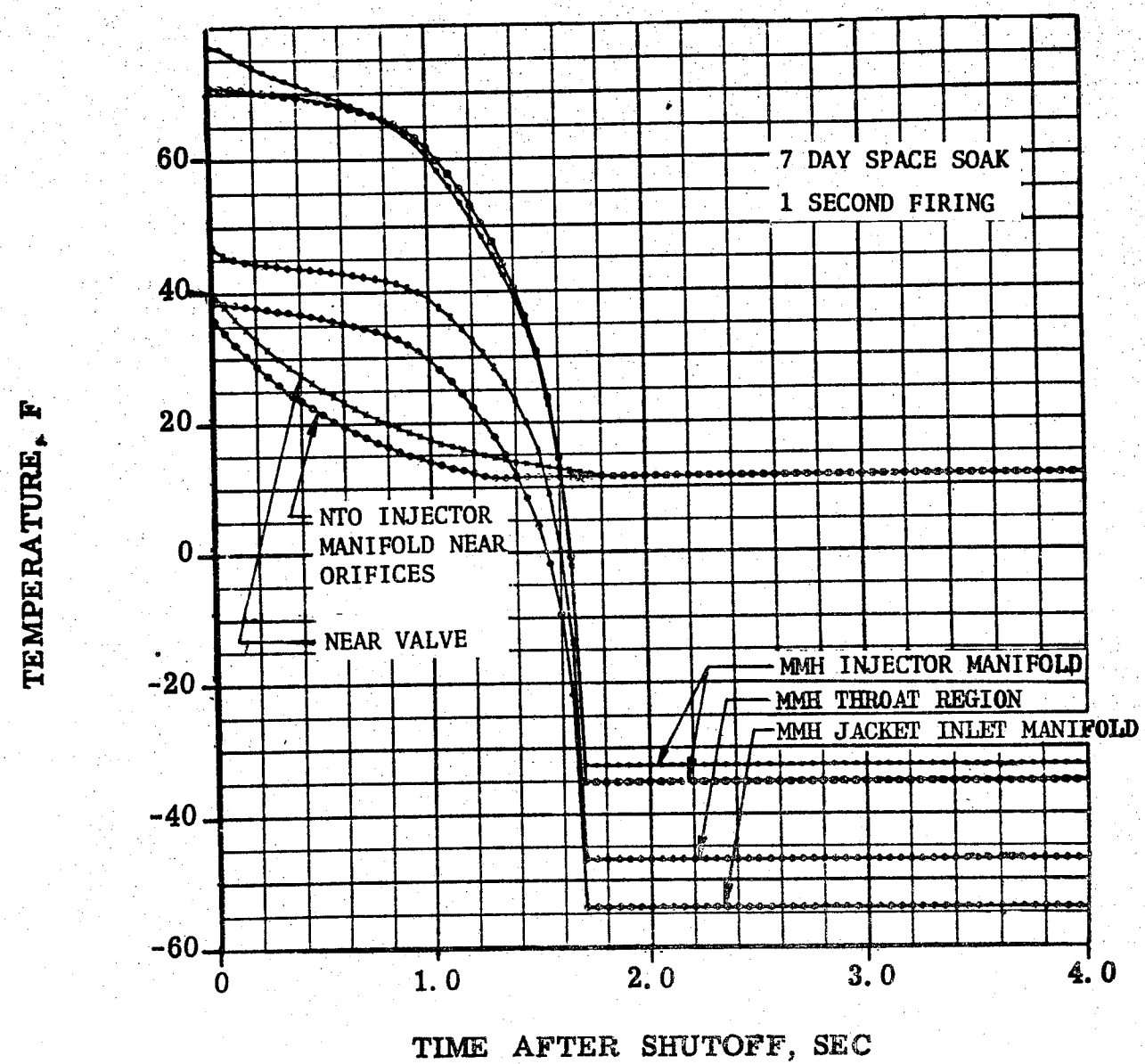

17

duty cycles include such a short firing duration but if such a requirement should develop the condition can be improved by maintaining the NTO at warmer than 40F or using heaters on the oxidizer feed system downstream of the engine valve.

OME SENSITIVITY

Sensitivity analyses were conducted to determine the effects of off-design engine inlet conditions on engine performance and safety. An engine steady-state model was used to analyze the effects of inlet pressure and temperature variations on chamber pressure and mixture ratio. The model includes variable C* effects and the pressure drops through indivudal components. The results of inlet pressure variations are plotted in Fig. 44 where 10 psi variations in individual tank pressure are shown to affect mixture ratio by approximately 0.1 units and chamber pressure by less than 4 psi for NTO inlet pressure variations are less than 2 psi for MMH inlet pressure variations. Inlet temperature effects are even less significant (Fig. 45) over the expected temperature ranges and particularly since the inlet temperatures are not expected to differ (between NTO and MMH) by more than approximately 10F. The effects of these variations on performance are shown in Fig. 46. The chamber pressure effect is seen to be negligible while the mixture ratio effect can result in performance variations of almost 2 seconds.

The effects of chamber pressure on the nominally designed regeneratively cooled thrust chamber wall temperature are shown in Fig. 47. The maximum wall temperature near the throat region increases from a nominal value of approximately 760F to slightly over 900F if the chamber pressure is increased from 125 to 200 psia. Operation is certainly safe under these conditions but the design life is slightly reduced. The temperature excursions of slightly over 200F occur if chamber pressure is increased to 200 psi. This temperature is within the operating capability of coated Columbium but is not recommended for long life application.

Figure 44. OME SENSITIVITY TO INLET PRESSURES

$P_{OI} = P_{FI} = 211$ PSIA NOMINAL

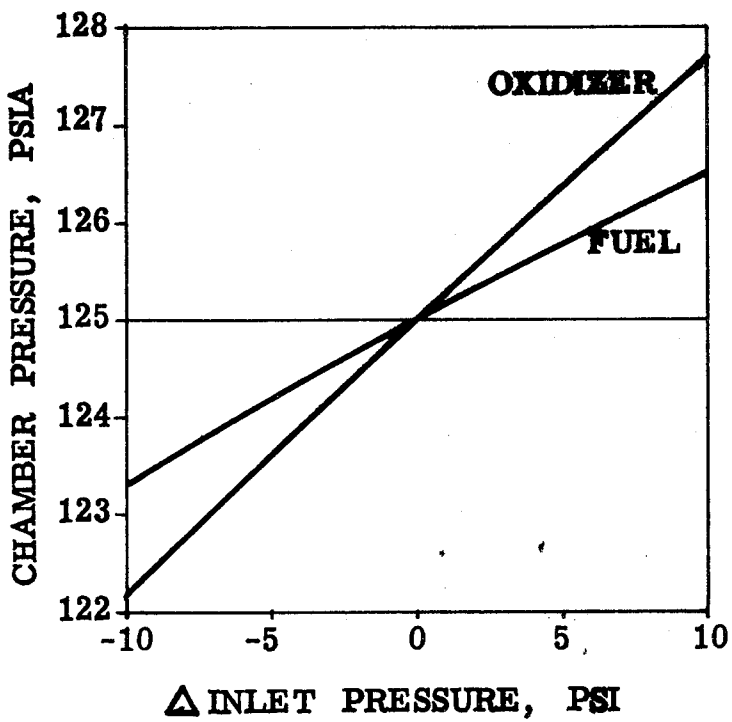

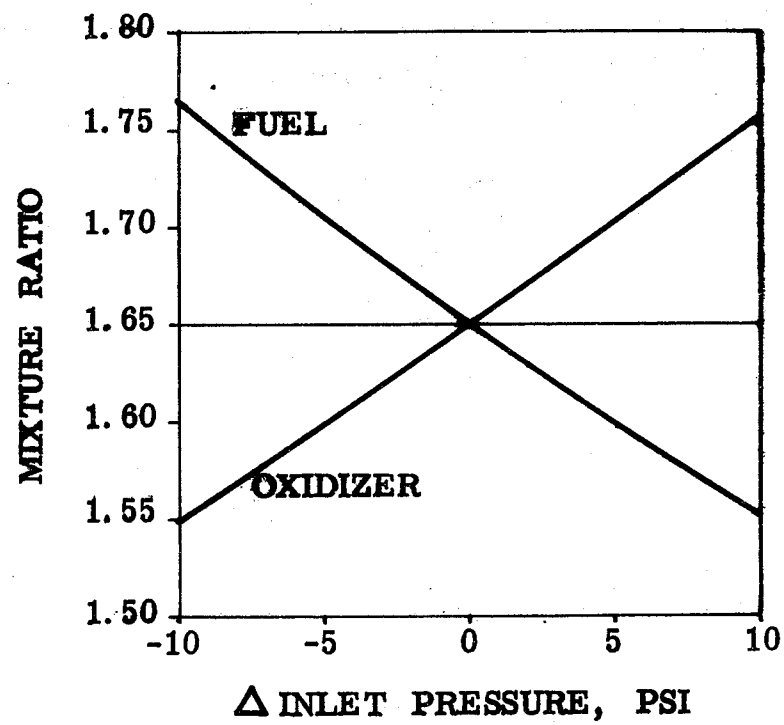

Figure 45. OME SENSITIVITY TO PROPELLANT INLET TEMPERATURES

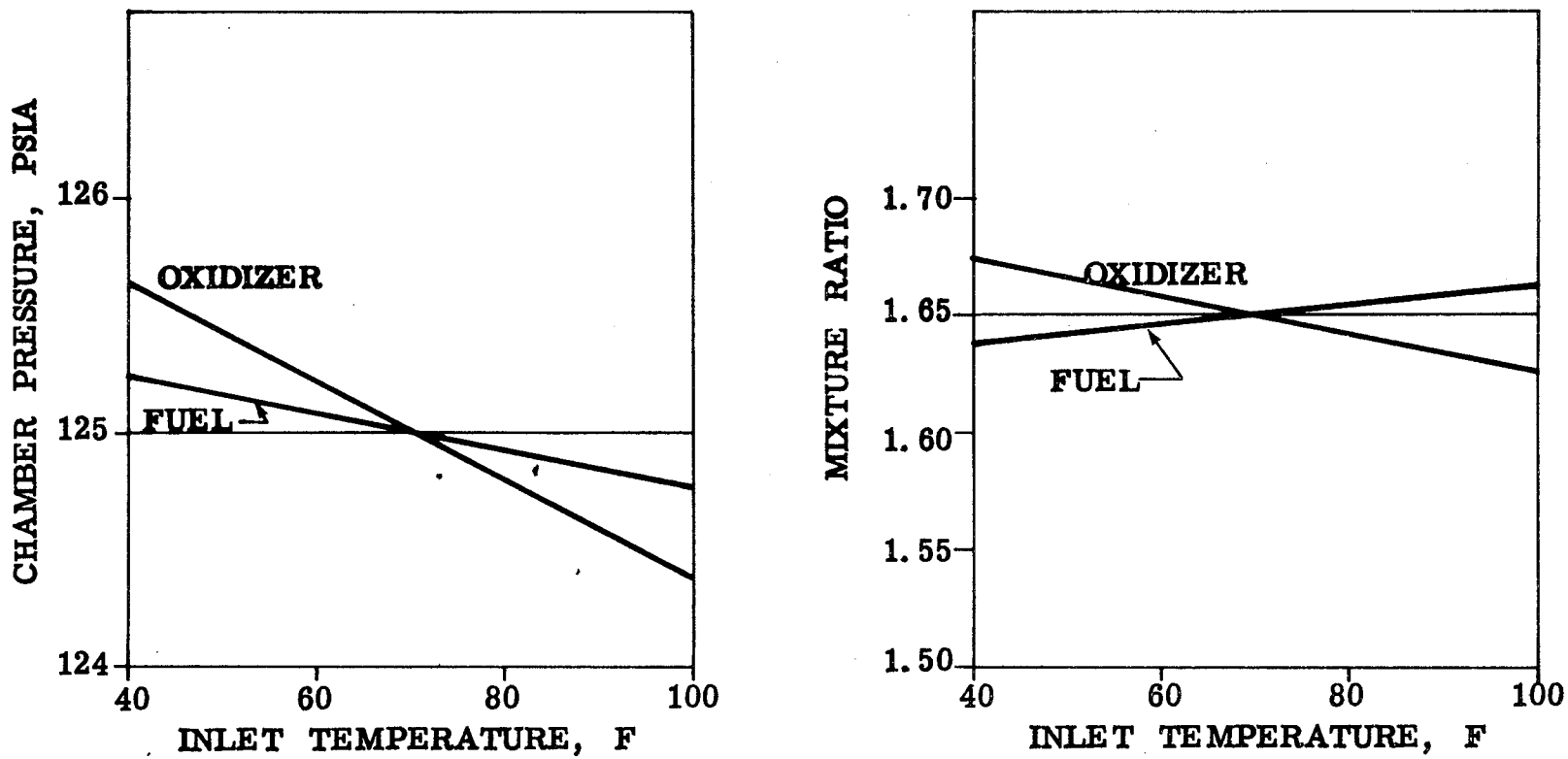

Figure 46. **OME PERFORMANCE SENSITIVITY**

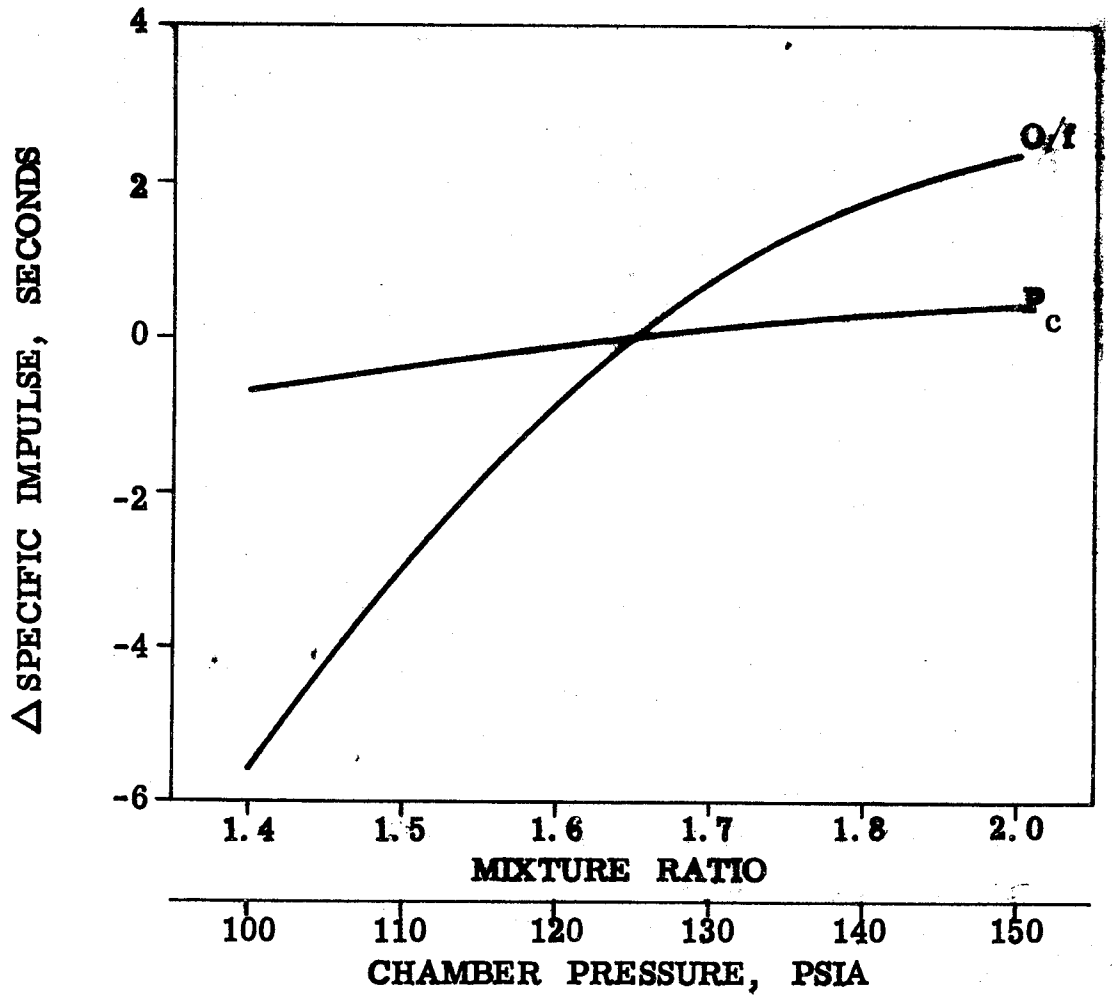

Figure 47. EFFECT OF CHAMBER PRESSURE ON MAXIMUM WALL TEMPERATURE AND LIFE

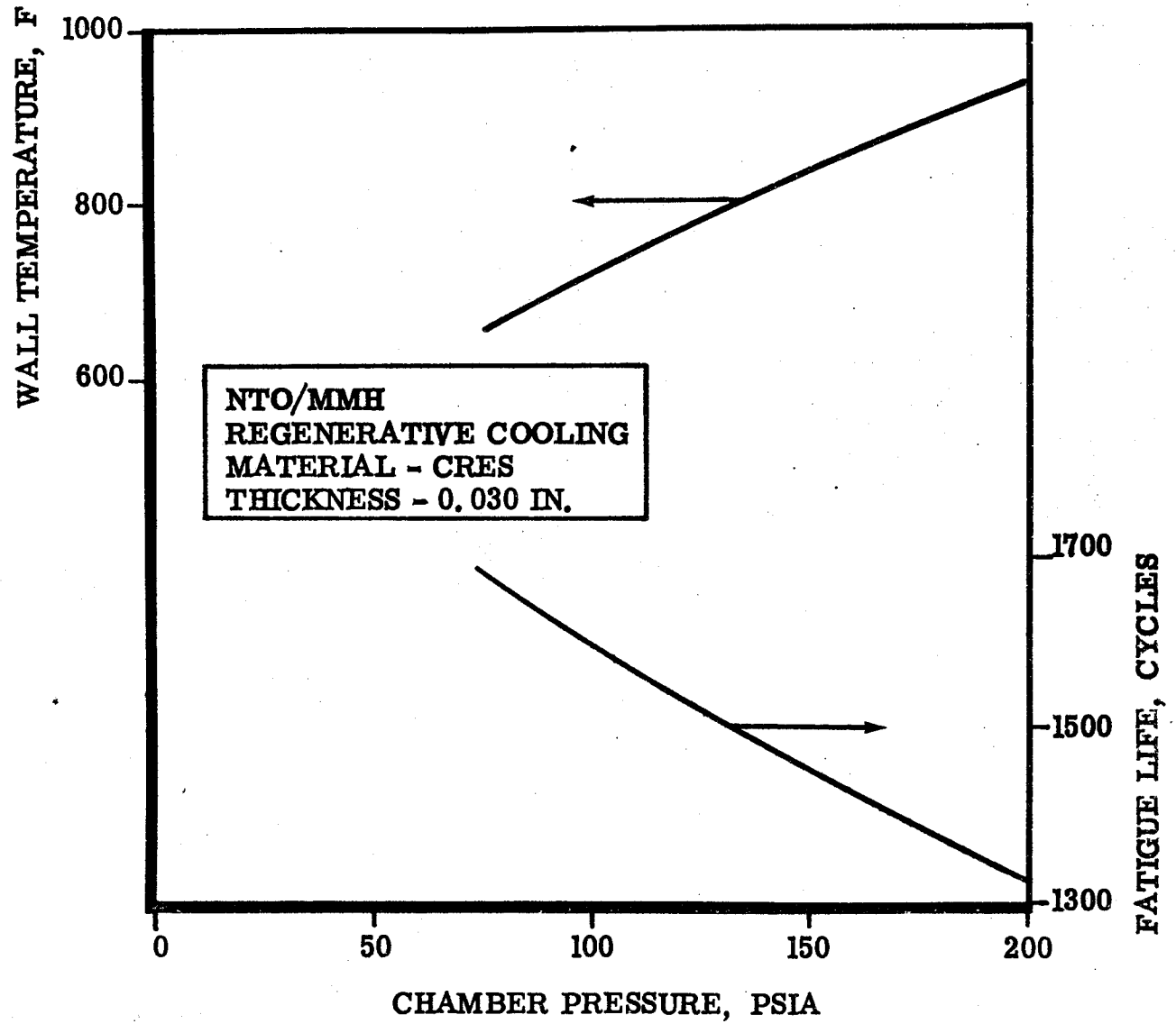

53

Figure 48. RADIATION NOZZLE TEMPERATURE SENSITIVITY TO CHAMBER PRESSURE AT ATTACH POINT

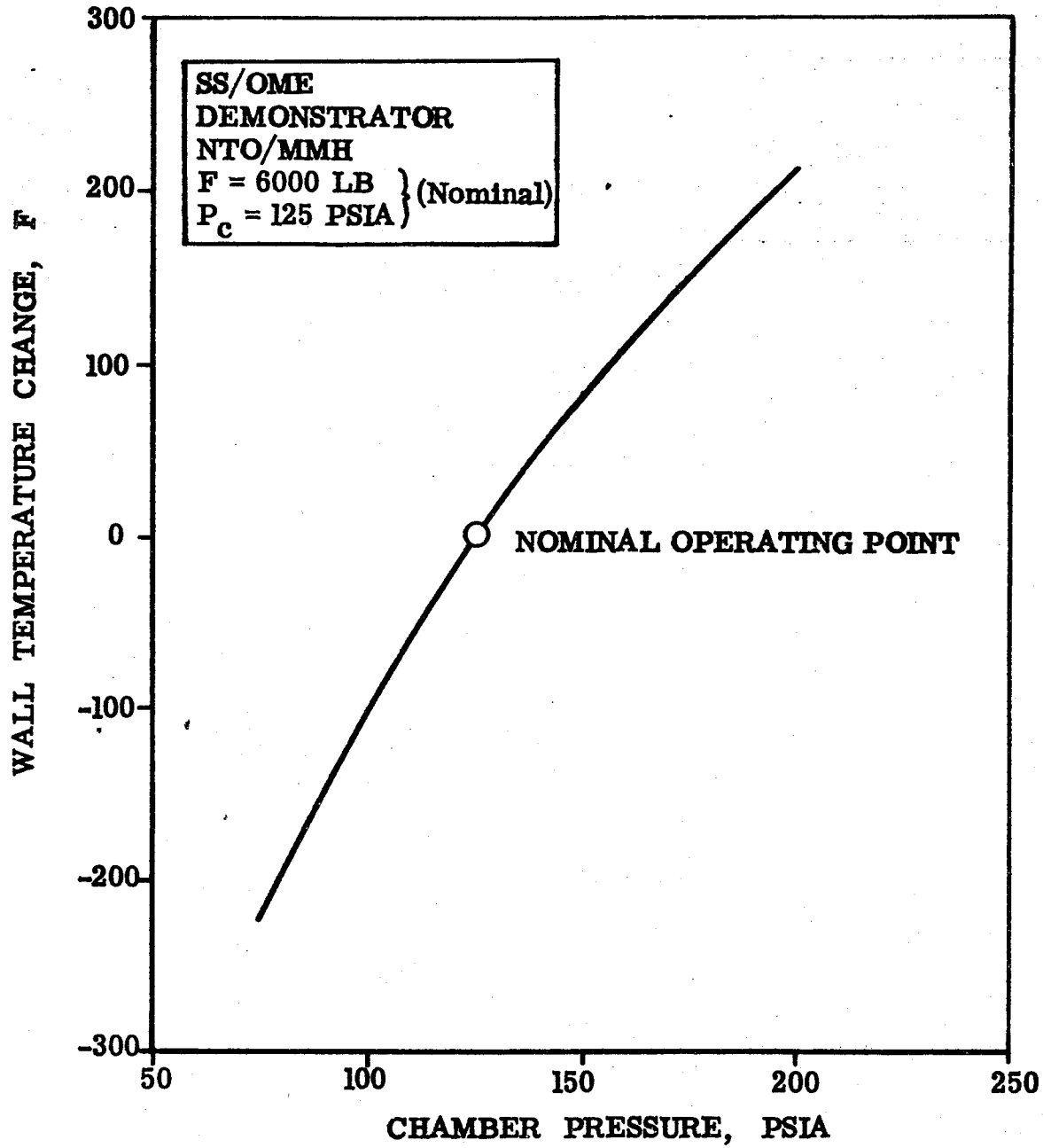

54

Chamber pressure effects not only the material temperatures but also the bulk temperature of the propellants as shown in Fig. 49. Increasing the chamber pressure actually results in a decrease of the coolant exit bulk temperature because the coolant flowrate increases more than the integrated heat flux. At the same time the saturation temperature of the MMH increases as shown because of the increased chamber pressure. The result is a significant increase in the subcooling as chamber pressure is increased. Increasing the mixture ratio increases the coolant exit temperature primarily because of the smaller amount of coolant available to absorb the heat of the chamber. The effects of increasing the inlet temperature of the coolant from 70 F to 90 F are also shown in Fig. 49. Thus, chamber pressure may be reduced to less than 100 psia or the inlet temperature may be increased to 90 F and the mixture ratio increased to 2.0 while maintaining a subcooling of greater than 50 F. The 50 F subcooling values is a conservative safe limit. Heated tube tests have been run with considerably lower subcooling values.

Varying the chamber pressure and mixture ratio result in different values of local velocity and subcooling in the coolant passages. These in turn effect the local burnout safety factor as shown in Fig. 50 . Again, the design chamber is seen to be capable of operating over a wide range of chamber pressures, mixture ratios, and coolant inlet temperatures.

Another off-design condition is the presence of gas in the propellants particularly in the fuel used to regeneratively cool the chamber. The gas may be present in solution or in the discrete gas phase. Pressurizing gas in solution constitutes no problem because the solubility of helium in MMH increases with temperature. Analysis indicated that helium in solution at engine inlet pressure and temperature will remain in solution throughout the engine. Heated tube tests have been conducted with helium-saturated MMH and indicate no effect on the burnout correlation (see Fig. 20).

Pressurant can enter the propellants in the undissolved gas phase as a result of failure of the OMS feed system bubble traps or upon switching from the normal to an alternate feed system. Gas phase pressurant can range from a

Figure 49. EFFECT OF MIXTURE RATIO AND CHAMBER PRESSURE ON COOLANT EXIT TEMPERATURE

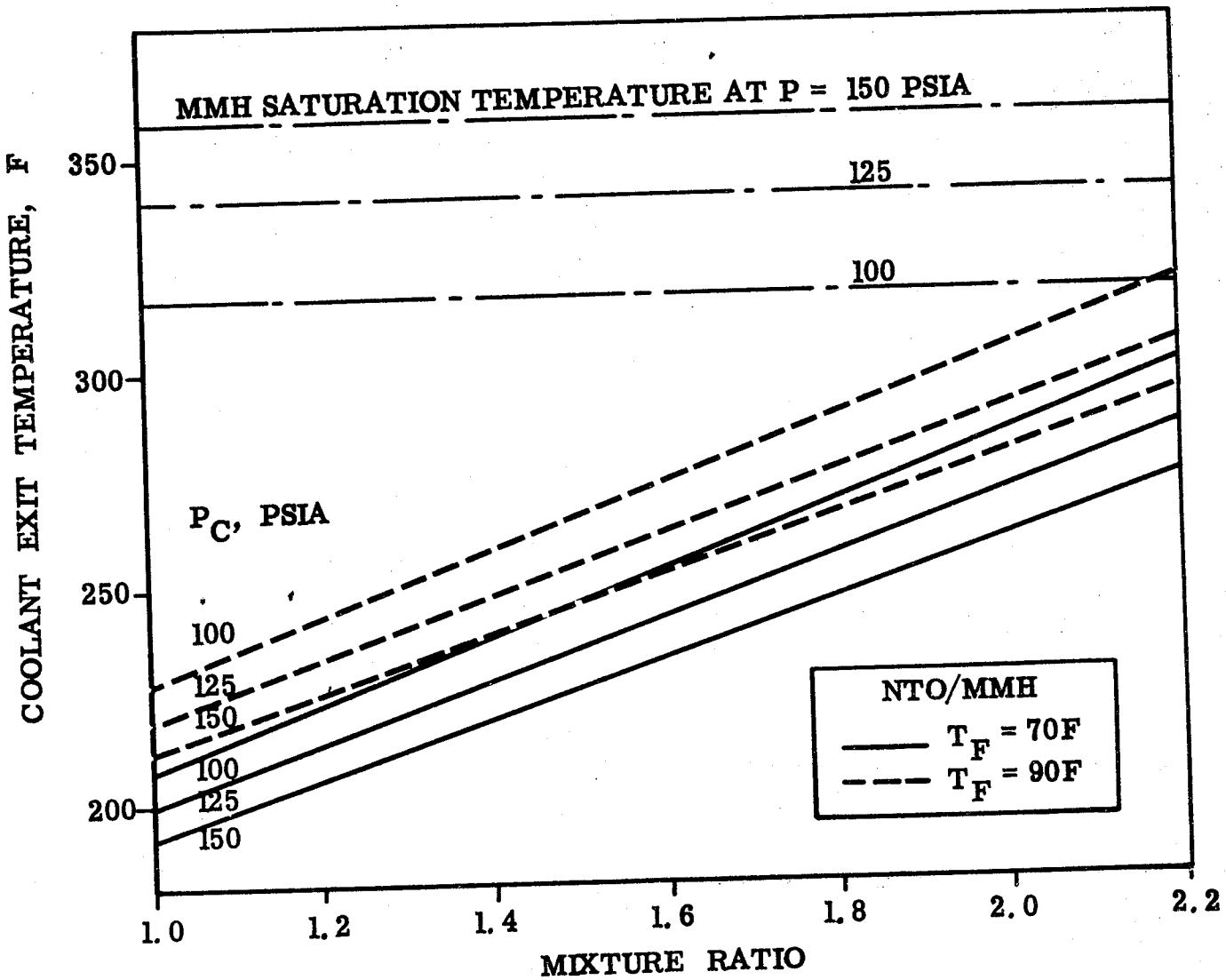

51

Figure 50. OFF-DESIGN OPERATING CAPABILITY

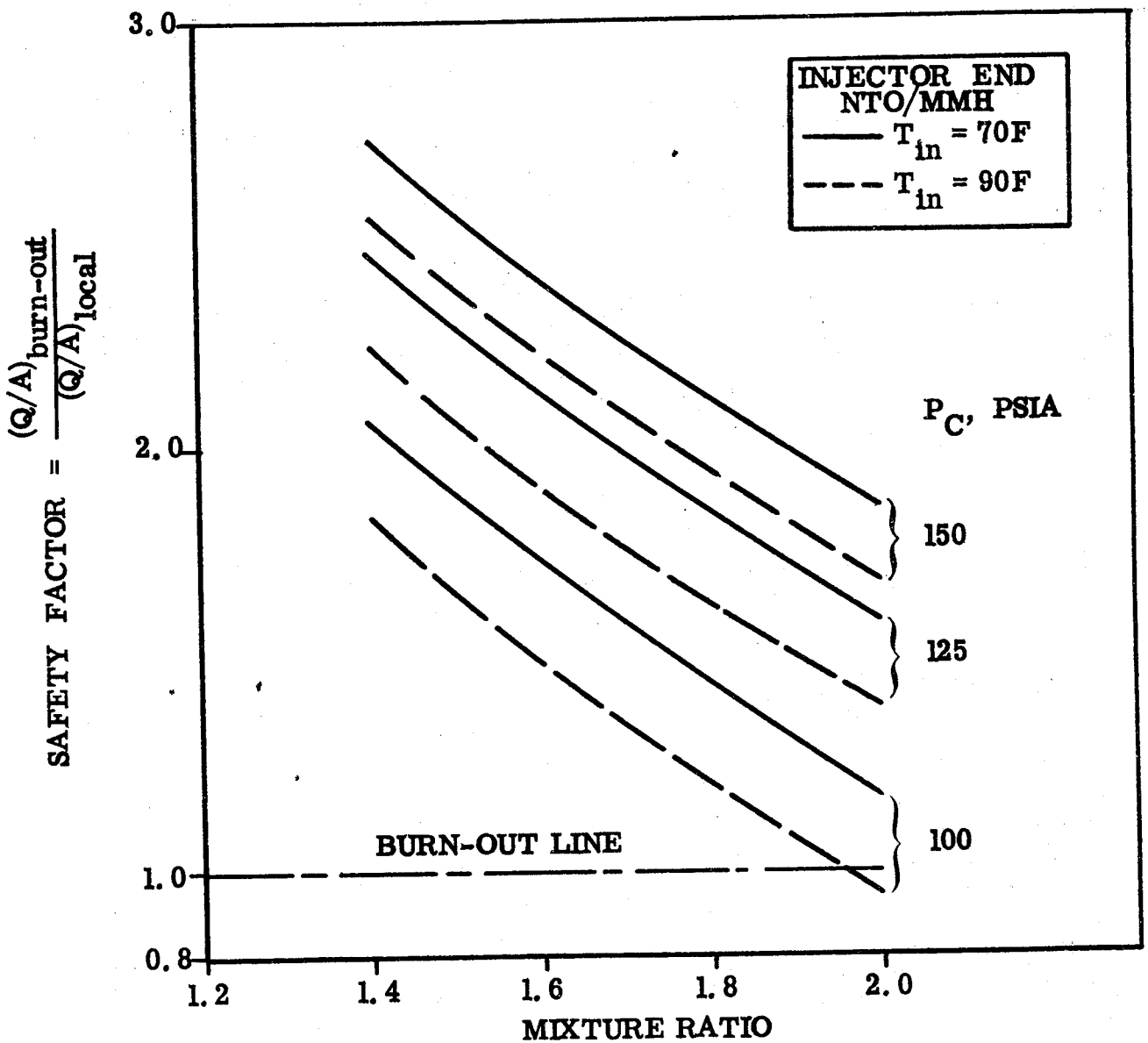

52

uniformly distributed froth to a large continuous bubble which completely interrupts the propellant flow. In the uniformly distributed situation the chamber pressure will be reduced and the mixture ratio changed as the froth reduces the effective density of the propellant. In addition to performance effects the presence of uniformly distributed bubbles in the fuel reduces the subcooling because of the resulting reduced fuel mass flowrate. However, there is sufficient safety margin that, at otherwise nominal inlet conditions, there is still 70 F subcooling with 25 percent by volume helium ingestion. The ingested helium increases the coolant velocity in the jacket so that the $V \Delta T$ product used to correlate burnout heat flux remains virtually unchanged with 25 percent ingestion. The applicability of the correlation to frothed coolant has not been experimentally verified.

Analyses were conducted to simulate the effect of a continuous bubble flowing through several channels by using a two-dimensional transient model of the chamber wall in the throat region. The analyses were conservative in that coolant flow was simply terminated; the cooling effect of the flowing bubble gas was not considered. Temperature transients for the coolant and combustion sides of the hot wall and for the coolant side of the back wall are shown in Fig. 51 for the nominal hot wall thickness of 0.030 inches.

Under nominal operating conditions only a small fin effect is present. However, as the wall temperature increases and the heat flux, consequently decreases, the fin effect becomes more pronounced and the hot wall temperature increases more slowly than a one-dimensional analysis would indicate.

If a gas bubble were to persist in the entire throat region for more than approximately 0.3 seconds it would drive all the fuel from the jacket and injector and combustion would cease. The analysis indicates that in this time the temperature of the combustion side of the hot wall would rise to 1290 F, a temperature at which the CRES liner would have a substantial structural safety factor. In fact, the hot wall is structurally adequate for uncooled operation for more than one second.

A NEW PRIEST

A new priest at his first mass was so scared he could hardly speak. After the mass he asked the Monsignor how he had done.

The Monsignor said fine, but next time it might help if he put Gin or Vodka in his water glass to help relax him.

The next Sunday the priest put Vodka in his glass and really talked up a storm. After mass he again asked the Monsignor how he had done. The Monsignor said fine, but there were a few things they should get straightened out.

1. There are TEN commandments, NOT TWELVE.

2. There were TWELVE Disciples, NOT TEN.

3. We do not refer to Jesus Christ as the late J.C.

4. David slew Goliath, he did not kick the shit out of him.

5. Next Sunday there is a taffy pulling contest at St. Peters, NOT A PETER PULLING CONTEST at St. Taffys.

6. The Father, Son, and Holy Ghost are not referred to as BIG DADDY, JUNIOR AND THE SPOOK.

Figure 51. WALL TEMPERATURE TRANSIENTS (NOMINAL T_{WALL} = 0.03 INCH)

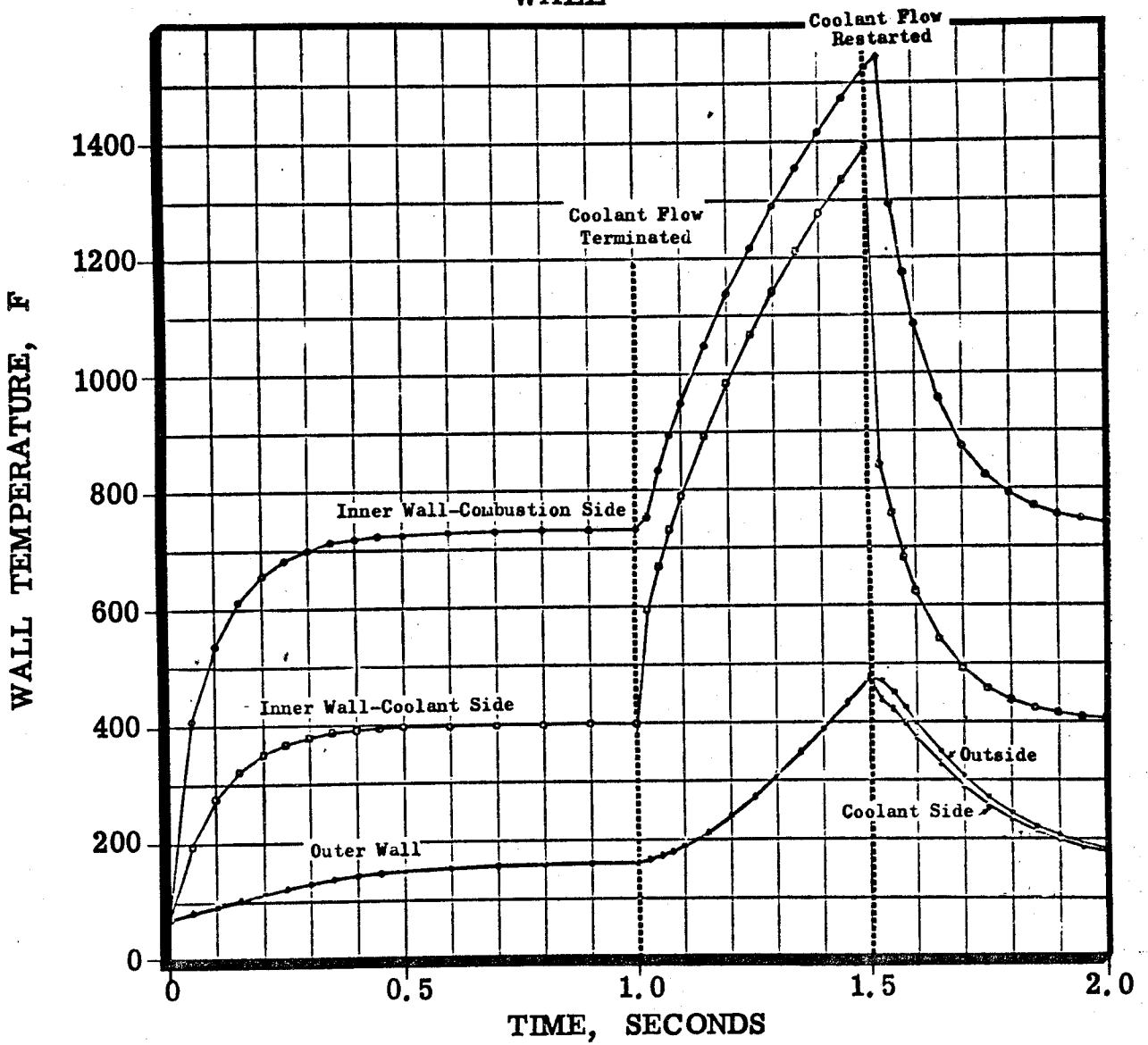

56

The other consideration is the consequence of fuel subsequently flowing over the inside of the CRES hot wall which, at 0.3 seconds, would be at a temperature of 1140 F. At this time the nickel back wall would be at a temperature of 310 F.

Pool boiling experiments indicate that the temperature of the MMH should be kept below approximately 550F. However, recent heated tube tests with MMH have demonstrated operation at inside wall temperatures as high as approximately 1200 F and coolant velocities below the nominal operating value without damage. Approximately 120 seconds of operation were accumulated on a single tube with inside hot-wall temperatures in excess of 1000 F without an increase in pressure drop through the tube. The implication of these test results is that neither explosive decomposition nor disposition would occur in the thrust chamber if the coolant flow were interrupted by a bubble.

DEMONSTRATOR THRUST CHAMBER AND NOZZLE FABRICATION

Manufacturing Operations and Schedules for the regeneratively cooled thrust chamber and for the nozzle extension are shown in Fig. 52 and 53. Fabrication of the CRES liner is begun by spinning to the approximate contour. Inside and outside contours are then machined and a light nickel electroform is applied to prepare the surface for the final electroform. Channels are then cut and their dimensions verified. Nickel electroform is applied and machined to provide an outer wall thickness of 0.030 inches. All channels are then cleaned and their flow characteristics determined. Manifolds, flanges, and ducts are machined and welded to the thrust chamber assembly. Final machining is followed by a proof and leak pressure test and a flow calibration of the completed assembly.

The nozzle extension is fabricated from a Columbium WC103 ring forging. This forging is machined to provide the 30 degree inside conical contour and the flange for attaching to the regeneratively cooled thrust chamber. After machining the nozzle is annealed and a final machining accomplished. A silicide coating is then applied and the nozzle mounted on the thrust chamber.

Figure 52. DEMONSTRATOR FABRICATION SEQUENCE

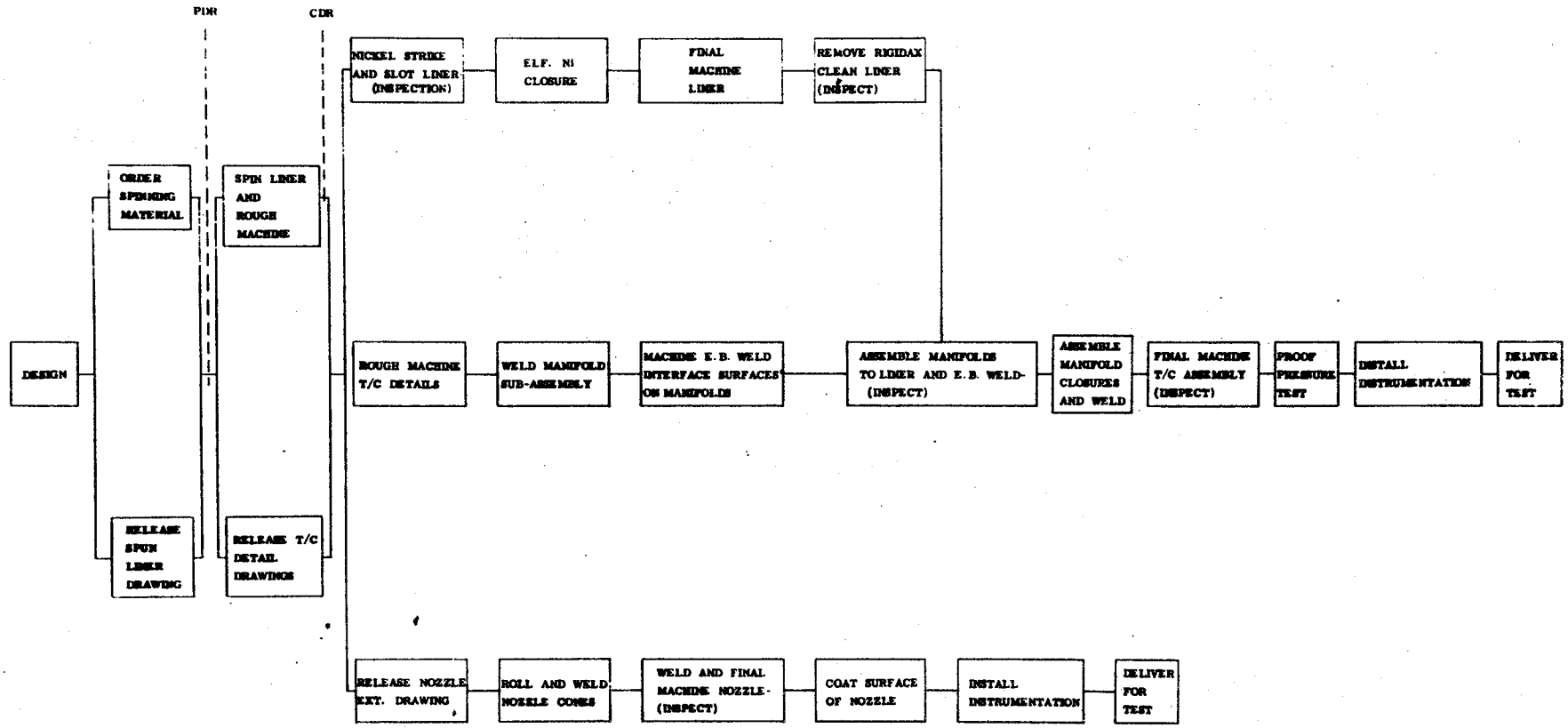

Figure 53. **DEMONSTRATION CHAMBER FABRICATION SCHEDULE**

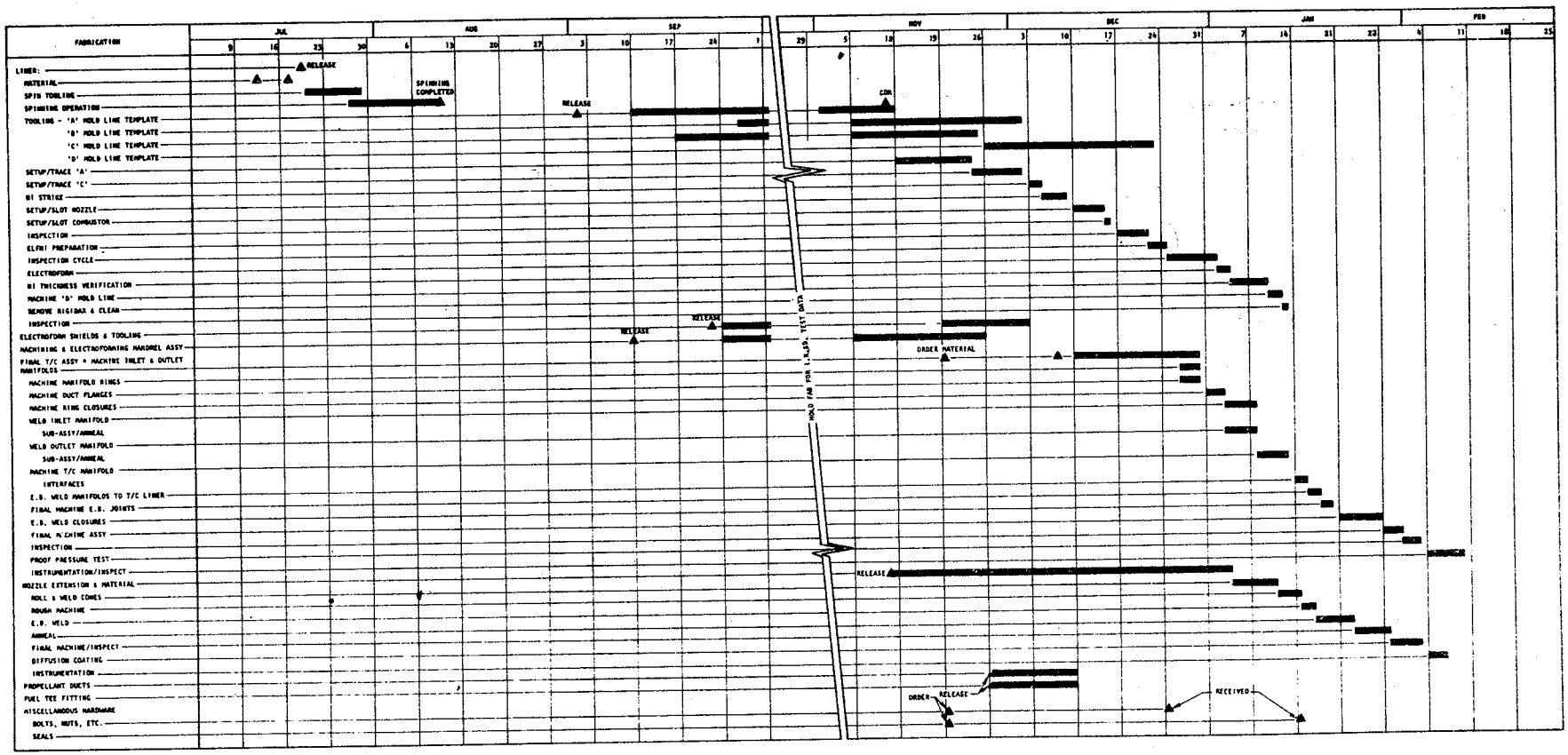

Exclusive of the spinning process and template cutting the entire fabrication is expected to take 15 weeks.

APPENDIX A

The results of Failure Modes and Effects Analyses for the injector and thrust chambers are summarized in Tables A-1 and A-2, respectively. Failure modes, causes, effects, and methods of detection are presented together with the design, fabrication, and operational controls which reduce the likelihood of the failure occurring.

Table A-1

Item: Injector

Function	Failure Mode/Mechanism	Failure Cause	Detection	Failure Effect on Engine	Failure Effect on Subsystem and Vehicle	Failure Effect on Mission	Controls in Effect to Eliminate or Reduce Failure Mode Occurrence or Effects	Criticality
The injector functions are as follows: (1) collect propellant from valve and regenerative cooling jacket and provide propellant isolation and distribution before mixing, (2) provide proper mixture ratio of propellants to obtain efficient combustion, (3) provide proper flow direction to both oxidizer and fuel to obtain efficient combustion, (4) provide proper characteristic propellant velocities to ensure combustion efficiency, (5) provide acoustic cavities for stability control	External Leakage: Material failure, corrosion, defective weld.	Installation damage. Inferior materials or weld.	Small leakage - unnoticed during operation. Visual inspection will show residues. Tape detectors. Small may be detectable Gross leakage - chamber pressure decrease and possible skin temperature change.	No effect with minor leakage. Fire possible. Performance loss and possible decrease in engine life with gross leakage.	No Effect: With minor leakage. Fire: Damage to to electrical systems and nonmetallic seals. Performance Loss: With major leakage	No Effect: With minor leakage. Fire: Depending upon the extent of fire may cause early mission termination	Generous wall thickness and machined bar stock utilized. Material compatible with propellants. Quality control of welding process. Electron beam welding & machine controlled welding will be used where possible. Ultrasonic inspection helpful. Leak check before EDMing orifices.	Reliability: Yes Hazard: Ground I Flight III
	Internal Leakage: Same as (External Leakage) above	Same as (External Leakage) above	Cannot be detected after assembly. Failure may be indicated by high skin temperature or low performance	Intermanifold leakage which would allow early mixing of propellants could cause fire, explosion, performance loss or chamber burnout depending upon the magnitude of leakage.	Engine Burnout: When performance loss noted by reduction in thrust or chamber pressure, may shutdown and switch OMS engines. Engine burnout may be damaging to surrounding equipment. If high skin temperatures picked up, OMS engine may be shutdown safely	Engine Burnout: Depending upon the extent of fire or damage may cause early mission termination regardless of spare engine. Performance Loss: OMS engine may be safely shutdown and mission completed with other engine	Same as for (External Leakage)	Reliability: Yes Hazard: Ground I Flight III

Table

Item: Injector

Function	Failure Mode/Mechanism	Failure Cause	Detection	Failure Effect on Engine	Failure Effect on Subsystem and Vehicle	Failure Effect on Mission	Controls in Effect to Eliminate or Reduce Failure Mode Occurrence or Effects	Criticality
	Instability.	Injector plugging changes in propellant flow distribution, changes in supply pressure, low supply pressure, feed system instability.	Excessive vibration and/or chamber pressure and feed system oscillations.	Structural Failure: Excessive vibration could result in rapid fatigue failure of chamber materials. Performance Loss: Reduction in combustion efficiency and resultant thrust loss.	No Effect: If properly decoupled from feed system except loss of engine. Could switch to second engine.	No Effect: As long as vehicle systems not damaged.	Feed system instabilities decoupled by proper orificing. Propellant filters used for supply fluids. Acoustic cavities suppress instabilities.	Reliability: Yes Hazard: Ground I Flight III
	Inefficient Combustion: Misimpingment (poor construction quality), contamination and plugging of orifices.	Inadequate control of manufacturing processes causing misimpingment, improperly configured injector holes, etc. Dirty fluids, components or assembly area.	Decreased chamber pressure. Possibly high skin temperature.	Performance degradation (thrust impulse, pressure). Could result in overheating depending upon misimpingment	No Effect: OMS engine may be switched to second engine.	No Effect:	Electrical discharge machining of injector orifices has been developed and is proved reliable in producing near perfect injectors. Area cleanliness methods during buildup, and implimentation of effective inspection practices. Injectors are cold flowed and hot fired after assembly for performance checkout.	

Table A-1

Item: Injector

Function	Failure Mode/Mechanism	Failure Cause	Detection	Failure Effect on Engine	Failure Effect on Subsystem and Vehicle	Failure Effect on Mission	Controls in Effect to Eliminate or Reduce Failure Mode Occurrence or Effects	Criticality
	Flow Restriction: Foreign material plugged flow passages. Improper machining, welding.	Contamination, corrosion products, processes residues, propellant residues, improper or no decontamination. Wrong dimensions, weld drop through or oxidation products from inadequate purging.	One or more of following: decreased chamber pressure, high skin temperature, excessive vibration.	One or more of the following: a) Injector or chamber overheating b) Loss of performance c) Combustion instability	No Effect: OMS engine may be switched to second engine.	No Effect	In-process cleanliness methods and contamination control procedures have been developed and are a matter of practice. Decontamination procedures include purges and vacuum exposure after each flight or test. Fluids are filtered through inlet line filters. Metal engine minimizes any blowback contamination from combustion. Injectors are cold flowed and hot fired after assembly for performance checkout.	Reliability: No Hazard: Ground I Flight II

Table

Item: Thrust Chamber

Function	Failure Mode/Mechanism	Failure Cause	Detection	Failure Effect on Engine	Failure Effect on Subsystem and Vehicle	Failure Effect on Mission	Controls in Effect to Eliminate or Reduce Failure Mode Occurrence or Effects	Criticality
To contain the combustion gases to obtain the desired chamber pressure and thrust. The channel wall of the thrust chamber provides regenerative cooling with fuel and film cooling at the injector end. The chamber distributes fuel to the injector manifold.	External Leakage: Structural failure.	Defective material, high internal stress, fabrication damage, excessive stresses (vibration).	Reduction of chamber pressure. Possible high skin or coolant outlet temperatures.	Engine Degradation: P Probable fire from fuel contacting hot combustion gases.	Possible Fire indicated damage on other systems.	No Effect: If fire contained and engine shutdown, can use second engine. Possible Mission Termination: If fire damaged other systems, mission may be terminated or limited depending upon the damage.	Integral wall chamber construction with channels. Low wall operating temperatures reduces likelihood of failure. Chamber proof pressure tested for structural check after fabrication.	Reliability: Yes Hazard: Ground I Flight III
	Internal Leakage of Inner Wall: Structural failure.	Same as above.	Possible high skin or coolant outlet temperatures.	Heating of wall at discharge end of channel due to reduction of coolant flow.	No Effect: If leakage small, no effect. Engine shutdown required by high temperature.	No Effect: Can use second engine.	High strength, compatible material used. Proof pressure testing for structural check after fabrication. Fuel cools wall at break.	Reliability: Yes Hazard: Ground I Flight II
	Fails to Maintain Geometrical Configuration: Erosion or melting.	Low coolant flow passages. off-limits operation. (high mixture ratio).	High skin temperatures. Possibly decreased performance.	Engine degradation: Possible inner wall failure.	No Effect: If engine shutdown before major wall failure, second engine can be used.	No Effect: Can use second engine.	Wide channels, proper distribution of fuel. All fuel must flow through walls. Design margin	Reliability: Yes Hazard: Ground I Flight II
	Structural failure of lands.	Improper fabrication methods, contamination, high stress levels.	Possibly none. Gross failure may be indicated by inner buckling.	Possibly no effect depending upon location and extent of failure	No Effect:	No Effect:	Low mechanical stress levels. Concept demonstrated at wide temperature cycles.	Reliability: Yes Hazard: Ground I Flight II

Table A-2

Item: Thrust Chamber

Function	Failure Mode/Mechanism	Failure Cause	Detection	Failure Effect on Engine	Failure Effect on Subsystem and Vehicle	Failure Effect on Mission	Controls in Effect to eliminate or reduce failure mode occurrence or effects	Criticality
	High Channel ΔP	Contamination, reaction products from propellant and air. Improper fabrication.	Reduced performance and/or chamber pressure. High skin temperatures.	Hotter Engine Operation; Restricted fuel flow increases mixture ratio (o/f) and engine operating temperatures. Channel burnthrough if completely plugged.	Possible engine overheating.	No Effect	Fluids filtered Components cleaned prior to assembly. Engine opened to vacuum after use and purged during field safing. Channels flow checked during fabrication.	Reliability: Yes Hazard: Ground I Flight II
Increase engine performance for orbital applications through optimum expansion of combustion gases.	Structural Damage to Nozzle: Due to buckling, burnout, erosion.	Manufacturing Defects: Extreme loading, overheating.	Visual inspection High skin temperature. Thrust misalignment.	Possible Structural Failure: Possible nozzle structural failure. Thrust vector error.	No Effect	No Effect: Switching to second engine if necessary.	Quality control provisions and strict visual inspection requirements	Reliability: Yes Hazard: Ground I Flight III
	Oxidization of Nozzle.	Loss of Coating: Manufacturing defects, mishandling.	Visual inspection High skin temperatures.	Possible Structural Failure: Oxidation and subsequent loss of material from nozzle resulting in structural failure from overheating.	No Effect	No Effect: Mission may be continued with second engine.	Quality control provisions and visual inspection requirements.	Reliability: Yes Hazard: Ground I Flight III

Internal Letter

North American Rockwell

Date	31 January 1973	No	ASR 72-303
To	R. Helsel D/578	FROM Address	R. P. Pauckert D/589-194
		Phone	2231

Addendum to Critical Design Review -
Reusable Thrust Chamber, NAS 9-12802

The following documentation is provided to questions asked at the OME Reusable Thrust Chamber Critical Design Review and subsequent telephone conversations.

R. Paster
P. Bailey
R. Tobin
D. Goracke
D. Leonard
M. Bensky

Q1. What impurities are included in calculating theoretical performance of NTO/MMH?

A1. The following concentrations of impurities are assumed: 1.00 percent H_2O in the MMH; 0.42 percent NO, 0.10 percent H_2O, and 0.08 percent NOCl in the NTO. These impurities are within the concentrations allowed by Mil Specs P-27404A (MMH) and P-26539C (NTO) except for the NOCl. Using Mil Spec concentration values for all impurities reduces C* by 6 fps and I_s by 0.3 seconds.

Q2. Experimental C* efficiencies were presented based on theoretical values of C*, which were determined for P_c = 125 psia and T_F = 70F. What are the implications of evaluating theoretical C* at the experimental values of these parameters?

A2. The C* efficiencies calculated with theoretical C* values based on P_c, T_F, and o/f for each particular test are shown in Fig. 1 for the injector using like-doublet elements. The effect of chamber pressure is very small so that the comparison of curves 1 vs 6 and 2 vs 7 is unaffected. The effect of fuel temperature is more significant. Previous data indicated that

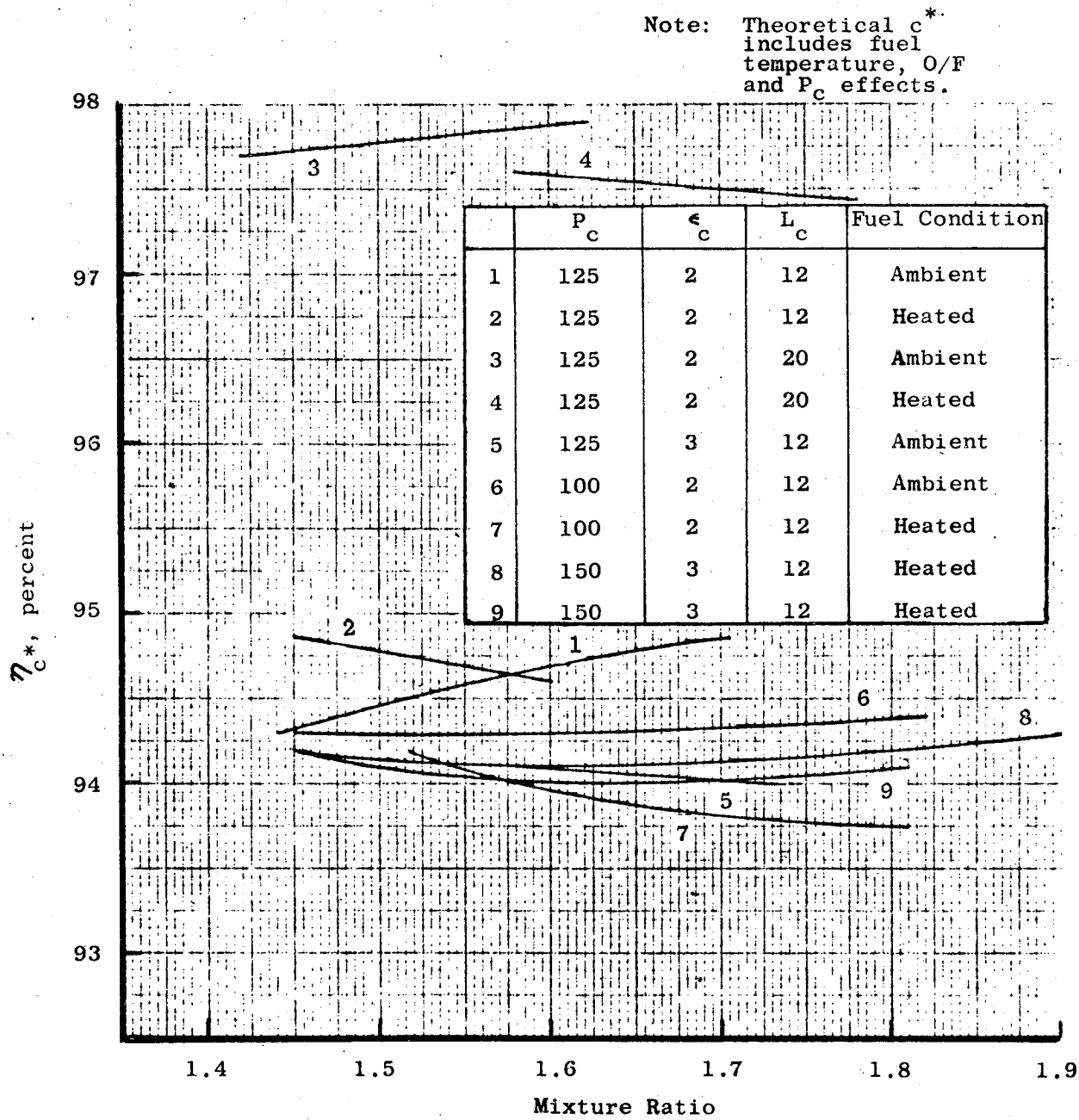

	P_c	ϵ_c	L_c	Fuel Condition
1	125	2	12	Ambient
2	125	2	12	Heated
3	125	2	20	Ambient
4	125	2	20	Heated
5	125	3	12	Ambient
6	100	2	12	Ambient
7	100	2	12	Heated
8	150	3	12	Heated
9	150	3	12	Heated

Figure 1. Experimental Like-Doublet Injector Performance.

heating the fuel has a slightly beneficial effect at nominal mixture ratio. The revised curves indicate a slightly negative effect (≈ 0.2 percent) resulting from heating the fuel. The predicted specific impulse values previously quoted are unaffected because the effect of the fuel temperature was accounted for in the prediction.

Q3. How do injector efficiency and inlet pressure trade off vs injector ΔP?

A3. Predicted injector efficiencies, shown in Volume A of the Critical Design Review Briefing, as a function of injector ΔP, were converted to delivered specific impulse variations. The inlet pressure variations were converted to equivalent specific impulse changes using a factor of 15 psi/sec. The optimum occurs at an injector orifice pressure drop of 50 psi. The effective specific impulse change is less than 0.3 seconds for ΔP values ranging from 35 to 70 psi. Doubling the inlet pressure-to-specific impulse trade factor to 30 psi/sec results in shifting the optimum ΔP to 70 psi; halving the factor to 7.5 psi/sec moves the optimum to 30 psi.

Q4. How does the nozzle percent length change as the combustor length is increased at constant (76 inch) engine length ?

A4. The engine design in the Final Data Dump was for a 73-inch engine with an 11-inch combustor and 70 percent nozzle. Allowing the engine length to increase to 76 inches (current Space Division design point) increases the nozzle length to 73.7 percent with an 11-inch combustor. Simultaneously increasing the engine length to 76 inches and the combustor length to 14.7 inches results in a 69 percent nozzle. The difference in nozzle efficiencies between 69 and 73.7 percent length nozzles is equivalent to approximately 0.9 seconds of I_s.

Q5. At the CDR an optimization of combustor length was shown based on η_{C*} and stratification loss variations. How would the optimization be affected if chamber weight and inlet pressure effects were also included?

A5. In the Final Data Dump it was shown that the combustor length optimization is most strongly effected by variations in η_{C*} and stratification losses resulting from film cooling. An optimization was conducted including effective specific impulse variations resulting from changes in coolant jacket pressure drop (15 psi ΔP/sec I_s) and engine weight (23 pounds/sec I_s). The chamber length resulting from the complete optimization is 0.2 in. shorter than the original optimization (15.5 vs 15.7 in.). The demonstrator chamber is being fabricated at a shorter length than optimum because:
(1) an existing spinning was available to make a chamber of 14.7 in. length
(2) it is anticipated that, with further effort, higher performing injectors will be built which characteristically have lower performance sensitivity to length. The latter characteristic, with the accompanying tendency toward higher heat flux levels near the injector, tends to favor shorter chanbers.

Q6. What are the weight implications of a 1-1/2 pass cooling configuration compared to an uppass cooling configuration?

A6. The coolant jacket weights of the two configurations can be made approximately the same. The weight of the attach flange for the radiation nozzle also remains virtually unchanged. Moving the inlet manifold from $\epsilon = 7$ to $\epsilon = 2.5$ results in a weight saving of 1 lb for the manifold and a smaller weight saving for the duct from the valve to the jacket. (There may actually be a weight increase because other ducting may have to be rerouted.) The 1-1/2 pass configuration would have a pressure drop 2 psi greater than the uppass circuit for equal jacket weights. To provide equal ΔP the channel heights of the 1-1/2 pass jacket would be increased with a consequent weight increase of approximately 4.5 lb.

Q7. What is the effect of propellant mixture ratio on theoretical throat heat flux?

A7. Theoretical values of heat flux vs o/f are shown in Fig. 2. The curve is so flat that during parametric analyses, the heat flux variation with mixture ratio is neglected. Experimental data points for the like doublet injector are shown which also indicate little variation with mixture ratio.

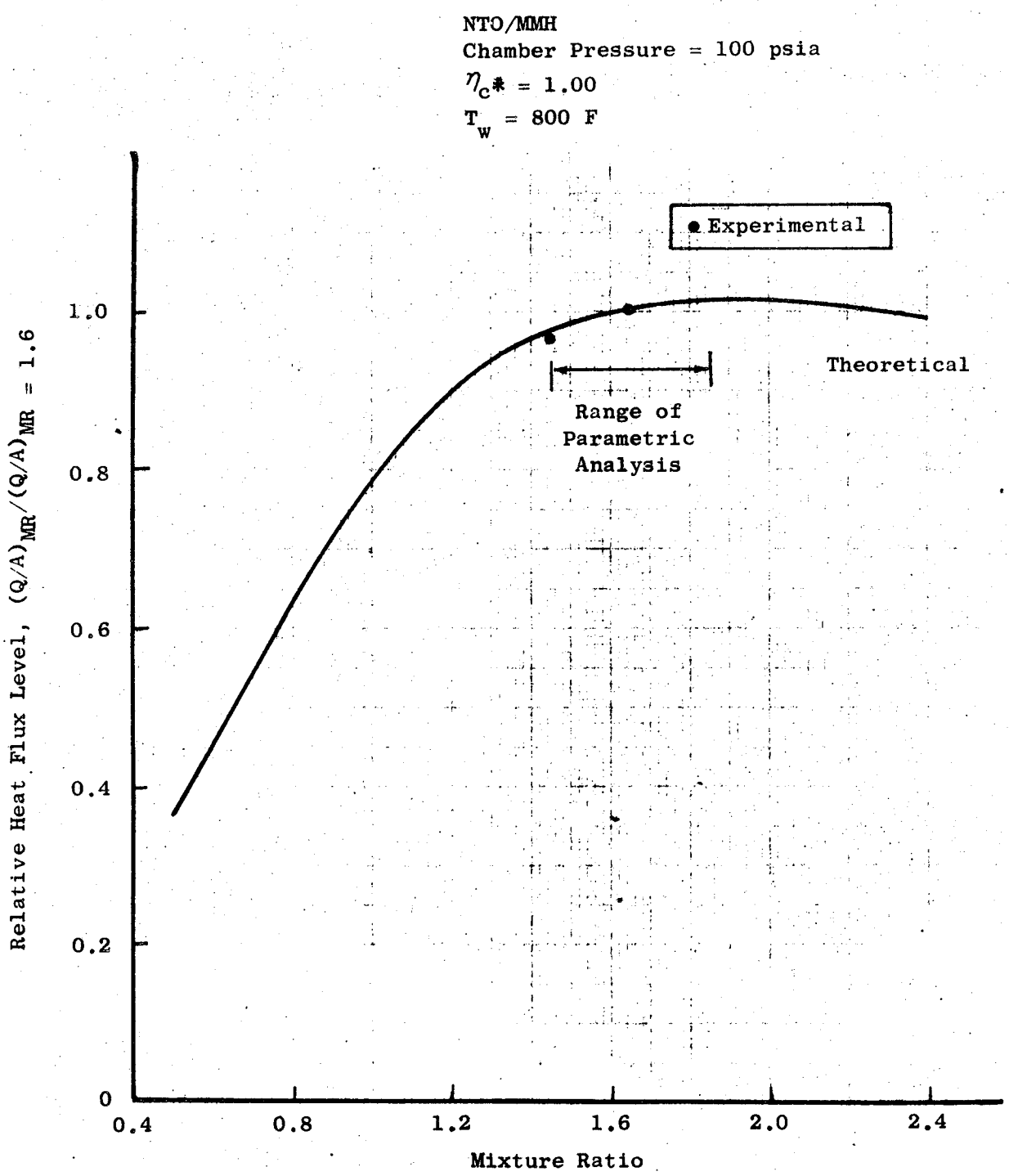

Figure 2. Theoretical Effect of Mixture Ratio on Relative Heat Flux Level

Q8. What is the minimum safety factor in the nozzle under sea level pressure operating conditions?

A8. The minimum safety factor in the nozzle under sea level operating conditions occurs at the point of flow separation at an area ratio of 3. The safety factor at this point is 2. At higher altitudes the minimum safety factor increases so that the chamber will operate safely at all altitudes.

Q9. What are the effects of operating at off-design chamber pressure and fuel flowrate on the minimum safety factor of the regeneratively cooled chamber?

A9. The minimum safety factor is shown vs P_c and o/f for off-design conditions in Fig. 3. The results are based on the assumption that the film coolant flow is constant fraction of the total fuel flow. A typical tank blowdown would result in a chamber pressure of approximately 85 psia and little change in mixture ratio from the initial value. If the initial mixture ratio were 1.65 the minimum safety factor would be approximately 1.4 for a fuel inlet temperature of 70F. If the blowdown were initiated when the fuel tank pressure was 10 psi lower than the oxidizer tank pressure the mixture ratio would be 1.76 and the minimum S.F. at 85 psia chamber pressure would be 1.3 for 70F fuel or 1.0 for 90F fuel. The 1.0 S.F. could be increased to 1.25 by increasing the film coolant from the nominal 2.4% to 3.5% and shortening the chamber to 13 in. The specific impulse under nominal conditions for this design would be 311 sec and the engine inlet pressure would be 208 psia.

Q10. What is the safety factor profile with no supplementary boundary layer coolant?

A10. The safety factor profile with no BLC is shown in Fig. 4. Under otherwise nominal conditions the minimum safety factor is 1.0 and occurs near the injector. The safety factor in the throat region is 1.8. The minimum safety factor can be increased to 1.5 under these conditions by two means: (1) the coolant channel area can be reduced near the injector end so

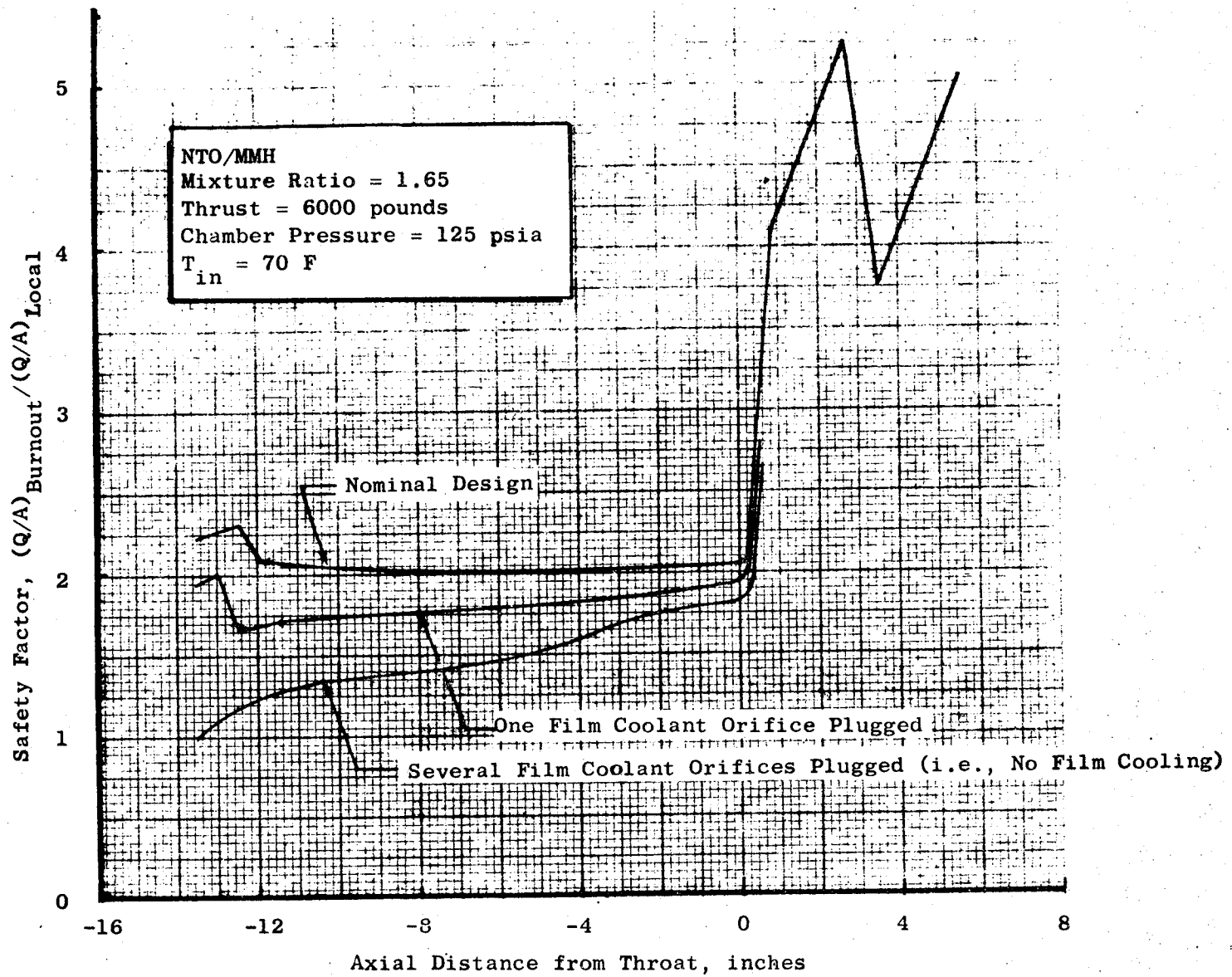

Figure 4. Safety Factor with Plugged Film Coolant Orifices, Nominal Condition

that the minimum S.F. is 1.5 with a resultant increase in jacket ΔP of 2 psi, (2) the channel area reduction described in (1) can be accomplished with no increase of pressure in the jacket ΔP by simultaneously enlarging the channels in the throat section. This would result in a S.F. of 1.5 in the throat region and 1.5 at the injector end with no BLC.

Q11. How does the temperature of the SS main engine nozzles affect the radiation cooled OME nozzles operation?

A11. The tubular wall nozzle of the main engine is cooled with cryogenic hydrogen. Since the driving potential for radiation cooling is the difference between the fourth power of the source temperature and the fourth power of the sink temperature; the temperature effect of the SSME nozzle is negligible. The reflectivity of the nozzles could increase the temperature of the radiation-cooled skirt slightly ($\approx$ 50F).

Q12. What strength properties were used for the design of the columbium film-cooled chamber and the columbium skirt of the regeneratively cooled chamber?

A12. The columbium film-cooled chamber was designed based on restricting the creep to 0.2 percent to limit performance variations. The creep data for WC-103 were obtained from the Technical Information Manual published by the Wah Chang Company. The Larson-Miller plot used in the design is shown in Fig. 5 reproduced from the Wah Chang manual.

The columbium nozzle design was based on the time to stress rapture criterion. A stress rupture data point given in the Wah Chang manual was theoretically extrapolated into the graph presented in the CDR and repeated here as Fig. 6 . A 2 percent creep line at 2400F has been added to the figure based on the aforementioned Larson-Miller plot to indicate the reasonableness of the stress rupture data shown.

Q13. The damping time of bomb induced oscillations on test 152 is longer than for the other tests and was stated to be a low frequency feed system conditions What is the damping time for high frequency oscillations on this test?

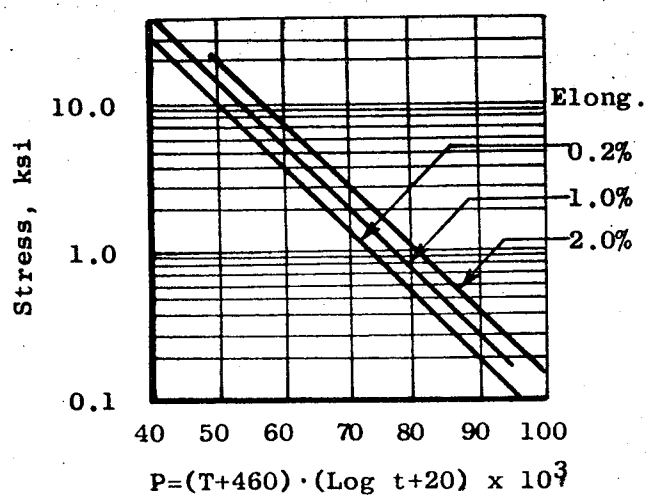

Figure 5. Larson-Miller Master Plot for Recrystallized WC-103.

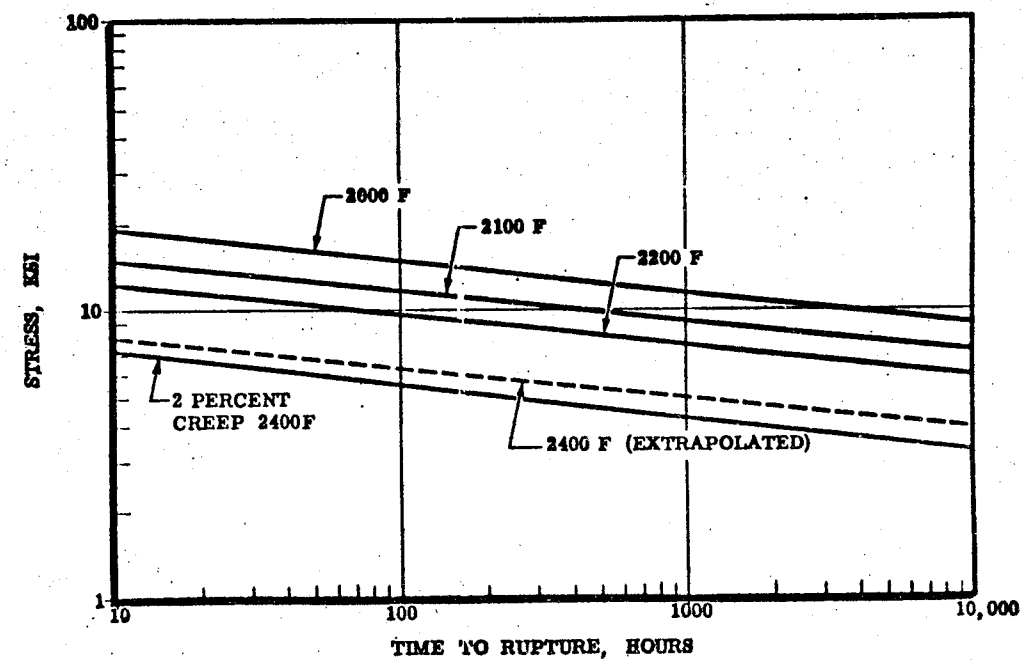

Figure 6. Stress Rupture Data, Columbium Alloy WC-103

A13. The damping time for high frequency oscillations was 8-9 msec, comparable with the times listed for the other tests.

Q14. How much will the throat area of the regeneratively cooled chamber change when operating compared to a value measured under ambient conditions?

A14. Pressure effects on the throat area are negligible. The predicted area increase resulting from thermal expansion is 0.7 percent.

A15. The acoustic cavity area expressed as a percent of the total area of the injector face presented at the CDR is in error. The corrected curve is shown in Fig. 7.

R. P. Pauckert
Systems Application
Advanced Programs

/c

VARIATION OF CHAMBER NATURAL FREQUENCY
WITH CONTRACTION AREA RATIO

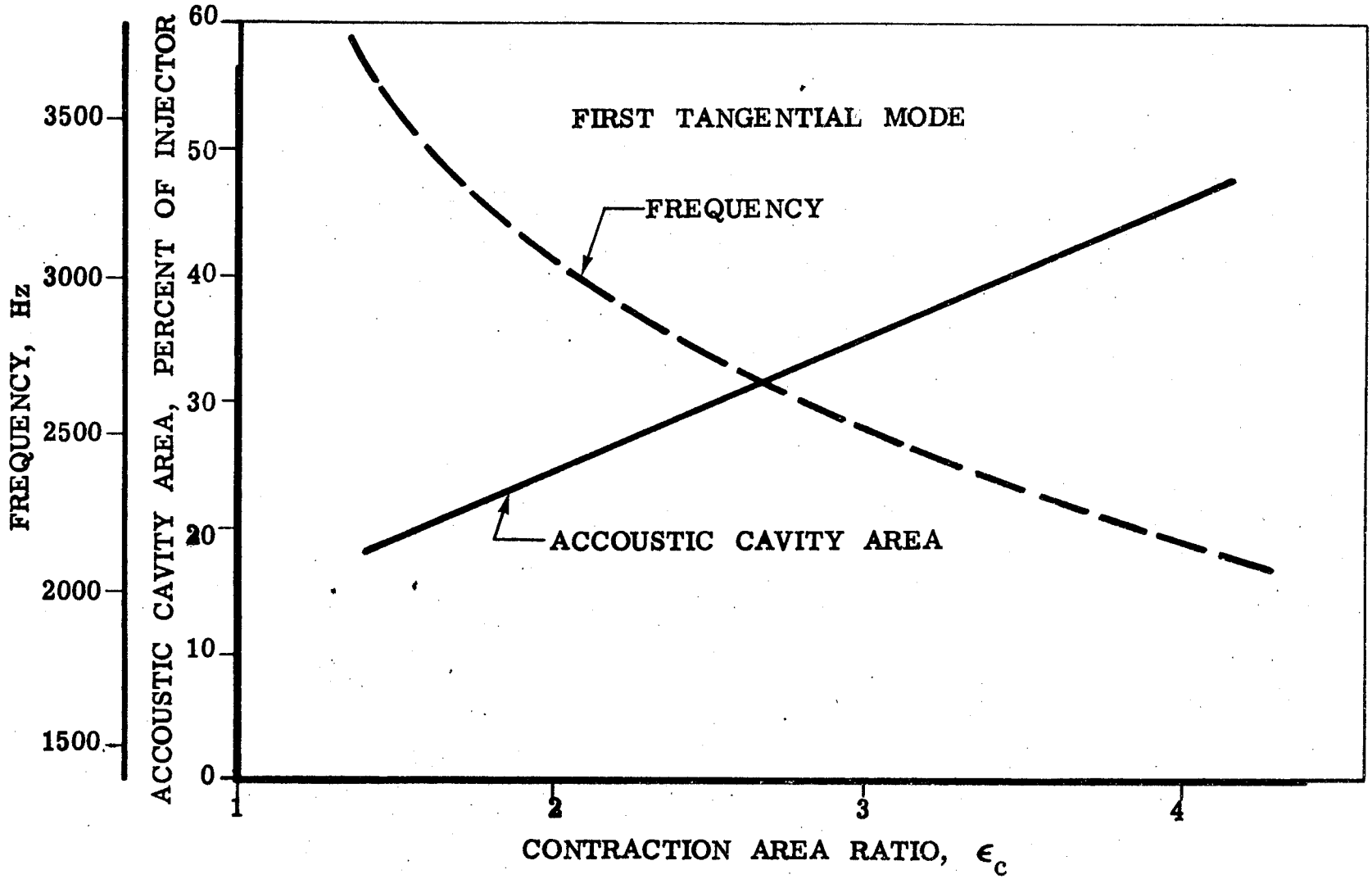

Figure 7.